Electronic Supporting Information

New routes to Cu(I)/Cu nanocatalysts for the multicomponent click synthesis of 1,2,3-triazoles

Pavel Abdulkin,[1] Yanina Moglie,[2] Benjamin R Knappett,[1] David A Jefferson[1], Miguel Yus[2], Francisco Alonso*[2] and Andrew E H Wheatley*[1]

[1]P. Abdulkin, B. Knappett, Dr. D. A. Jefferson, Dr. A. E. H. Wheatley
Department of Chemistry, University of Cambridge, Lensfield Road, Cambridge, CB2 1EW (UK)
Fax: (+)44-1223-336362; E-mail: aehw2@cam.ac.uk

Dr. Y. Moglie, Prof. M. Yus, Prof. F. Alonso
[2]Departamento de Química Orgánica, Facultad de Ciencias and Instituto de Síntesis Orgánica (ISO), Universidad de Alicante, Apdo. de Correos 99, 03080 Alicante, Spain; Fax: (+)34-96-5903549;
E-mail: falonso@ua.es

Contents

General details of catalyst synthesis

Chemicals, including a stock solution of hydrazine (1 M in THF), were purchased from Sigma-Aldrich (reagents: analytical grade; solvents: HPLC grade) and used without further purification. Aqueous solutions were prepared using deionized water (Millipore, specific resistivity ≥18.2 MΩ cm). Ethanol was distilled immediately prior to use. Prior to synthesis, flasks were flushed and all solutions were degassed with argon.

Catalyst characterization

High-resolution Transmission Electron Microscopy (HRTEM)

Analysis on a JEOL JEM-3011 high-resolution transmission electron microscope required preparation by droplet coating of MeOH suspensions on carbon coated Ni grids (Agar Scientific, 300 mesh). Electron optical parameters: C_S = 0.6 mm, C_C = 1.2 mm, electron energy spread = 1.5 eV, beam divergence semi-angle = 1 mrad). Elemental analysis was by energy dispersive X-ray spectroscopy (EDS). In this work, narrow beam EDS is defined as using a 7 nm beam diameter (note that this does not reflect the true area over which data was collected due to secondary effects). Broad beam EDS is defined as using a 50 nm beam diameter. A PGT prism Si/Li detector and an Avalon 2000 analytical system were employed. Observed Ni Kα and Kβ emission lines were attributed to scattered electrons impinging on the bars of the nickel support grid. Any minor Fe Kα and Co Kα emission lines were due to parasitic scattering from the lens pole-piece. Some significant CuKα and Kβ x-rays, however, were generated from stray electrons impinging on the specimen holder itself. Allowance for this was made by examining a specimen of CeO_2 nanoparticles of similar dimensions (3-10 nm) on a nickel grid in both the standard specimen holder used in this work and also a specially manufactured titanium holder. From the latter, the Ni Kα/NiKβ intensity ratio was determined to be 6.7±0.1. This knowledge enabled calculation of the mean value of the CuKα contribution to the combined CuKα + NiKβ peak recorded in the standard specimen holder. The resulting value was approximately 40% of the observed NiKα signal. This correction for the contribution from the specimen holder was made to EDS analyses of CuZn samples.

Samples analysed on an image aberration corrected FEI Titan 80-300 operated at 300 kV providing an information limit of 0.08 nm in TEM mode were prepared by dropping a suspension of the NPs in MeOH onto carbon coated Ni grids (Quantifoil). Scanning transmission electron microscopy (STEM) was performed using a high-angle annular dark-field (HAADF) detector with a nominal spot size of 0.14 nm. For spectroscopy, a nominal spot size of ~0.5 nm was used in STEM mode with a Gatan Tridiem image filter for electron energy loss spectroscopy (EELS) and an EDAX S-UTW EDS detector.

The particle size were analysed using Macnification 2.0.1 by counting the diameters of 100 particles in lower magnification images, defining size intervals of 0.2 nm between $d_{min} \leq d \leq d_{max}$ and counting the number of particles falling into these intervals, the data was then used to construct particle size distributions using DataGraph 3.0.

The detailed analysis of particle morphology was done using Digital Micrograph 3.6.5. The values of average *d*-spacing were obtained from Fourier transforms of high magnification images (x800K, x1M, x1.2M) using the expression $d = D/20$ where D is the diameter (nm) of rings obtained. The average *d*-spacing was then verified using the profile tool in Digital Micrograph counting at least 10 *d*-spacings. To determine the error in the value of *d*-spacing thus obtained, detailed TEM examination of CeO_2 and Au nanoparticles was undertaken. The relationship between the diameter of the FT rings and the DV value (a measure of the objective lens focusing voltage) was established for DV values between –6 and +6 and the value of standard deviation in *d*-spacing was established to be 10% when compared to literature values.Where oxidation state was determined based on *d*-spacings obtained by TEM measurements, values within 1 standard deviation (±5%) of literature values were used.

Powder X-ray diffraction (XRPD)

XRPD data were collected on a Roentgen PW3040/60 XPert PRO powder X-ray diffractometer with a high resolution PW3373/00 Cu LFF (unmonochromated) tube at $\lambda = 1.5404$ Å (Cu Kα). Sample preparation was by solvent evaporation from colloidal suspensions deposited on the 0.5 mm deep ground area of a glass flatplate sample holder using a microscope slide so that the powder sample was smooth, flat and flush with the sample holder surface. The holder was inserted onto the sample stage (PW3071/60 Bracket) such that the sample was just free of the reference plane of the sample stage.

X-ray photoelectron spectroscopy (XPS)

XPS spectra were measured on a Kratos Axis Ultra DLD XPS System using a dual Al-Mg X-ray anode with a circular spatial resolution of 15μm. Samples were prepared by droplet coating of the methanol dispersed NPs on Si wafers under an atmosphere of air.

Inductively coupled plasma optical emission spectroscopy (ICP-OES)

ICP-OES was carried out using a Perkin-Elmer 7300DV spectrometer at an RF power of 1300 W. Gas flows (l/min) were: 15 (plasma), 0.2 (auxiliary), 0.85 (nebulizer).

Synthesis and characterization of nanoparticles

Cu/PVP40 1(reaction pav55)

$CuSO_4•5H_2O$ (249.70mg, 1.00 mmol) and PVP40 (average M_w = 40000, 1.11 g, 10.00 mmol) were dissolved in ethylene glycol (120 ml) under an Ar atmosphere and the mixture was stirred for 2 h at 80°C. After cooling to 0°C the pH was adjusted to *ca*. 10 by adding NaOH (1 M in deinolozed water, 5 ml). The mixture was stirred for 15 min after which $NaH_2PO_2•H_2O$ (211.98 mg, 2.00 mmol) in deionized water (2 ml) was added. The reaction was stirred at 140°C for 90 min to give a crude NP dispersion, an aliquot of which was purified by extraction using excess acetone (1:10) over not more than 90 min. After sedimentation of the particles, the supernatant was decanted and the remaining suspension centrifuged. Upon removal of the solvent layer, the precipitate was resuspended in methanol.

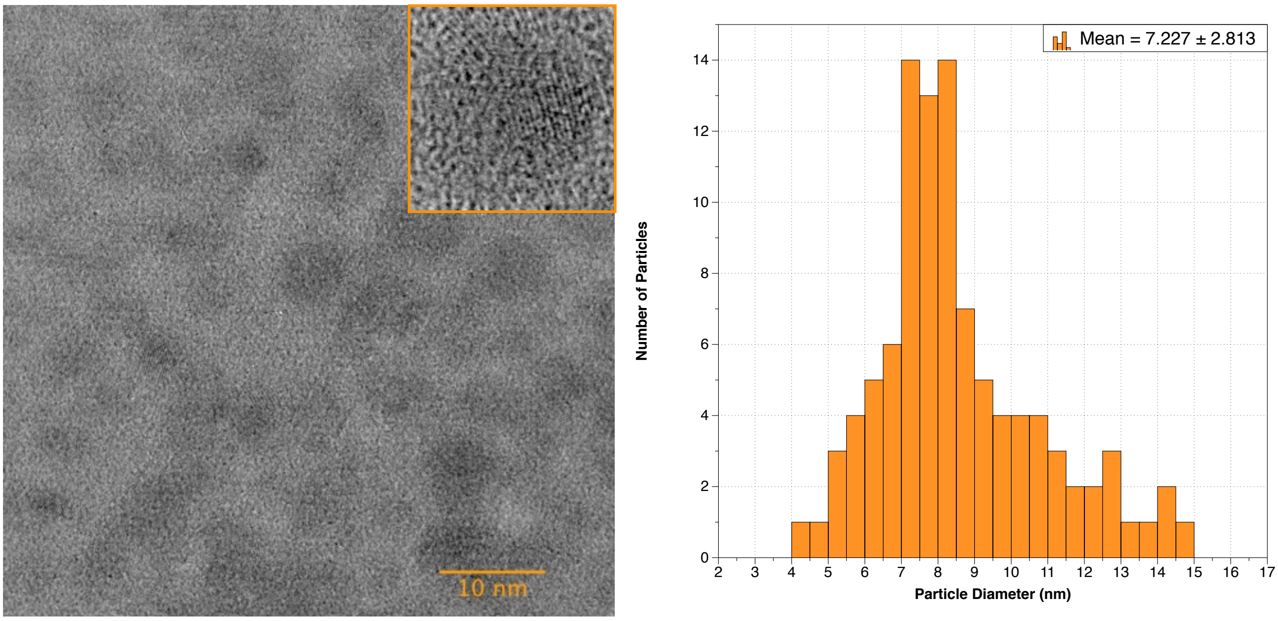

Figure S1a Representative TEM image of catalyst 1 at x300k with a magnified insert *(left)* and particle size distribution *(right)*

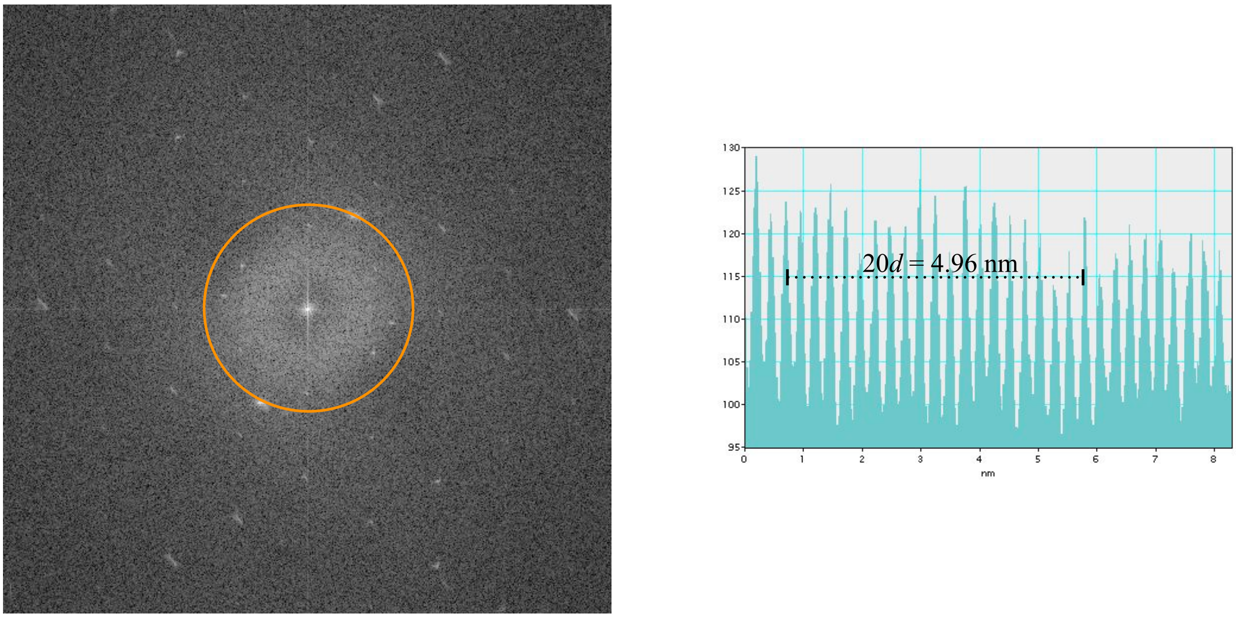

Figure S1b Representative Fourier transform image and fringe space analysis for catalyst 1 demonstrate an average *d* spacing of 2.48 Å corresponding to Cu_2O (111)

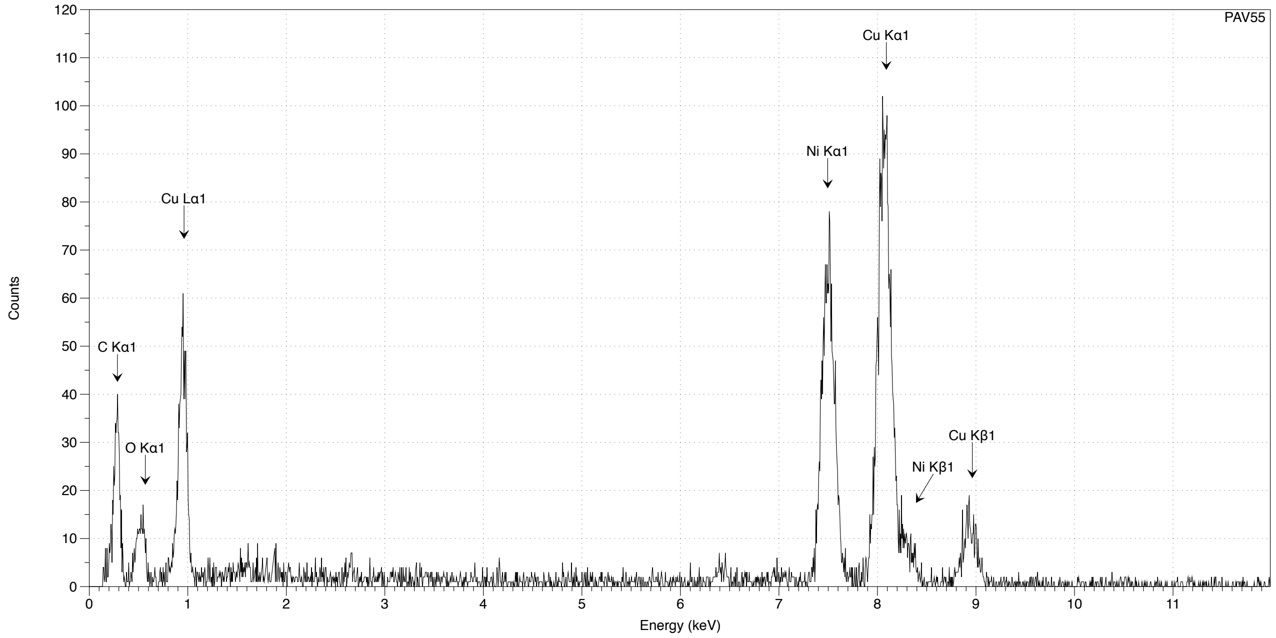

Figure S1c Representative narrow beam ED spectrum

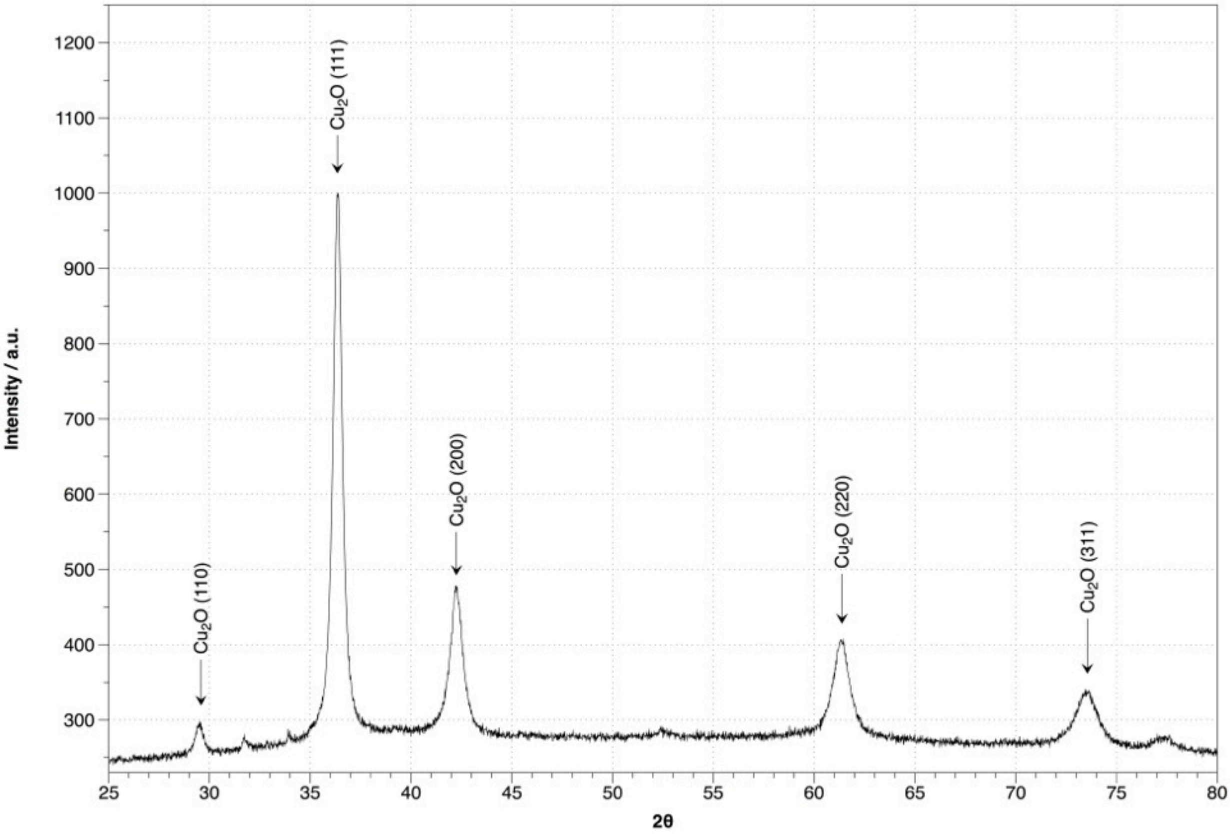

Figure S1d XRPD pattern of fresh catalyst 1 reveals Cu_2O only

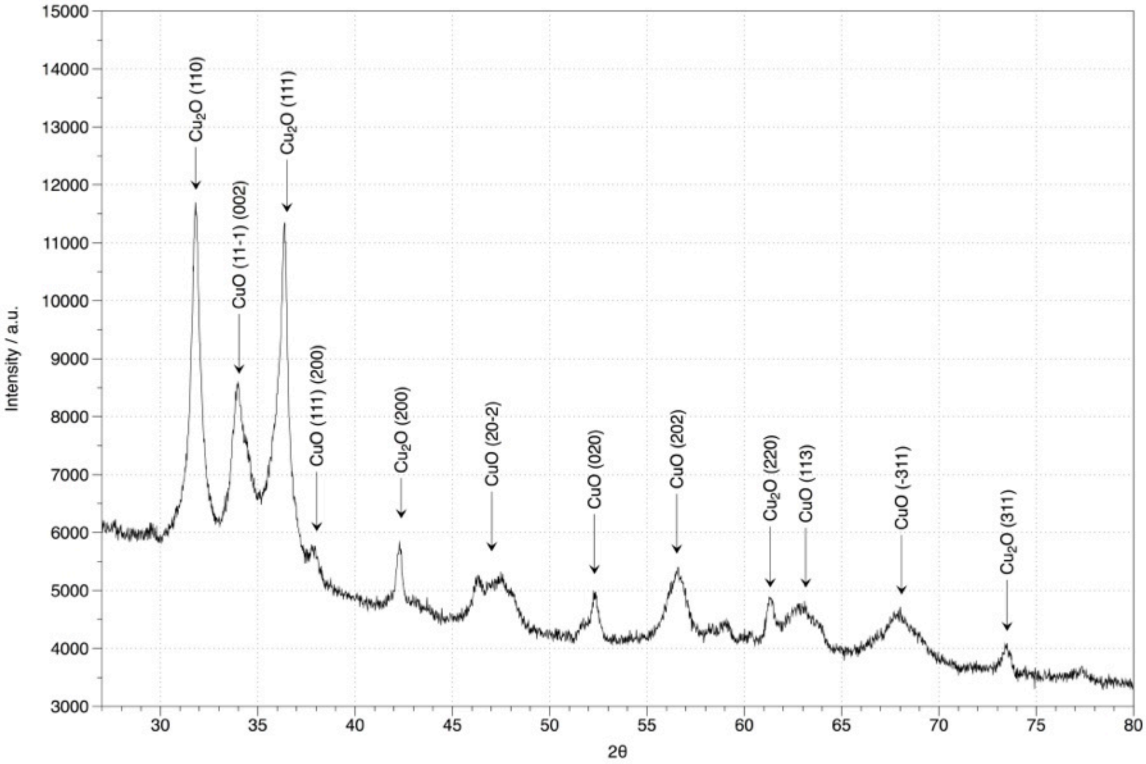

Figure S1e XRPD pattern of catalyst 1 reveals Cu_2O and CuO after 14 days of air exposure

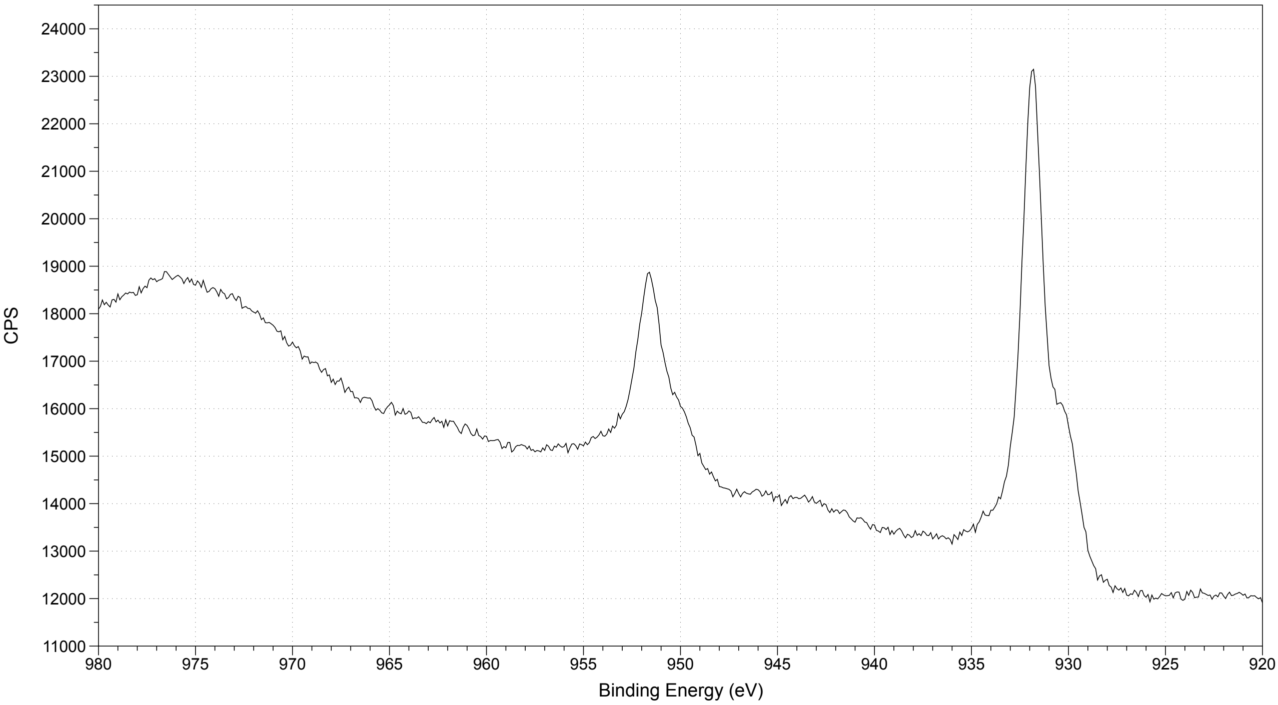

Figure S1f XPS data Cu $2p_{1/2}$ and $2p_{3/2}$ region demonstrates a large signal at 932.5 eV and a minor signal at 930.7 eV corresponding to Cu_2O and Cu respectively

Cu/PVP40 2(reaction pav70)

$CuSO_4$ (159.62 mg, 1.00 mmol) and PVP40 (1.11 g, 10.00 mmol) were dissolved in ethylene glycol (120 ml) under an Ar atmosphere and the mixture was stirred for 2 h at 80°C. After cooling to 0°C the pH was adjusted to *ca*. 10 adding by NaOH (1 M in ethylene glycol, 5 ml). The mixture was stirred for 15 min after which NaH_2PO_2 (175.96 mg, 2.00 mmol) in ethylene glycol (10 ml) was added. The reaction was stirred at 140°C for 90 min to give a crude NP dispersion, an aliquot of which was purified and redispersed as for catalyst 1.

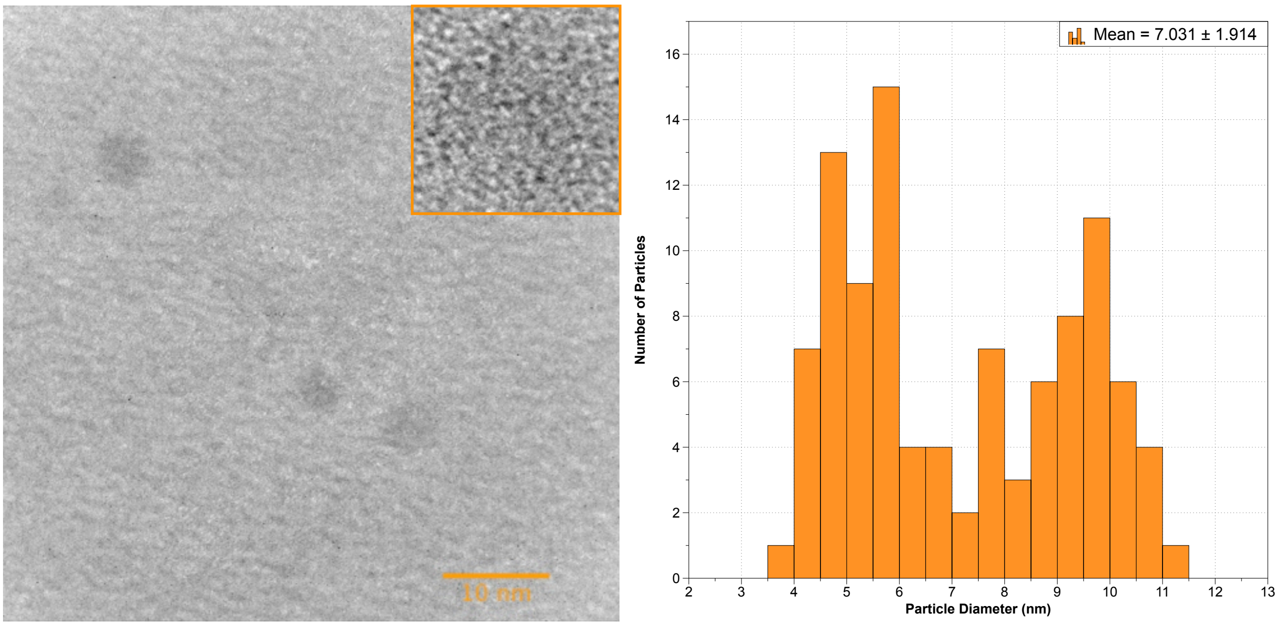

Figure S2a Representative TEM image of catalyst 2 at x300k with a magnified insert *(left)* and particle size distribution *(right)*

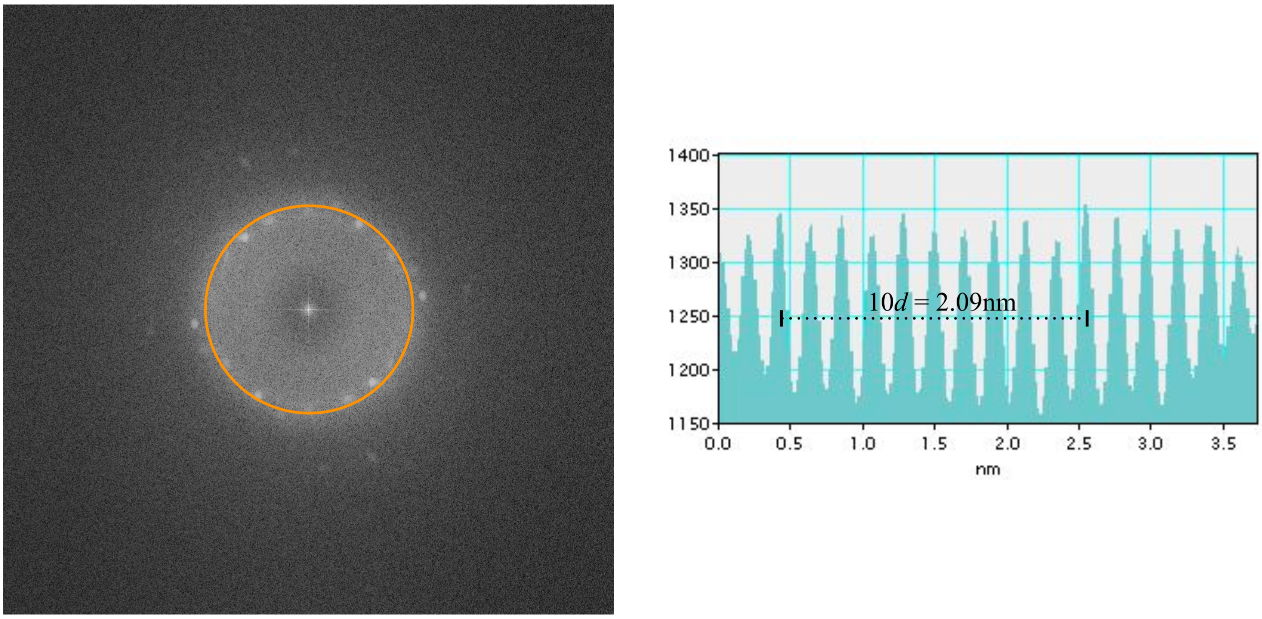

Figure S2b Representative Fourier transform image and fringe space analysis for catalyst 2 demonstrate an average *d* spacing of 2.09 Å corresponding to Cu (111)

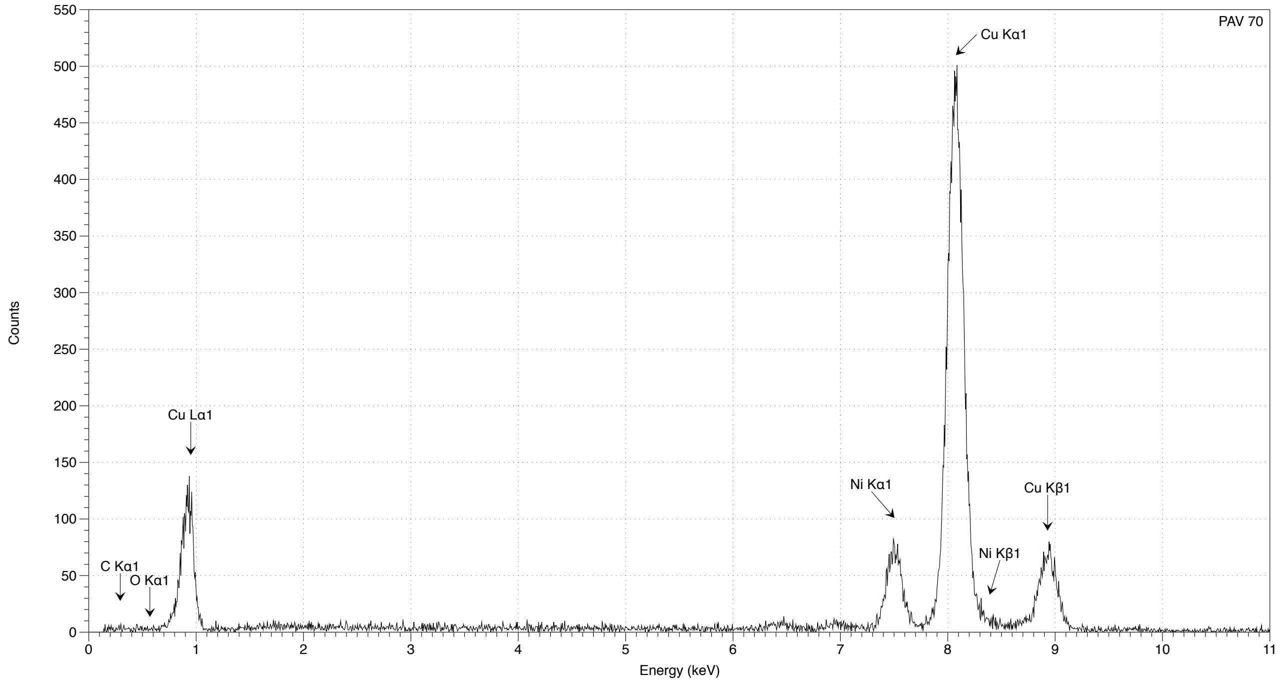

Figure S2c Representative narrow beam ED spectrum

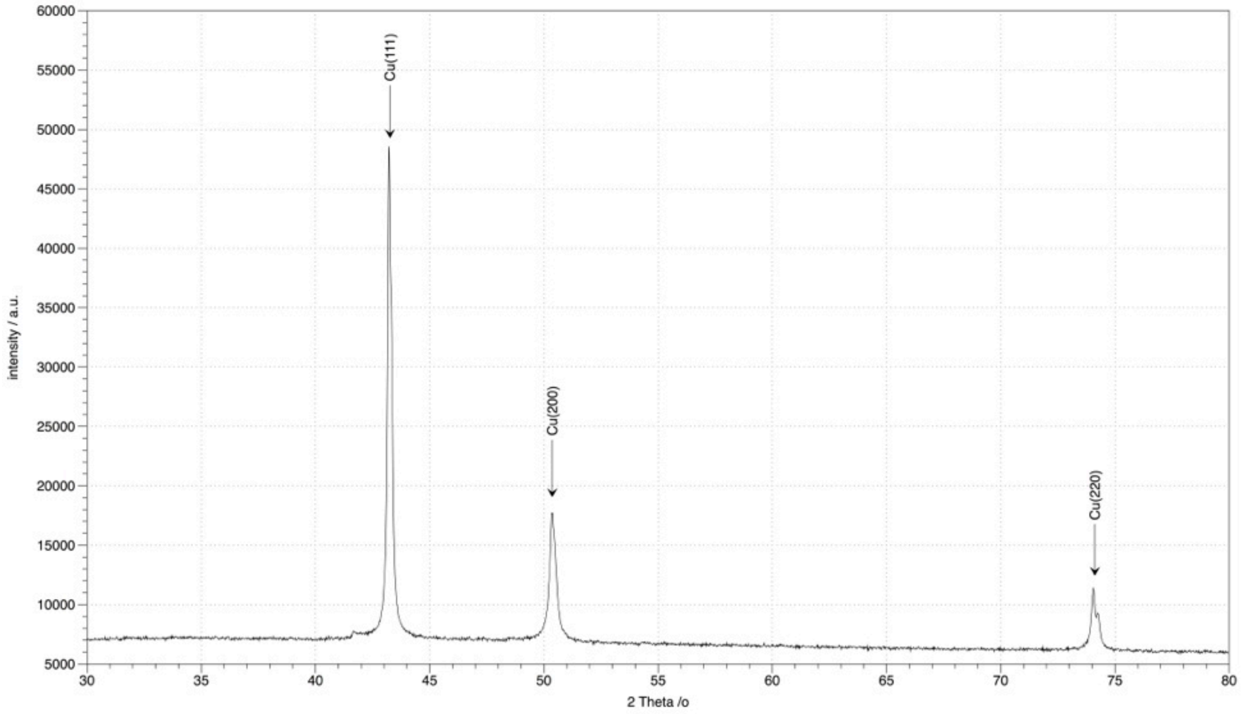

Figure S2d XRPD pattern of fresh catalyst 2 demonstrates the presence of metallic copper only

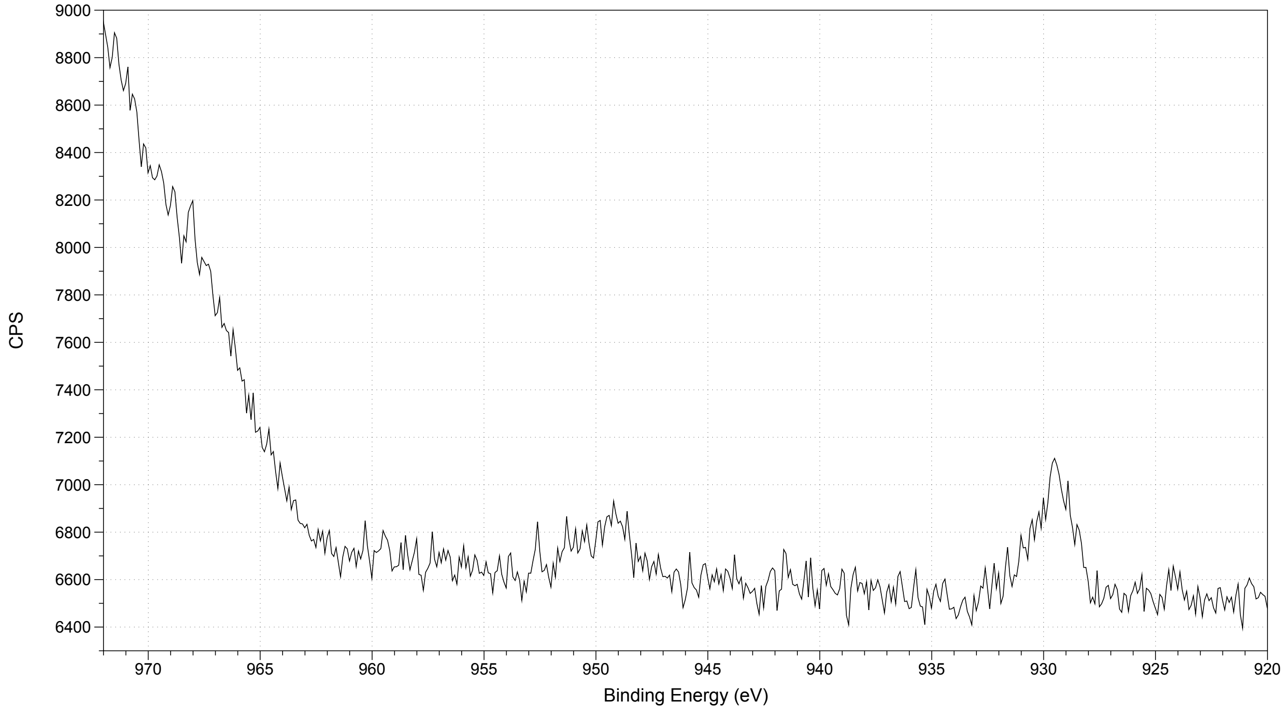

Figure S2e XPS data: Cu $2p_{1/2}$ and $2p_{3/2}$ region showing little evidence of Cu_2O at 932.5 eV

Cu PVP29 3(reaction pav52)

$CuSO_4•5H_2O$ (249.70mg, 1.00 mmol) and PVP29 (average M_w = 29000, 1.11 g, 10.00 mmol) were dissolved in ethylene glycol (120 ml) under Ar and the mixture was stirred for 2 h at 80°C. After cooling to 0°C the pH was adjusted to *ca*. 10 by adding NaOH (1 M in deinolozed water, 5 ml). The mixture was stirred for 15 min after which $NaH_2PO_2•H_2O$ (211.98 mg, 2.00 mmol) in deionized water (2 ml) was added. The reaction was stirred at 140°C for 90 min to give a crude NP dispersion, an aliquot of which was purified and redispersed as for catalyst 1.

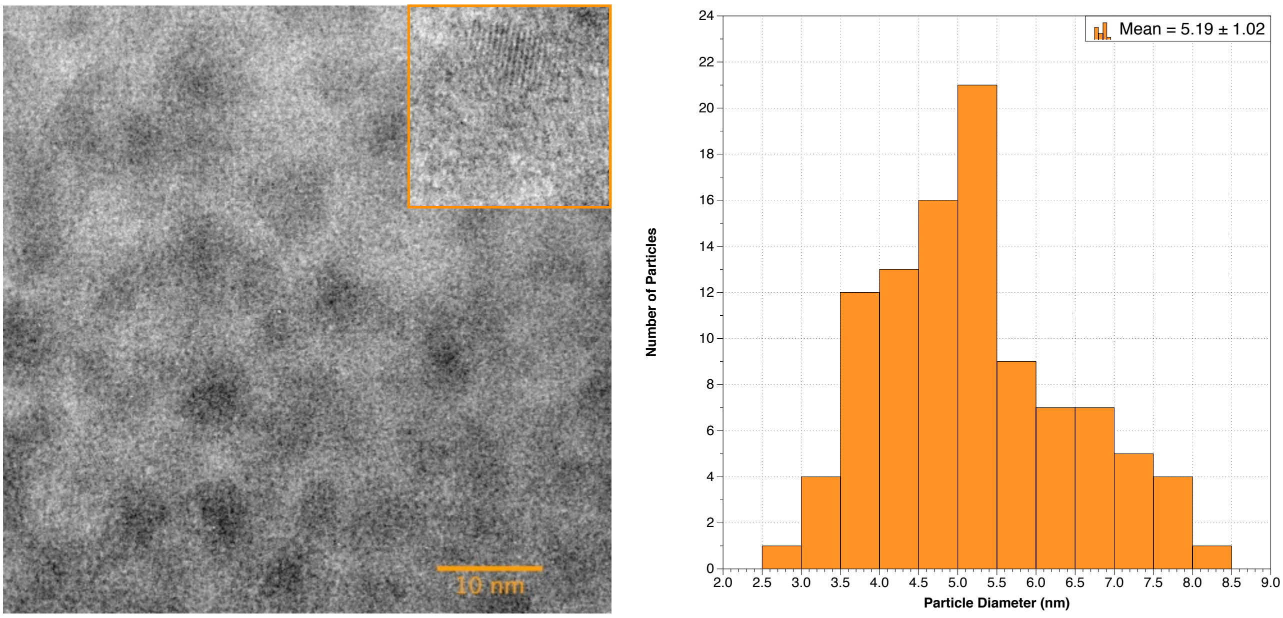

Figure S3a Representative TEM image of catalyst 3 at x300k with a magnified insert *(left)* and particle size distribution *(right)*

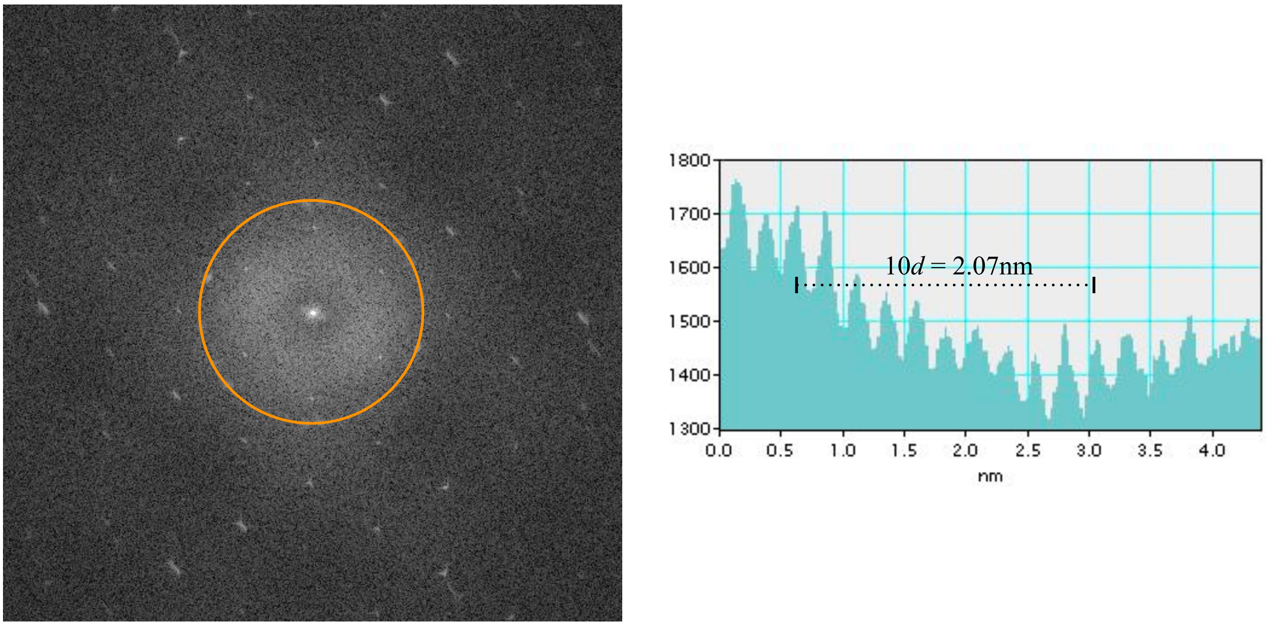

Figure S3b Representative Fourier transform image and fringe space analysis for catalyst 3 demonstrate an average *d* spacing of 2.07 Å corresponding to Cu (111)

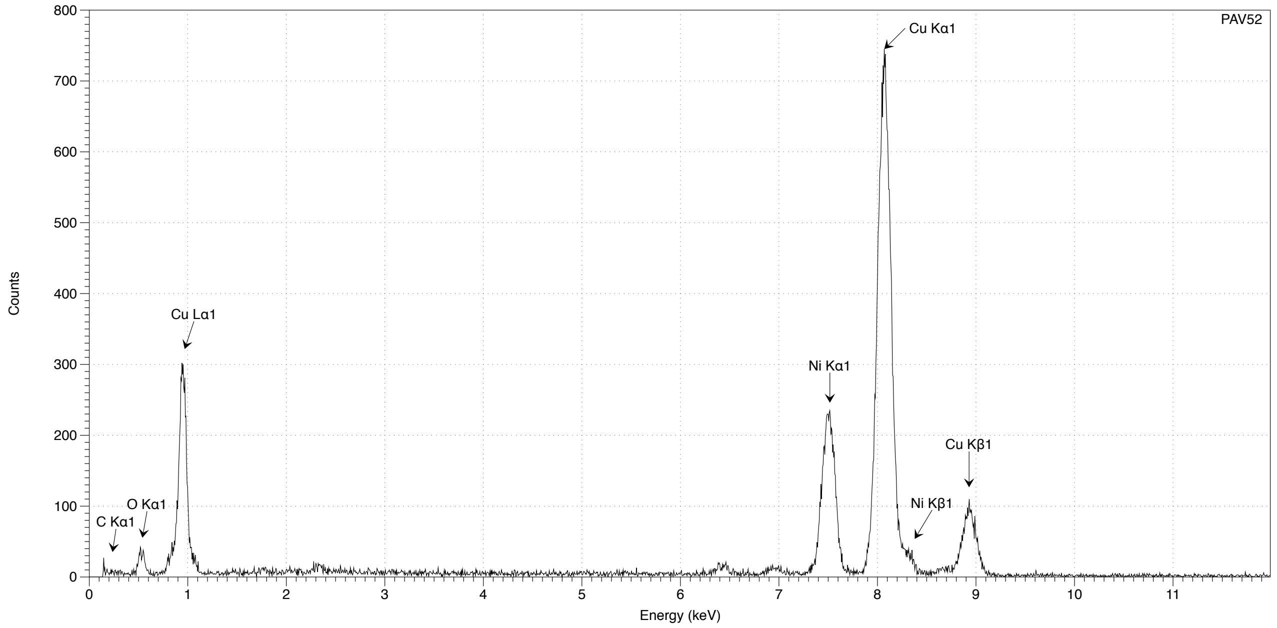

Figure S3c Representative narrow beam ED spectrum

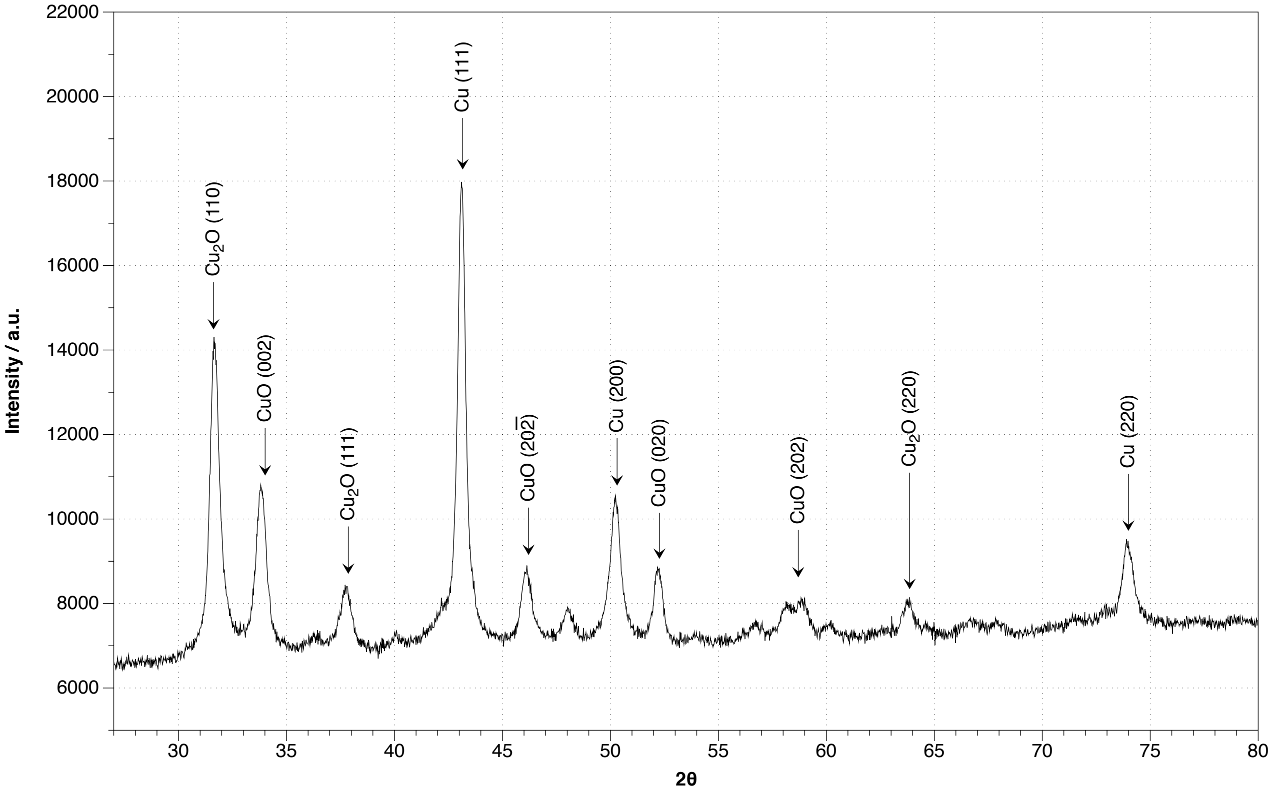

Figure S3d XRPD pattern demonstrates the presence of Cu, Cu_2O and CuO

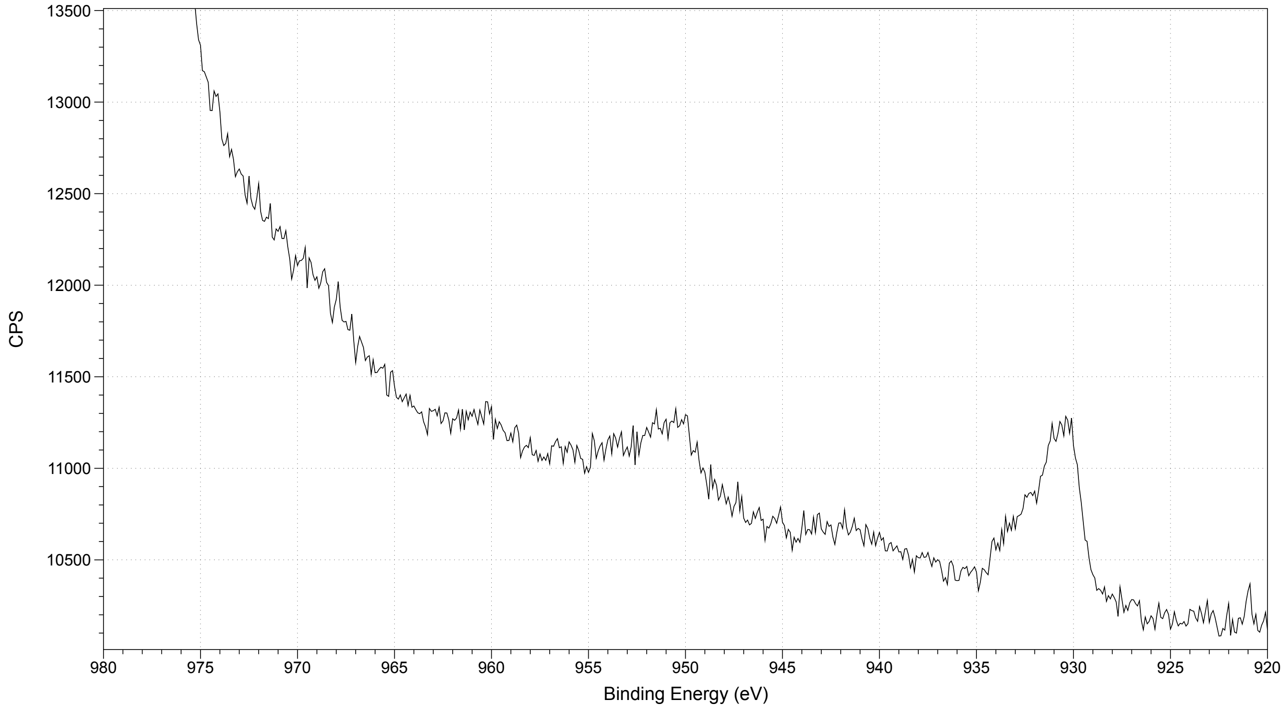

Figure S3e XPS data: Cu $2p_{1/2}$ and $2p_{3/2}$ region demonstrates Cu_2O signal at 932.5 eV and Cu signal 930.5 eV

Cu/PVP29 4(reaction pav60)

$CuSO_4$ (159.62 mg, 1 mmol) and PVP29 (1.11 g, 10.00 mmol) were dissolved in anhydrous ethylene glycol (120 ml) under Ar and the mixture was stirred for 2 h at 80°C. After cooling to 0°C the pH was adjusted to *ca*. 10 by adding NaOH (1 M in ethylene glycol, 5ml). The mixture was stirred for 15 min after which NaH_2PO_2 (175.96 mg, 2 mmol) in ethylene glycol (5 ml) was added. The reaction was heated to 140°C for 90 min to give a crude NP dispersion, an aliquot of which was purified and redispersed as for catalyst 1.

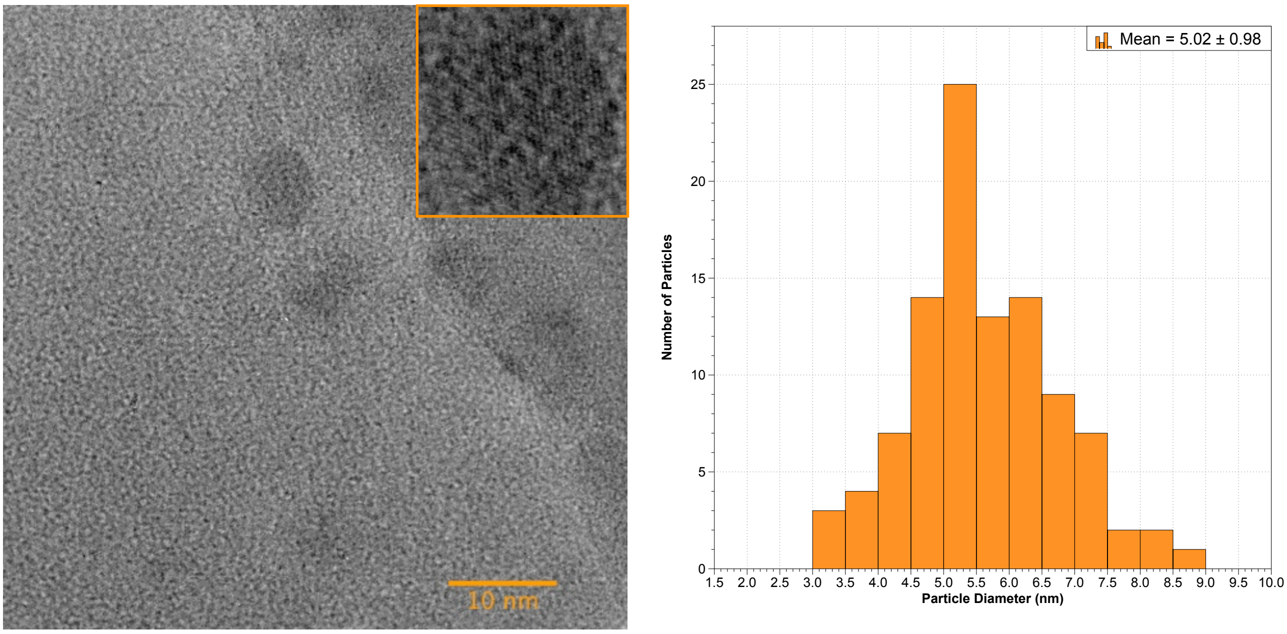

Figure S4a Representative TEM image of catalyst 4 at x300k with a magnified insert *(left)* and particle size distribution *(right)*

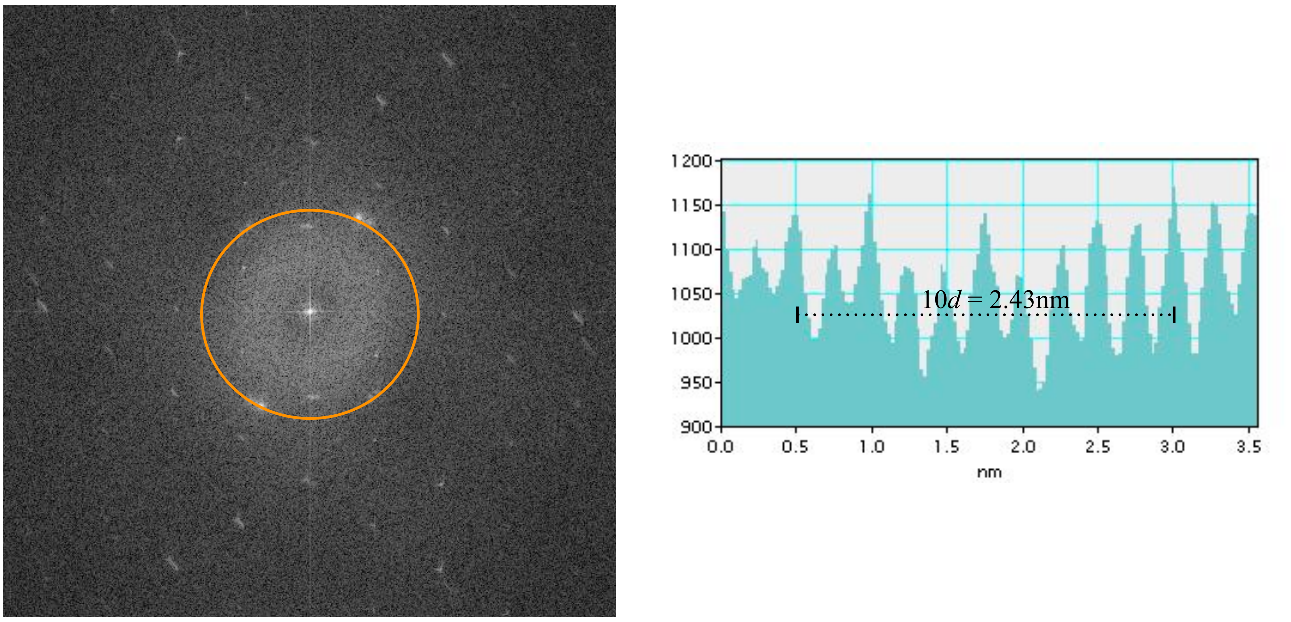

Figure 4b Representative Fourier transform image and fringe space analysis for catalyst 4 demonstrate an average d spacing of 2.43 Å corresponding to Cu_2O (111)

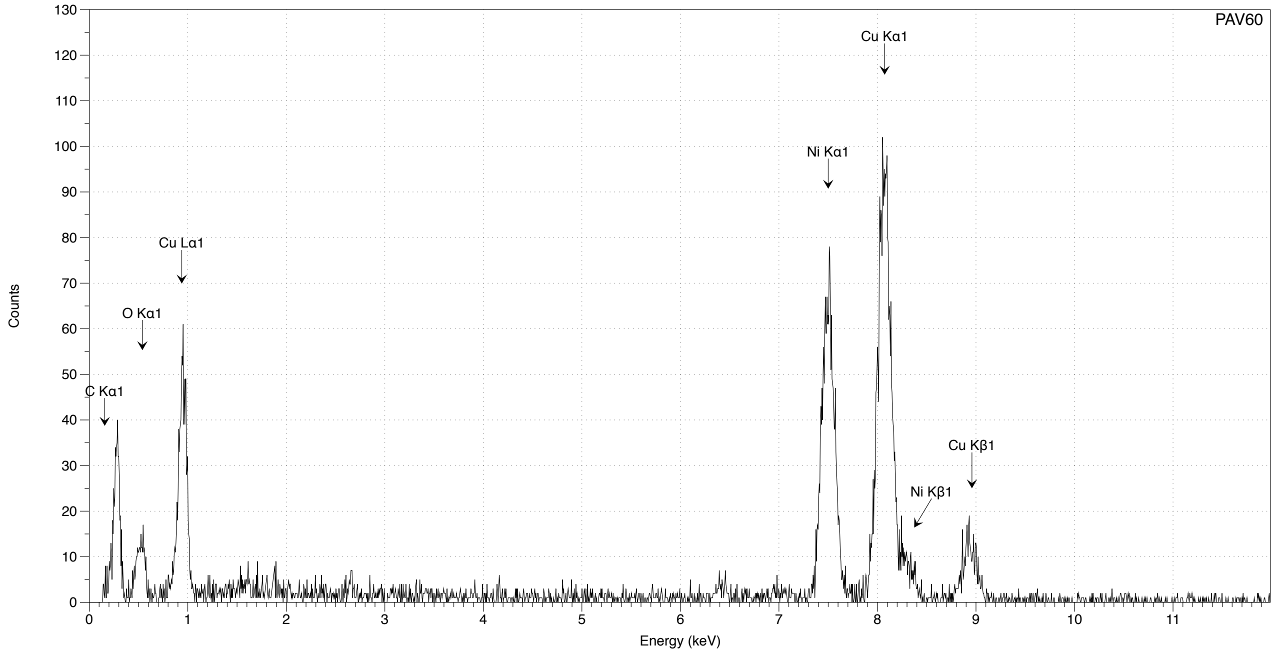

Figure S4c Representative narrow beam ED spectrum

Cu/PVP29 5(reaction pav97)

$CuSO_4$ (79.81 mg, 0.50 mmol) and PVP29 (333 mg, 3.00 mmol) were dissolved in EtOH (40 ml) under Ar and the mixture was stirred for 2 h at 40°C. The mixture was heated to reflux after which $NaBH_4$ (37.83 mg, 1.00 mmol) in EtOH (10 ml) was added. The reaction was allowed to run to completion over additional 90 min to give a crude NP dispersion, an aliquot of which was purified by extraction using excess acetone (1:10) over not more than 240 min. After sedimentation of the particles, the supernatant was decanted and the remaining suspension centrifuged, washed with 3x10ml portions of 50:50 hexane/ethanol mixture and 1x 5 ml portion of ethanol. Upon removal of the solvent layer, the precipitate was resuspended in either ethanol or methanol.

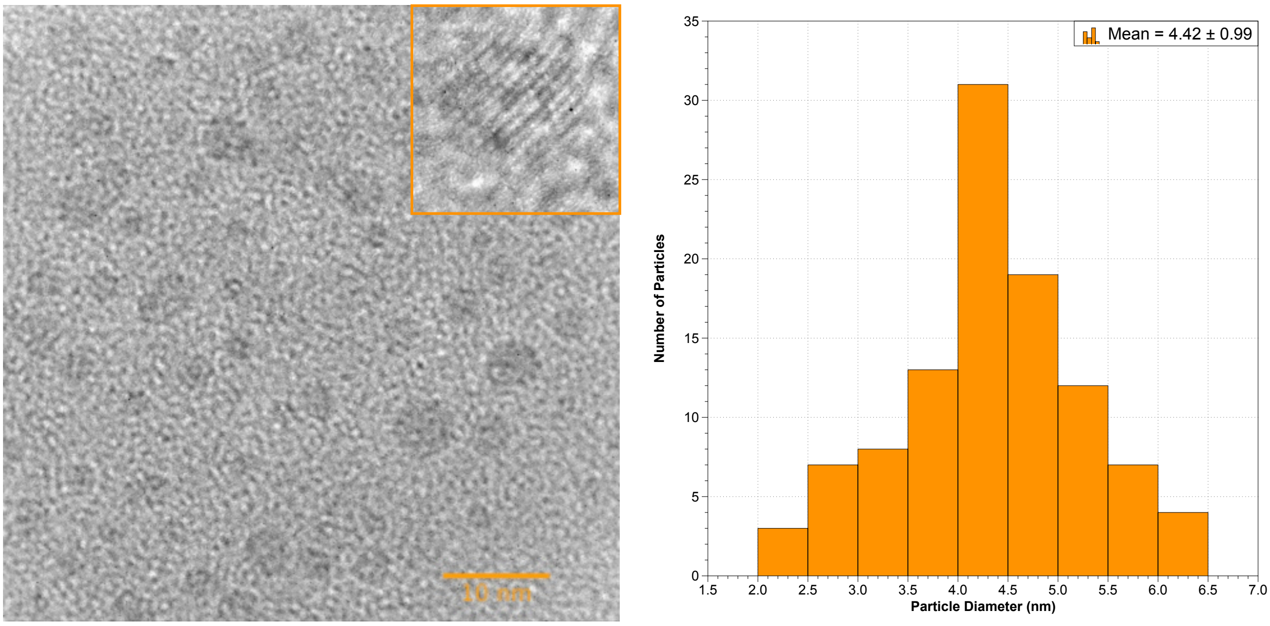

Figure S5a Representative TEM image of catalyst 5 at x300k with a magnified insert *(left)* and particle size distribution *(right)*

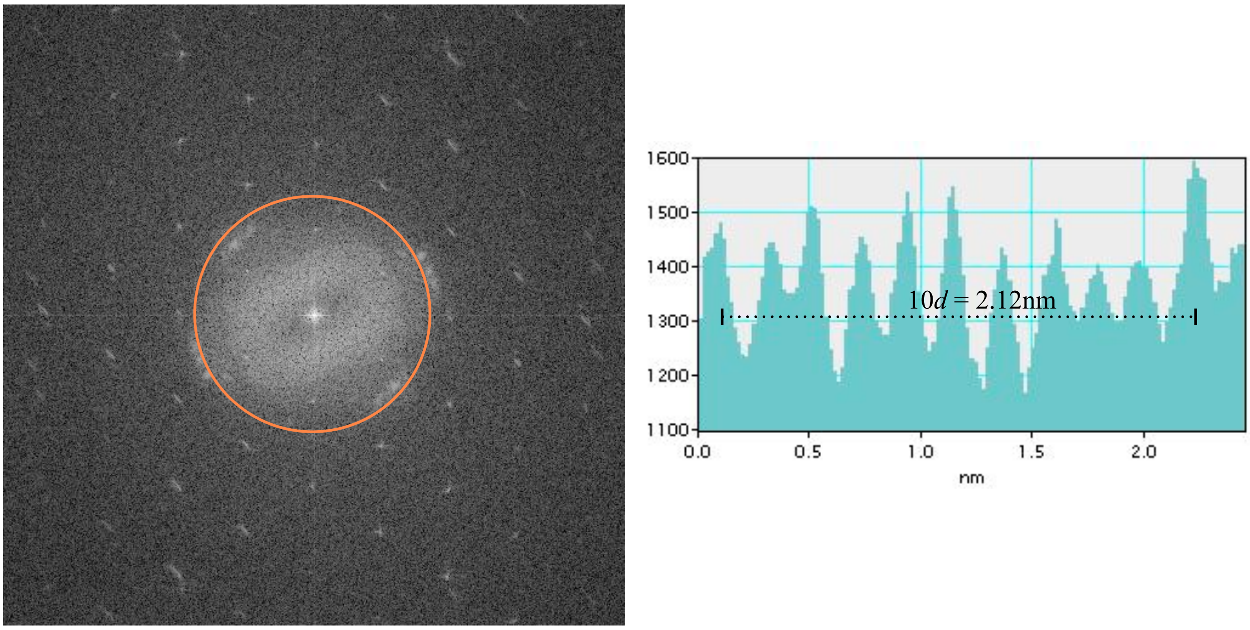

Figure S5b Representative Fourier transform image and fringe space analysis for catalyst 5 demonstrate an average *d* spacing of 2.12 Å corresponding to Cu (111)

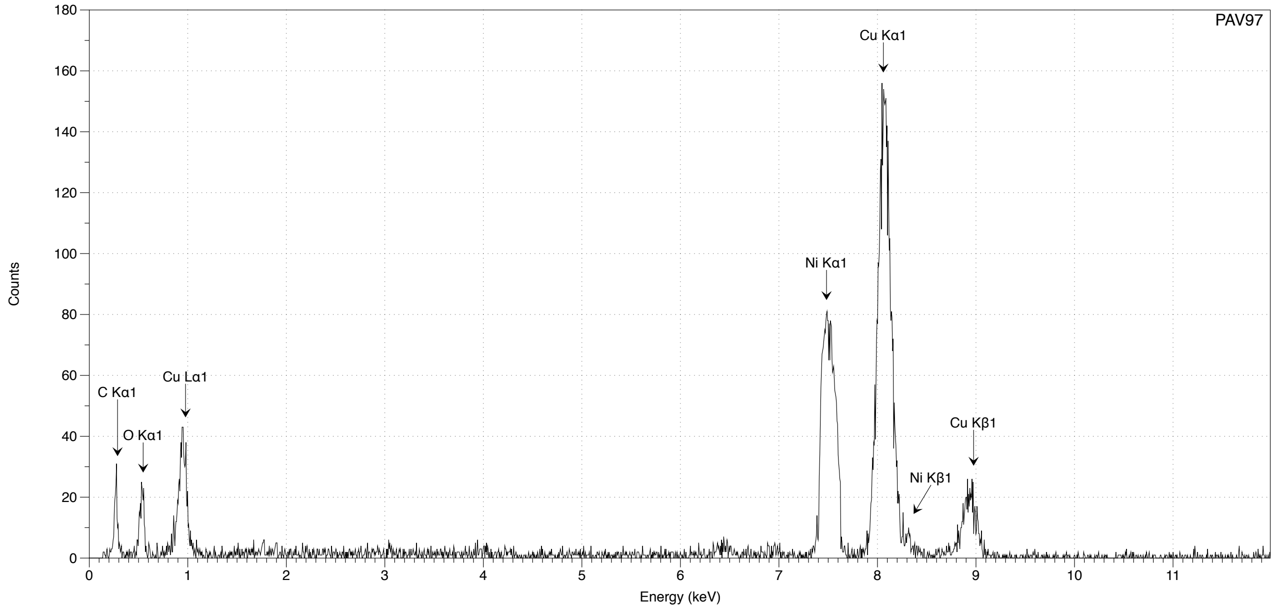

Figure S5c Representative narrow beam ED spectrum

Cu/PVP29 6(reaction pav105)

$CuSO_4$ (79.81 mg, 0.5 mmol) and PVP29 (333 mg, 3.00 mmol) were dissolved in EtOH (40 ml) under Ar and the mixture was stirred for 2 h at 40°C. The mixture was cooled to 25°C and $NaBH_4$ (37.83 mg, 1.00 mmol) in 10 ml ethanol was added. The reaction was allowed to run to completion over 90 min to give a crude NP dispersion, an aliquot of which was purified and redispersed as for catalyst 5.

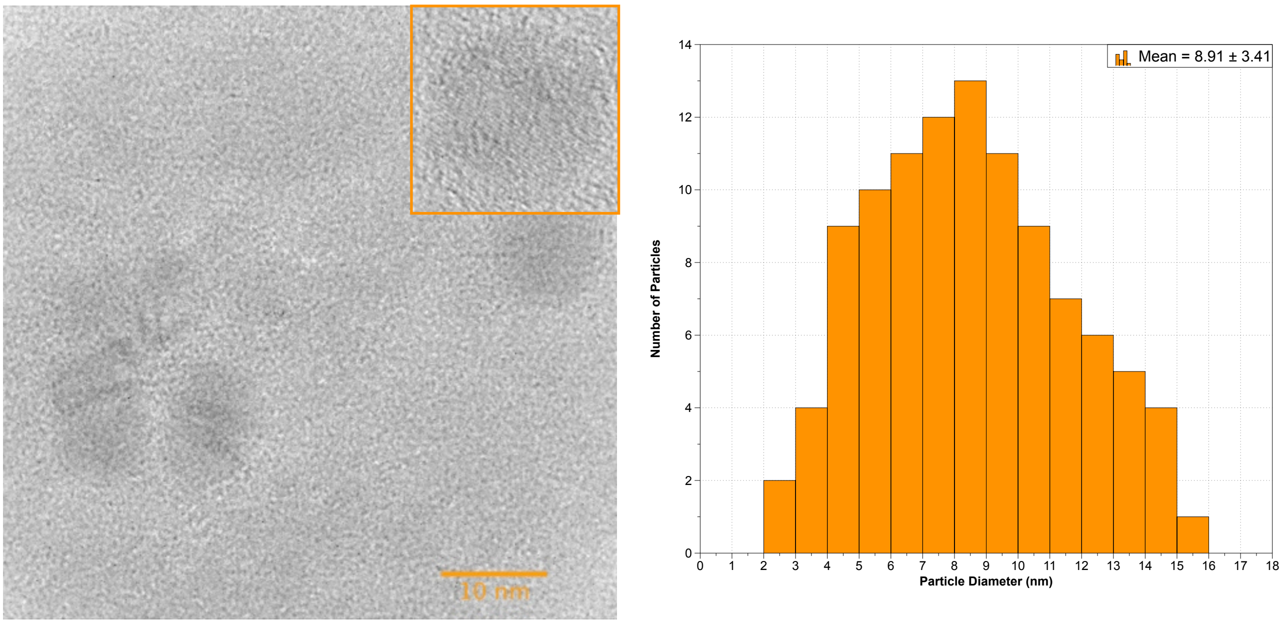

Figure S6a Representative TEM image of catalyst 6 at x300k with a magnified insert *(left)* and particle size distribution *(right)*

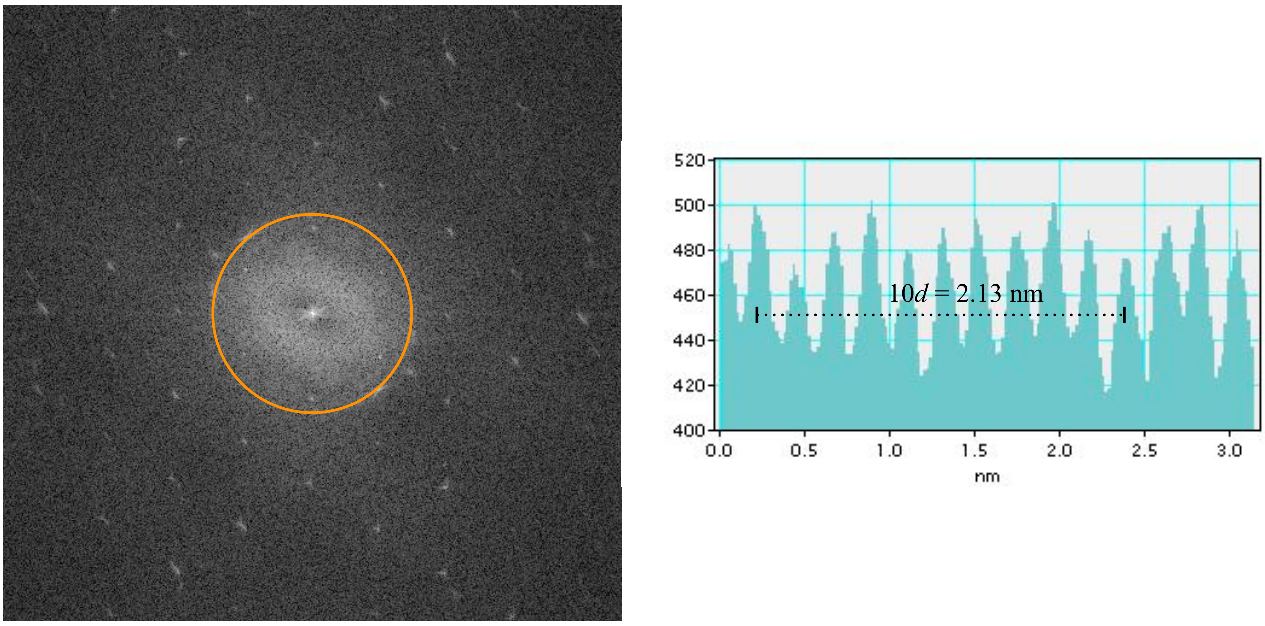

Figure 6b Representative Fourier transform image and fringe space analysis for catalyst 6 demonstrate an average *d* spacing of 2.13 Å corresponding to Cu (111)

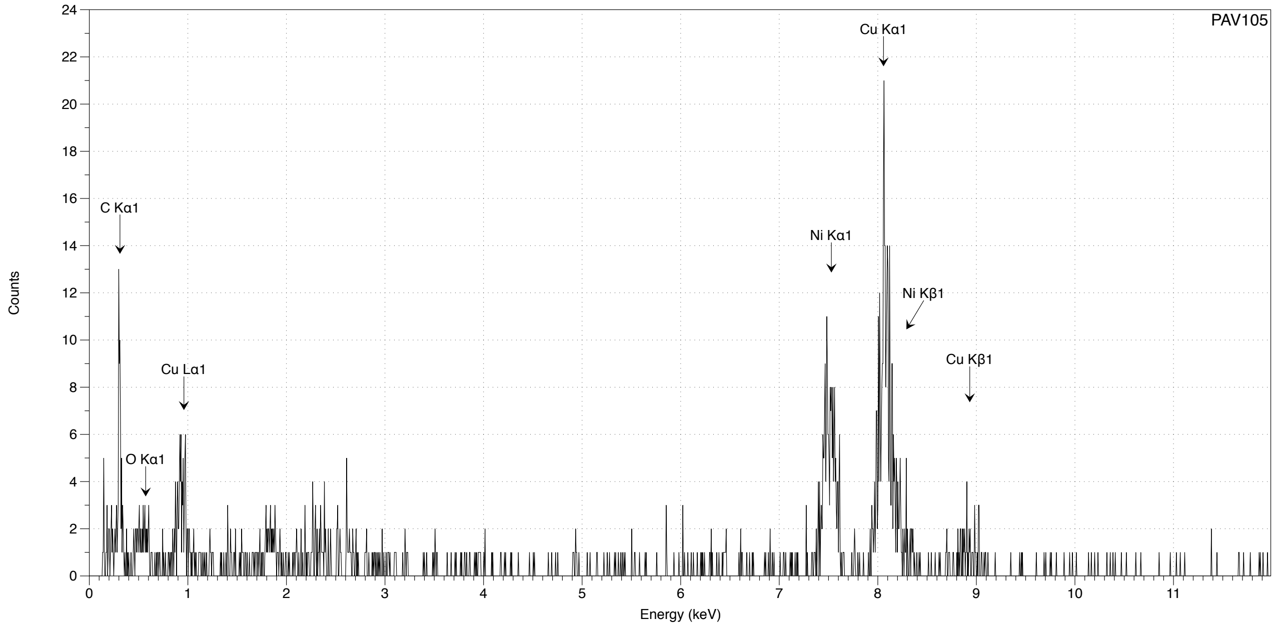

Figure S6c Representative narrow beam ED spectrum

Cu/PVP29 7(reaction pav200)

$Cu(OAc)_2$ (90.81 mg, 0.50 mmol) and PVP29 (333 mg, 3.00 mmol) were dissolved in EtOH (40 ml) under Ar and the mixture was stirred for 2 h at 40°C. The mixture was cooled to 25°C after which $NaBH_4$ (37.83 mg, 1.00 mmol) in EtOH (10 ml) was added. The reaction was allowed to run to completion over 90 min to give a crude NP dispersion, an aliquot of which was purified and redispersed as for catalyst 5.

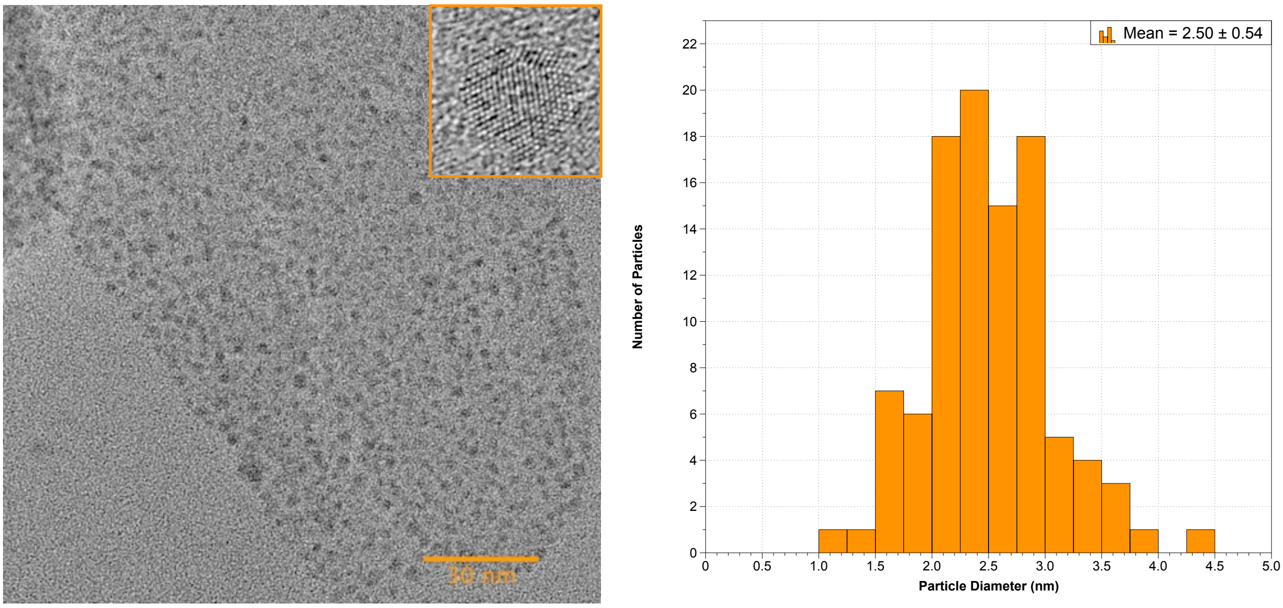

Figure S7a Representative TEM image of catalyst 7 at x145k with a magnified insert *(left)* and particle size distribution *(right)*

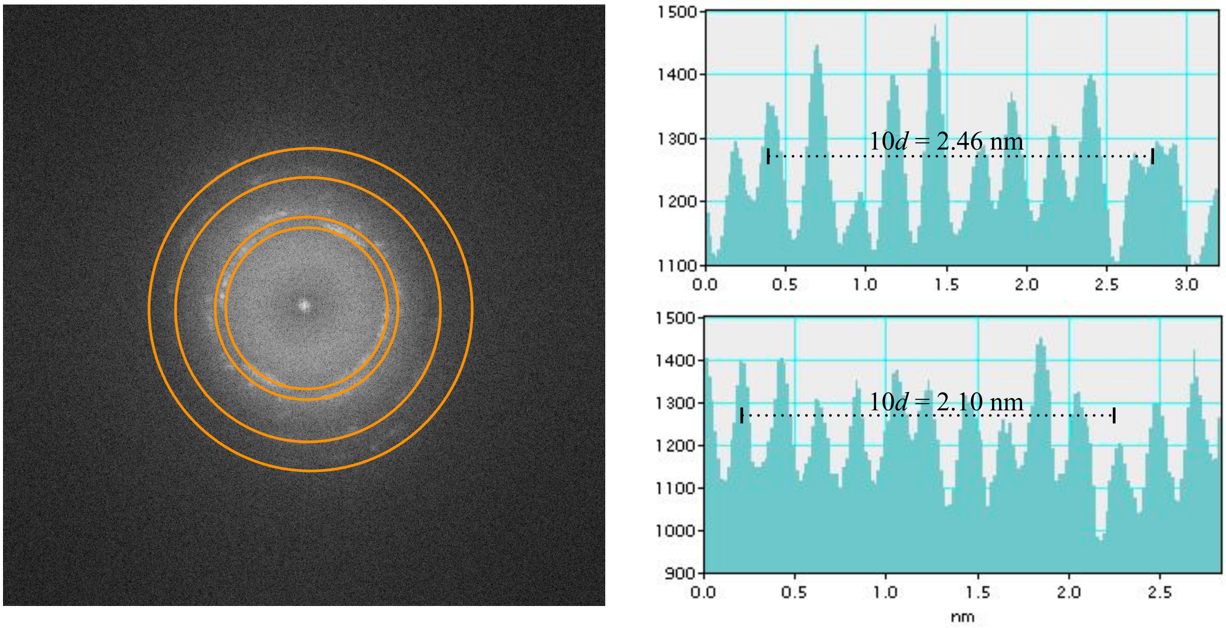

Figure S7b Representative Fourier transform image and fringe space analysis for catalyst 7 demonstrates average *d* spacings of 2.46 Å (*top right*), 2.10 Å (*bottom right*), 1.47 Å, 1.29 Å corresponding to Cu_2O (111), Cu (111), Cu_2O (220) and Cu (220) respectively

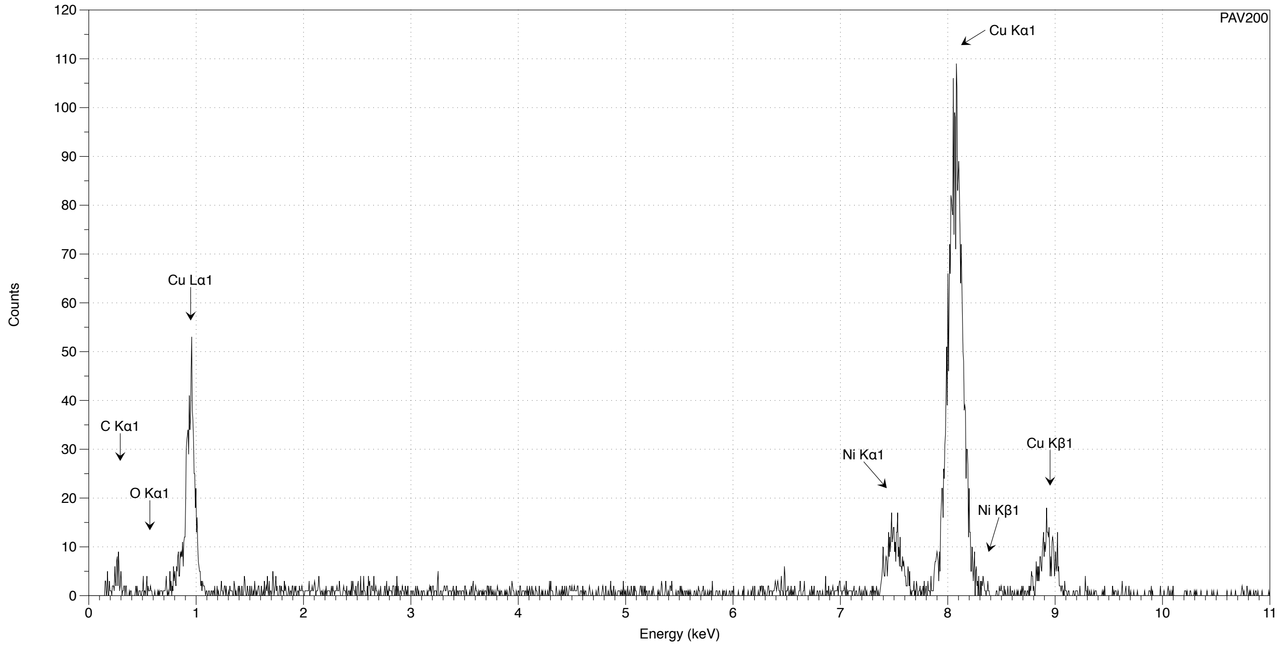

Figure S7c Representative narrow beam ED spectrum

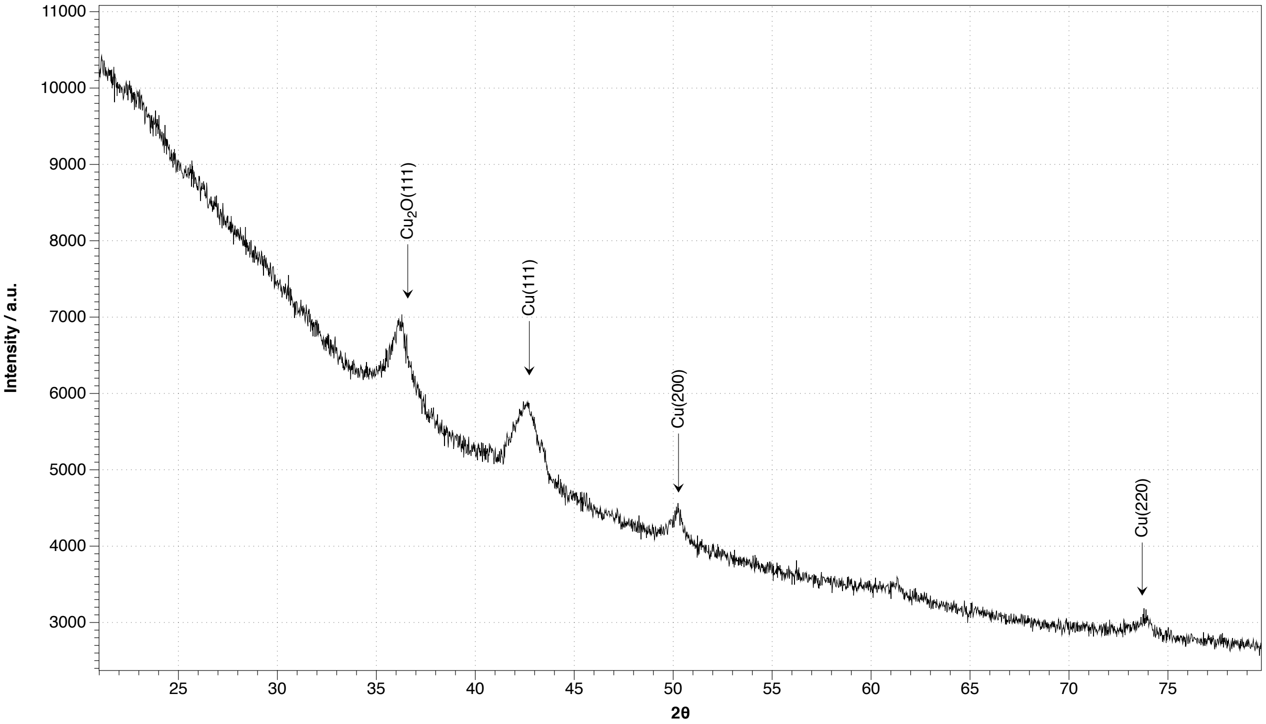

Figure S7d XRPD pattern of fresh catalyst 7 demonstrates the presence of Cu and Cu_2O

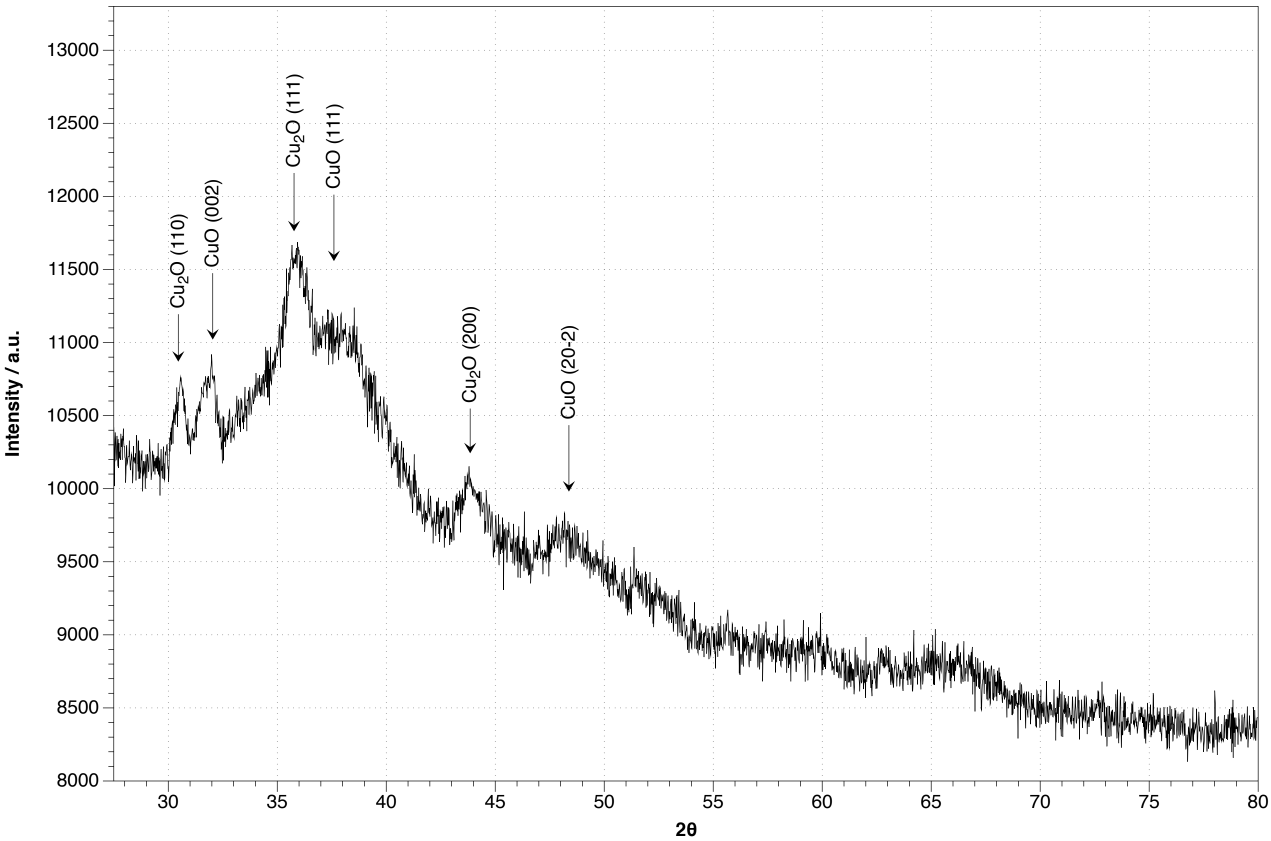

Figure S7e XRPD pattern after 14 days of air exposure demonstrates the presence of Cu_2O and CuO

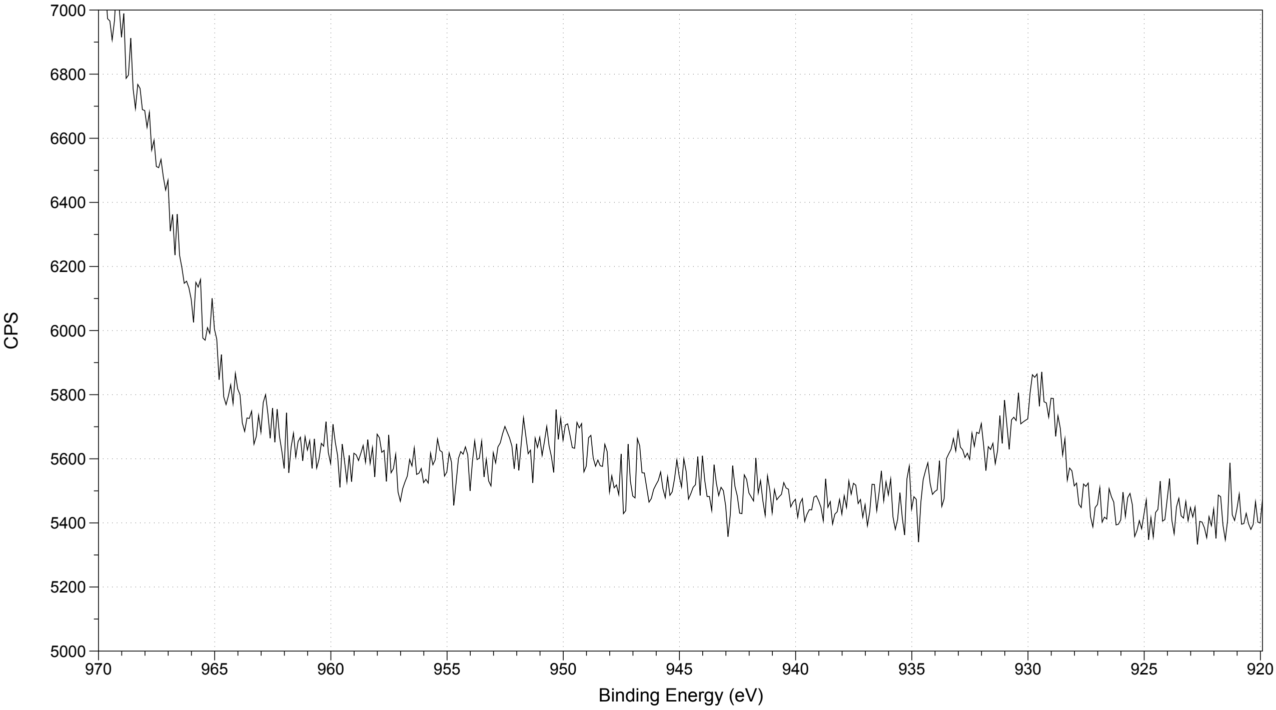

Figure S7e XPS data: Cu $2p_{1/2}$ and $2p_{3/2}$ region demonstrates Cu_2O signal at 932.5 eV and Cu signal at 929.5 eV

Cu/PVP29 8(reaction pav95)

$Cu(OAc)_2$ (90.81 mg, 0.50 mmol) and PVP29 (333 mg, 3.00 mmol) were dissolved in EtOH (40 ml) under Ar and the mixture was stirred for 2 h at 40°C. The mixture was then heated to reflux after which $NaBH_4$ (37.83 mg, 1.00 mmol) in EtOH (10 ml) was added. The reaction was allowed to run to completion over the period of additional 90 min to give a crude NP dispersion, an aliquot of which was purified and redispersed as for catalyst 5.

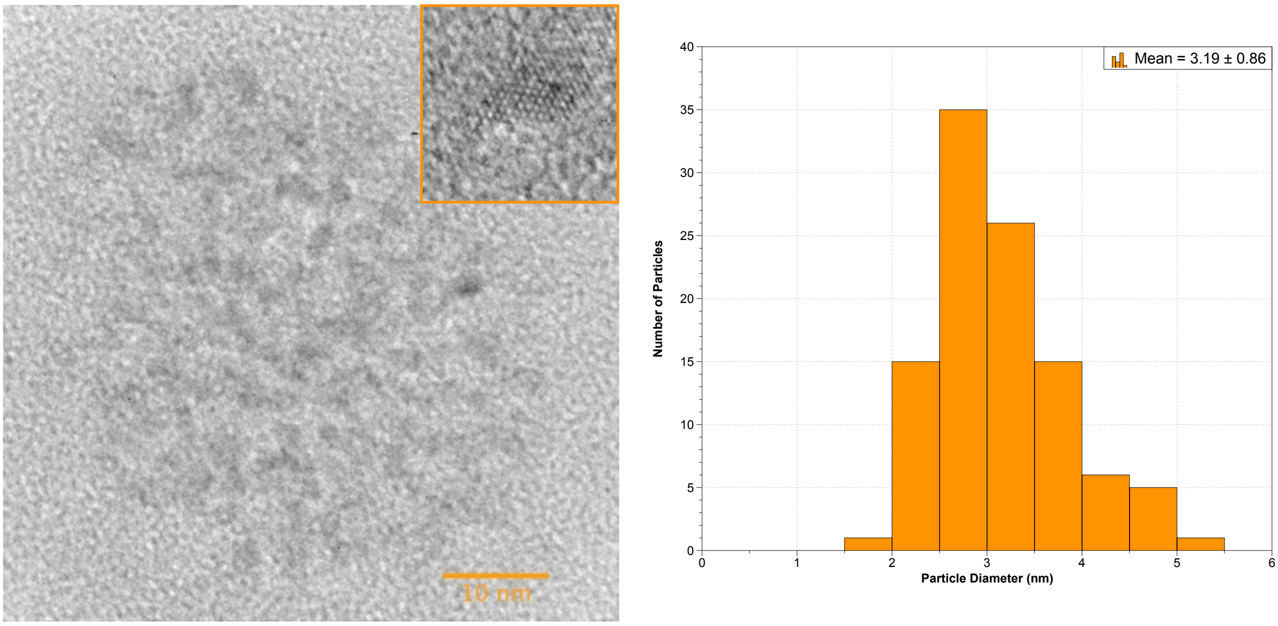

Figure S8a Representative TEM image of catalyst 8 at x300k with a magnified insert *(left)* and particle size distribution *(right)*

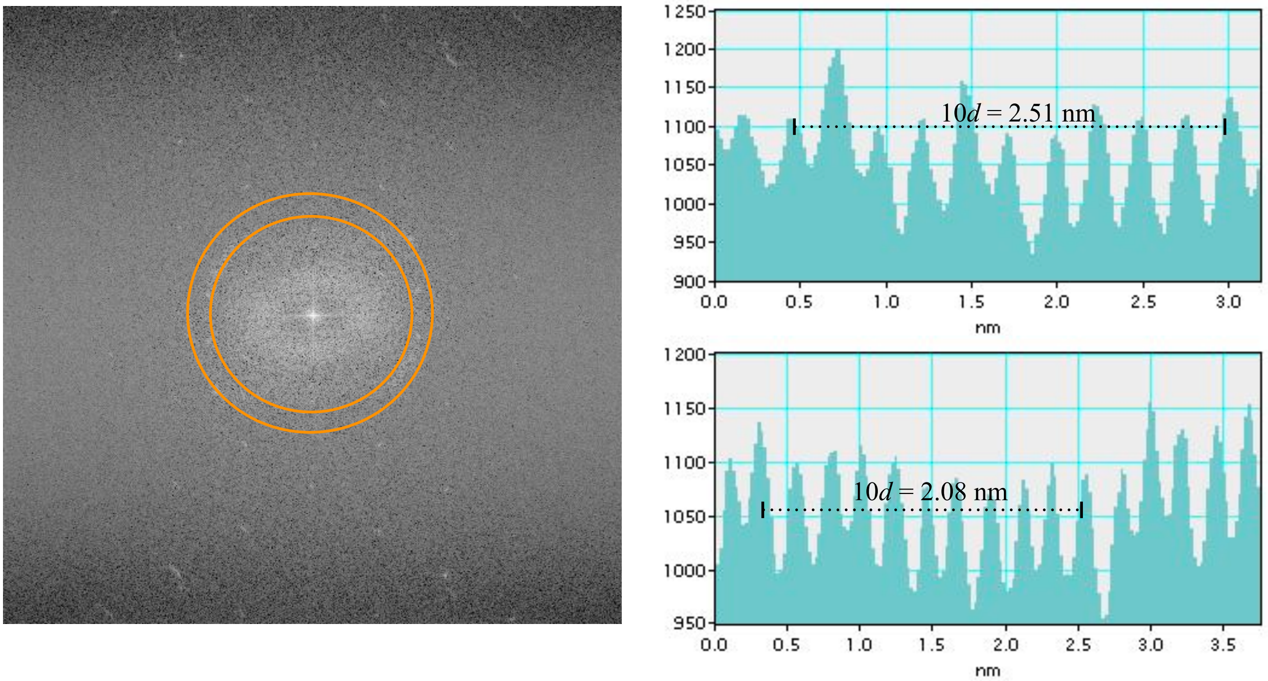

Figure S8b Representative Fourier transform image and fringe space analysis for catalyst 8 demonstrate average *d* spacings of 2.51 Å (*top right*), 2.08 Å (*bottom right)* corresponding to Cu_2O (111), Cu (111) respectively

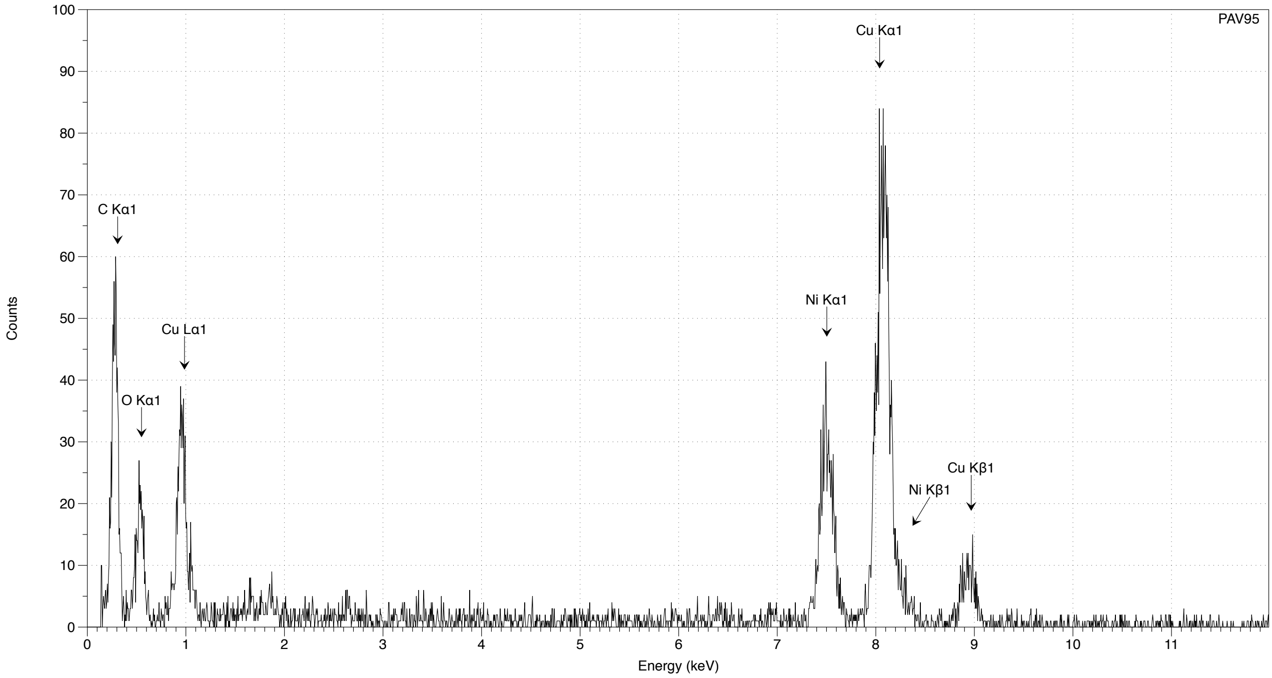

Figure S8c Representative narrow beam ED spectrum

Cu/PVP29 9(reaction pav210)

$Cu(OAc)_2$ (90.81 mg, 0.50 mmol) and PVP29 (333 mg, 3.00 mmol) were dissolved in EtOH (40 ml) under Ar and the mixture was stirred for 2 h at 40°C. The reaction temperature was maintained at 40°C and a stock solution of N_2H_4 (1M in THF, 1.00 ml, 1.00 mmol) was added. The reaction was allowed to run to completion over 120 min to give a crude NP dispersion, an aliquot of which was purified and redispersed as for catalyst 5.

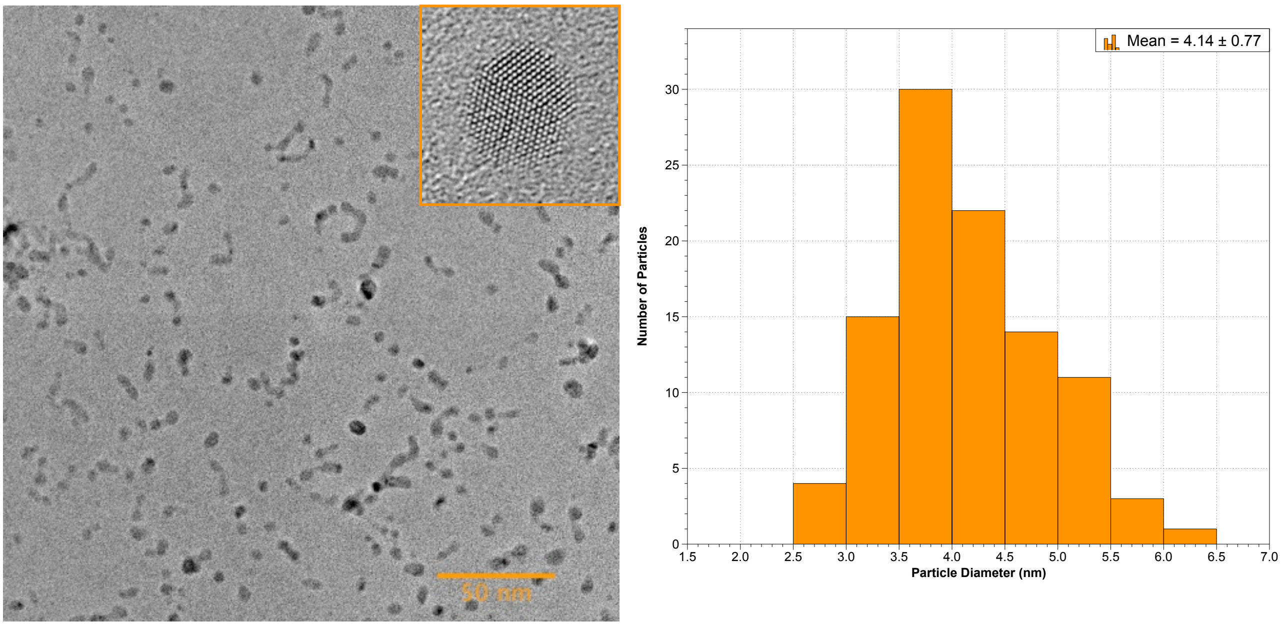

Figure S9a Representative TEM image of catalyst 9 at x145k with a magnified insert *(left)* and particle size distribution *(right)*

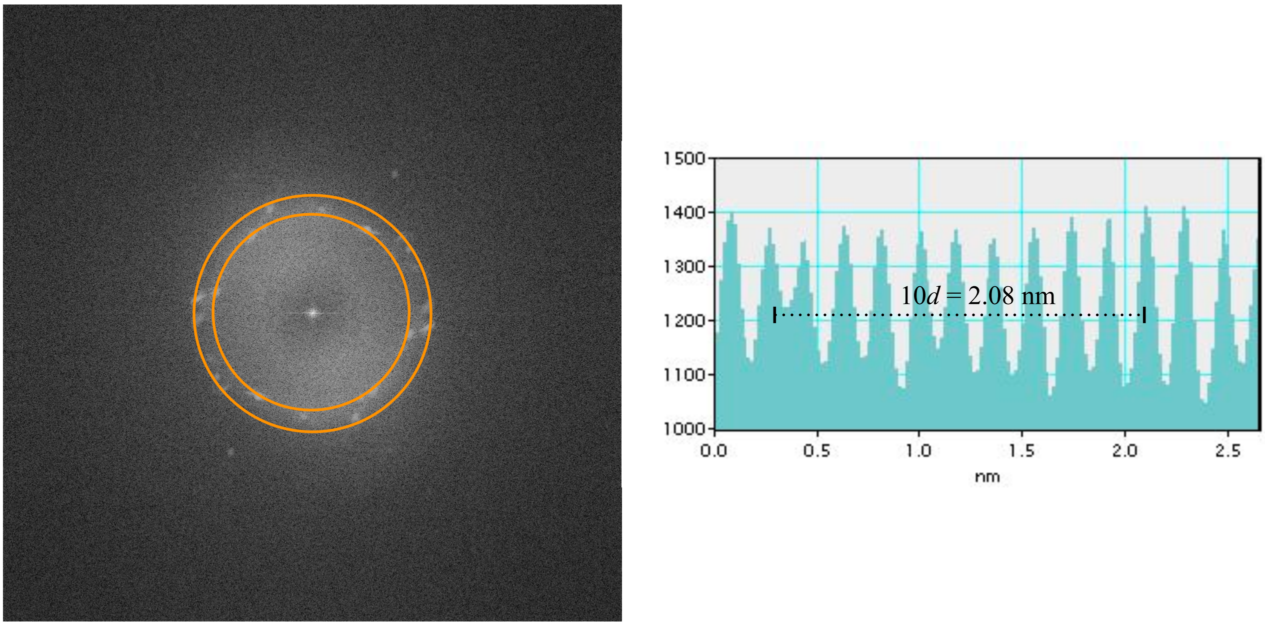

Figure S9b Representative Fourier transform image and fringe space analysis for catalyst 9 demonstrate average *d* spacings of 2.08 Å, 1.86 Å corresponding to Cu (111), Cu (200) respectively

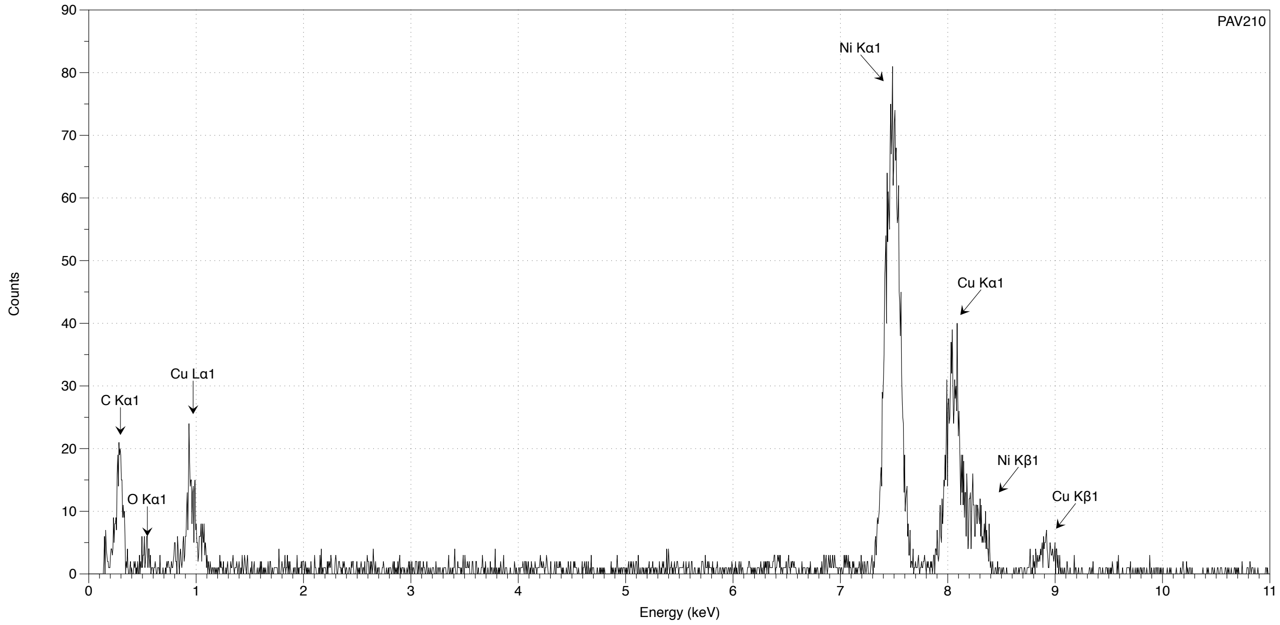

Figure S9c Representative narrow beam ED spectrum

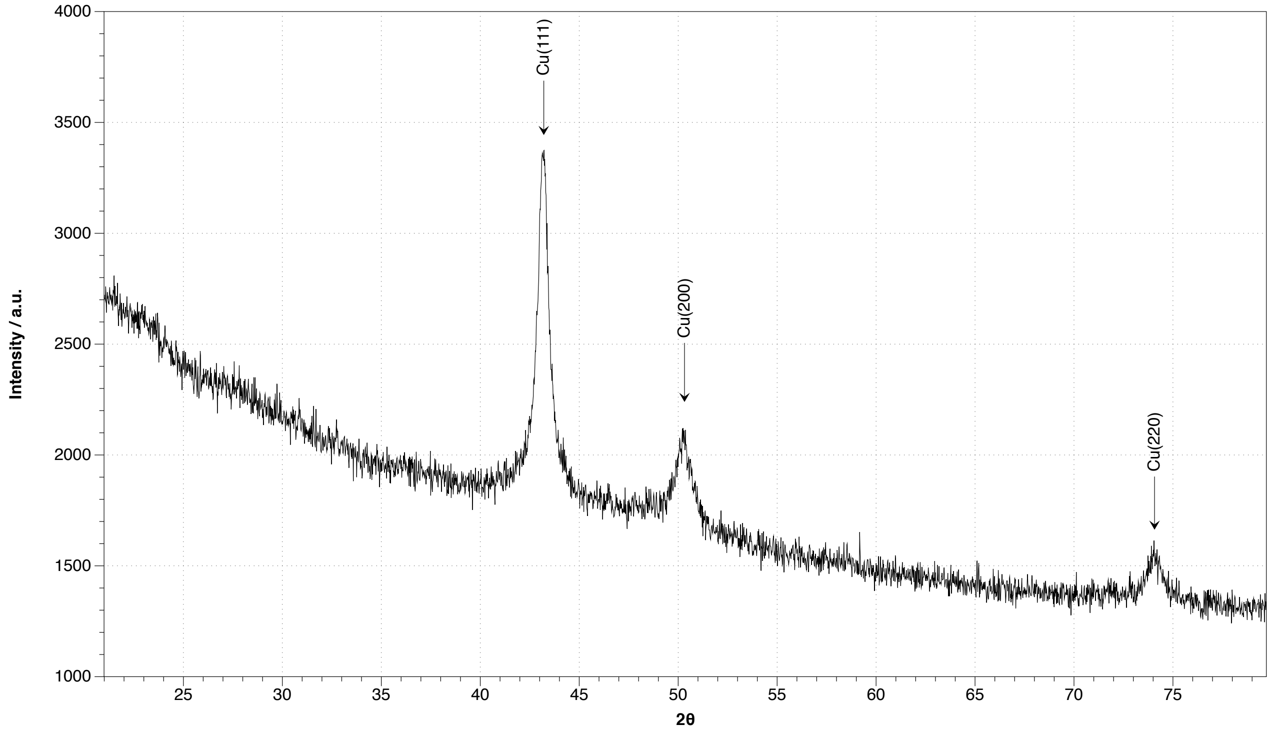

Figure S9d XRPD pattern of fresh catalyst 9 demonstrates the presence of Cu only

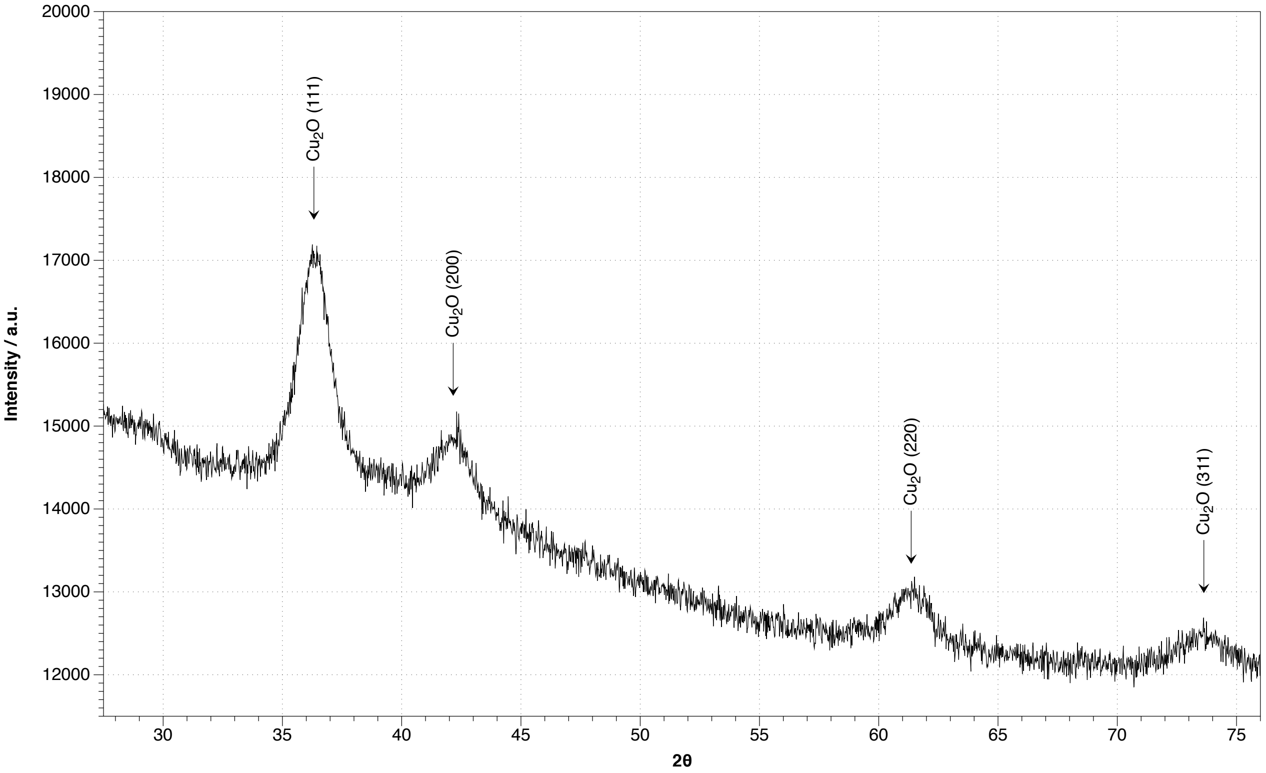

Figure S9e XRPD pattern of catalyst 9 demonstrates the presence of Cu_2O after 14 days of air exposure

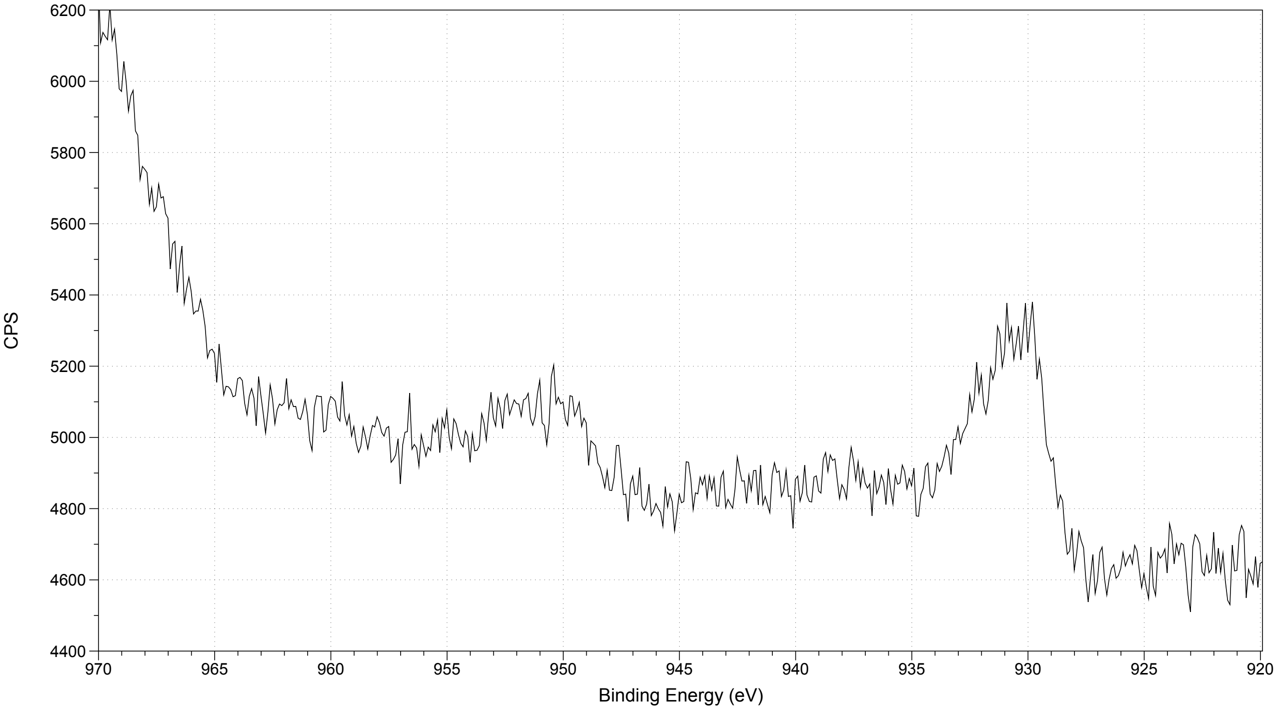

S9f XPS data: Cu $2p_{1/2}$ and $2p_{3/2}$ region shows evidence of both Cu_2O signal at 932.5 eV and Cu signal at 930 eV

Cu/PVP29 10(reaction pav96)

$CuCl_2$ (67.23 mg, 0.50 mmol) and PVP29 (333 mg, 3.00 mmol) were dissolved in EtOH (40 ml) under Ar and the mixture was stirred for 2 h at 40°C. The mixture was heated to reflux after which $NaBH_4$ (37.83 mg, 1.00 mmol) in EtOH (10 ml) was added. The reaction was allowed to run to completion over additional 90 min to give a crude NP dispersion, an aliquot of which was purified and redispersed as for catalyst 5.

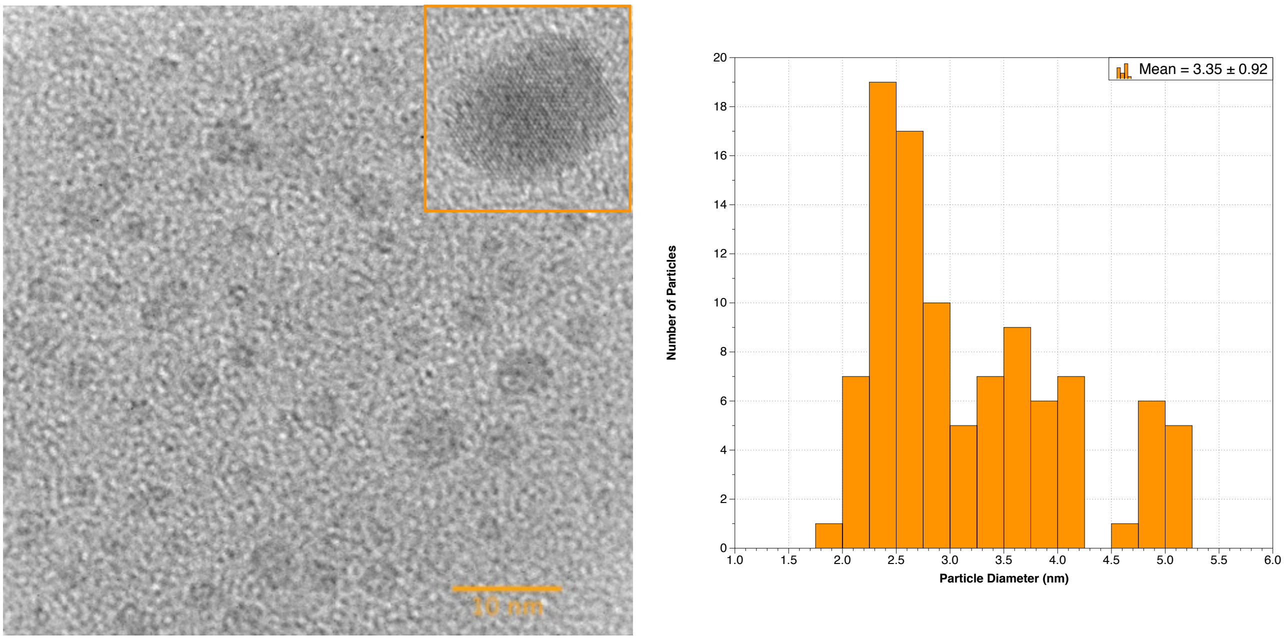

Figure S10a Representative TEM image of catalyst 10 at x300k with a magnified insert *(left)* and particle size distribution *(right)*

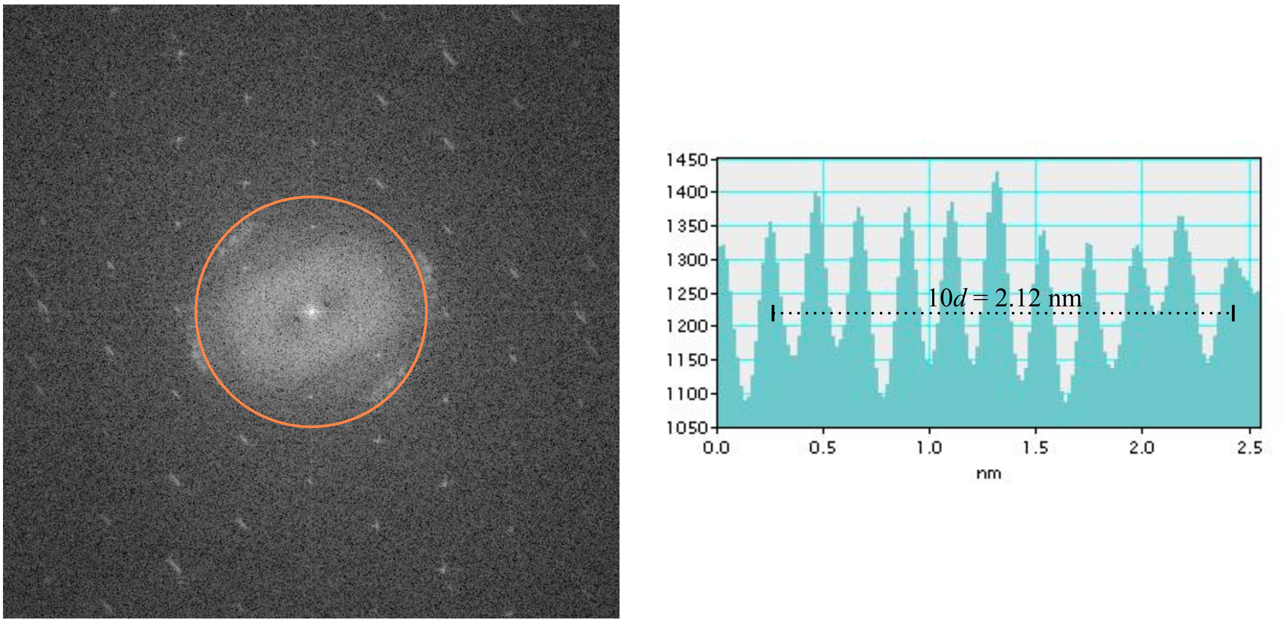

Figure 10b Representative Fourier transform image and fringe space analysis for catalyst 10 demonstrate an average *d* spacing of 2.12 Å corresponding to Cu (111)

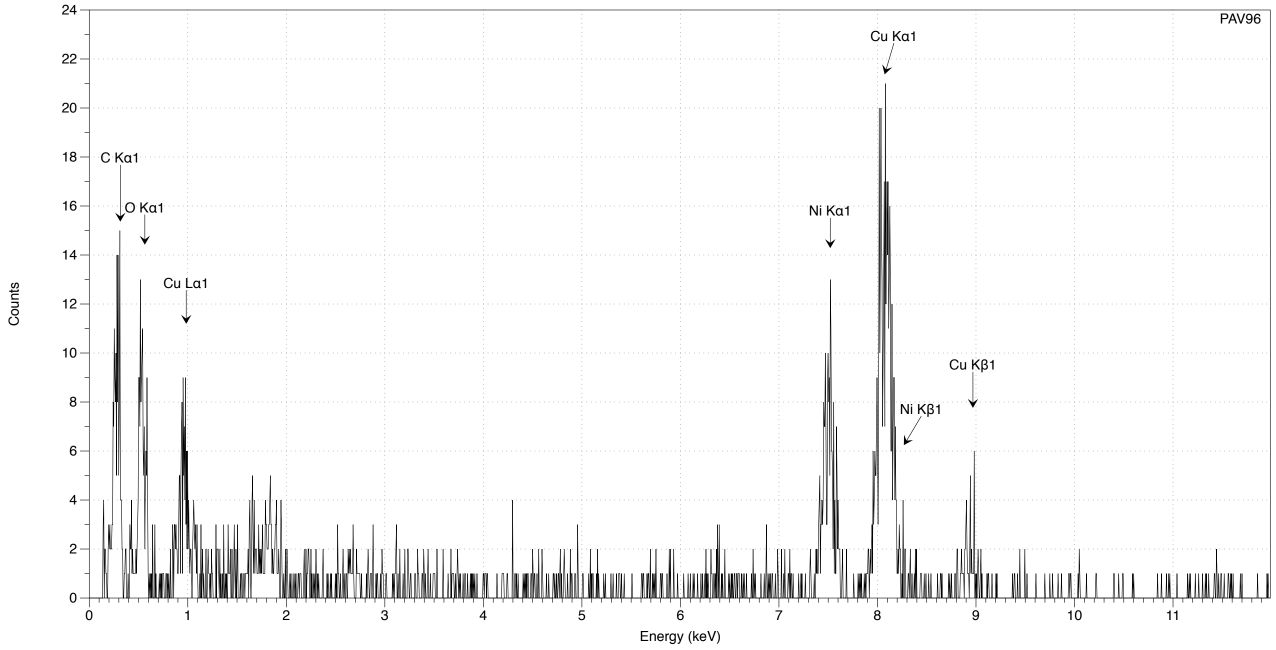

Figure S10c Representative narrow beam ED spectrum

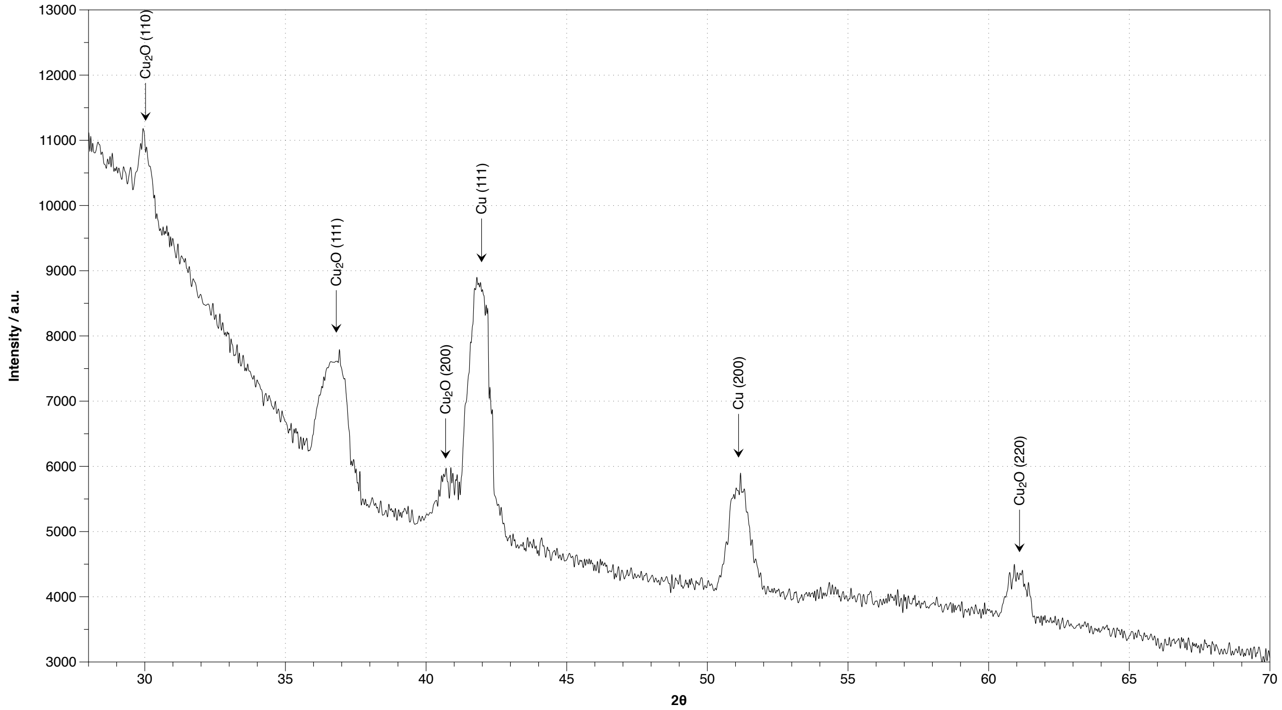

Figure 10d XRPD pattern reveals Cu and Cu_2O

Cu/PVP29 11(reaction pav151)

$CuCl_2$ (67.23 mg, 0.50 mmol) and PVP29 (333 mg, 2.70 mmol) were dissolved in EtOH (40 ml) under Ar and the mixture was stirred for 2 h at 40°C. The reaction temperature was maintained at 40°C and a stock solution of N_2H_4 (1M in THF, 1.0 ml, 1.0 mmol) was added. The reaction was allowed to run to completion over 120 min to give a crude NP dispersion, an aliquot of which was purified and redispersed as for catalyst 1.

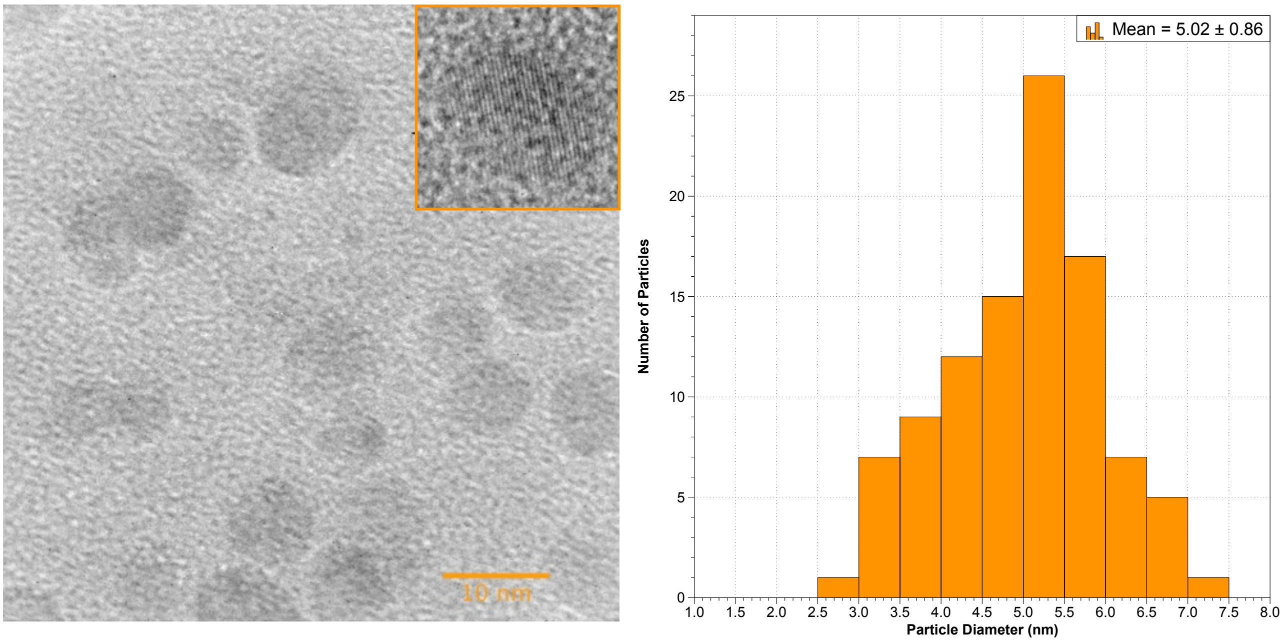

Figure S11a Representative TEM image of catalyst 11 at x300k with a magnified insert *(left)* and particle size distribution *(right)*

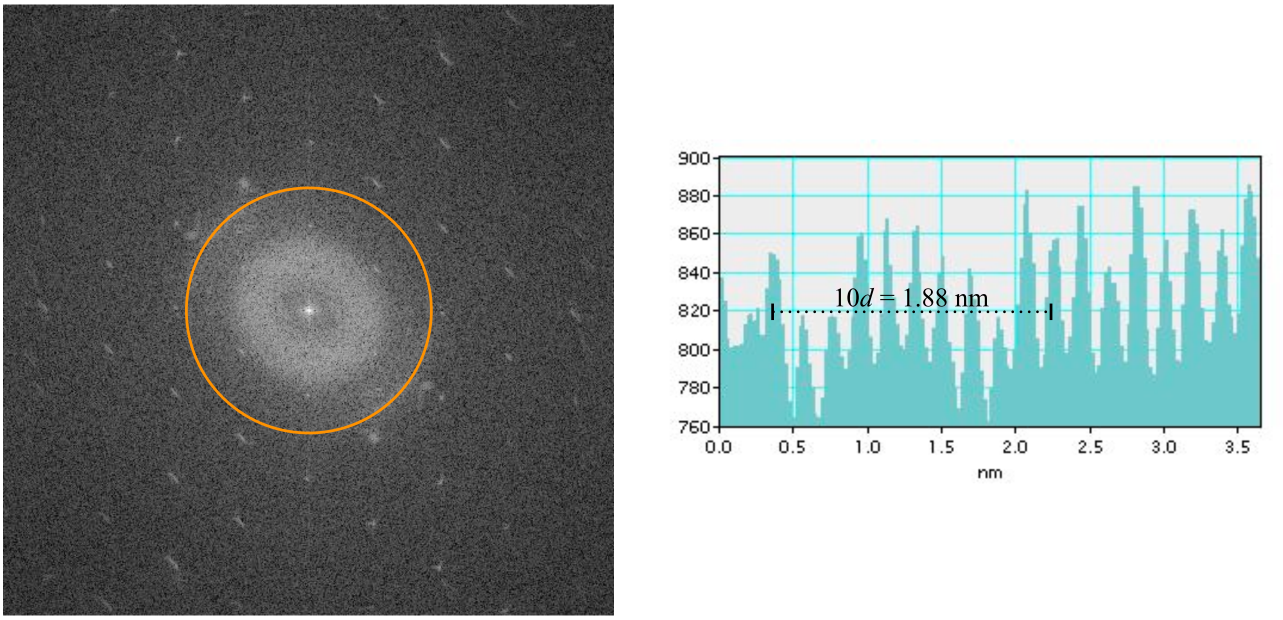

Figure 11b Representative Fourier transform image and fringe space analysis for catalyst 11 demonstrate an average *d* spacing of 1.88 Å corresponding to Cu (200).

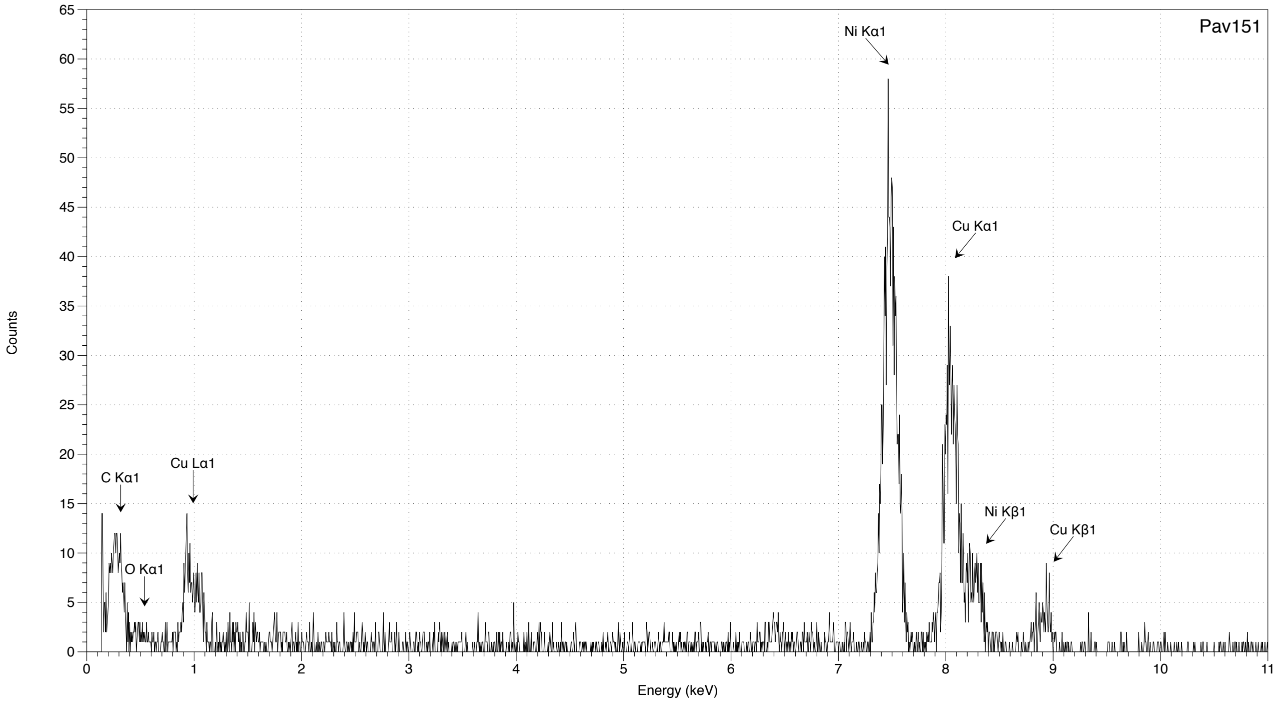

Figure S11c Representative narrow beam ED spectrum

Cu/PVPy60 12(reaction pav65)

$CuSO_4$ (159.62 mg, 1.00 mmol) and PVPy60 (average M_w = 60,000, 1.05 g, 10.00 mmol) were dissolved in ethylene glycol (120 ml) under Ar and the mixture was stirred for 2 h at 80°C. After cooling to 0°C the pH was adjusted to *ca.* 10 by adding NaOH (1 M in ethylene glycol, 5 ml). The mixture was stirred for 15 min after which NaH_2PO_2 (175.96 mg, 2.00 mmol) in ethylene glycol (10 ml) was added. The reaction was heated to 140°C for 90 min to give a crude NP dispersion, an aliquot of which was purified and redispersed as for catalyst 1.

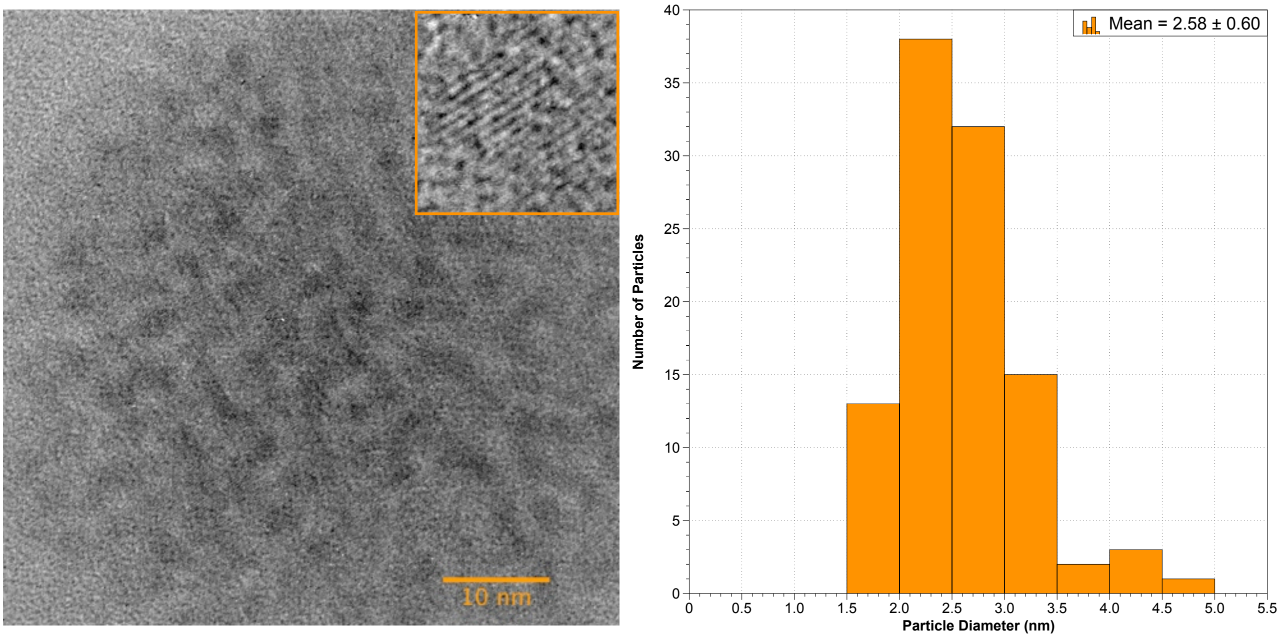

Figure S12a Representative TEM image of catalyst 13 at x300k with a magnified insert *(left)* and particle size distribution *(right)*

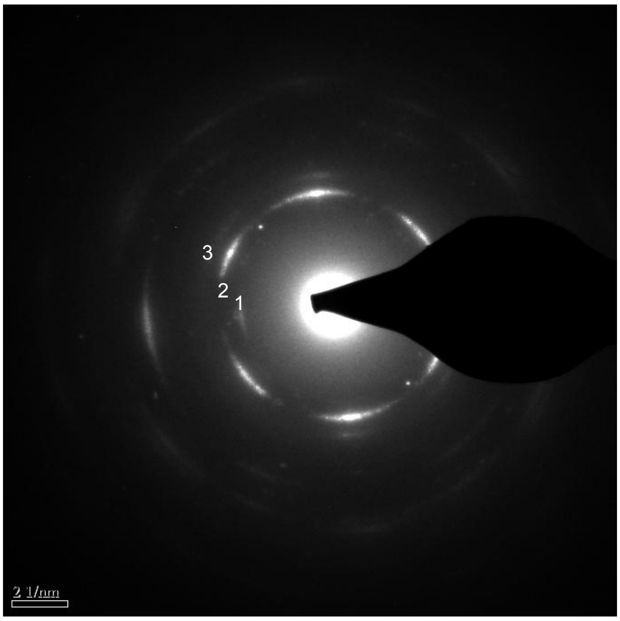

Lattice spacing / Å	Phase
2.96	Cu_2O (110)
2.43	Cu_2O (111)
2.11	Cu_2O (200)

Figure S12b Electron diffraction pattern demonstrates the presence of Cu_2O

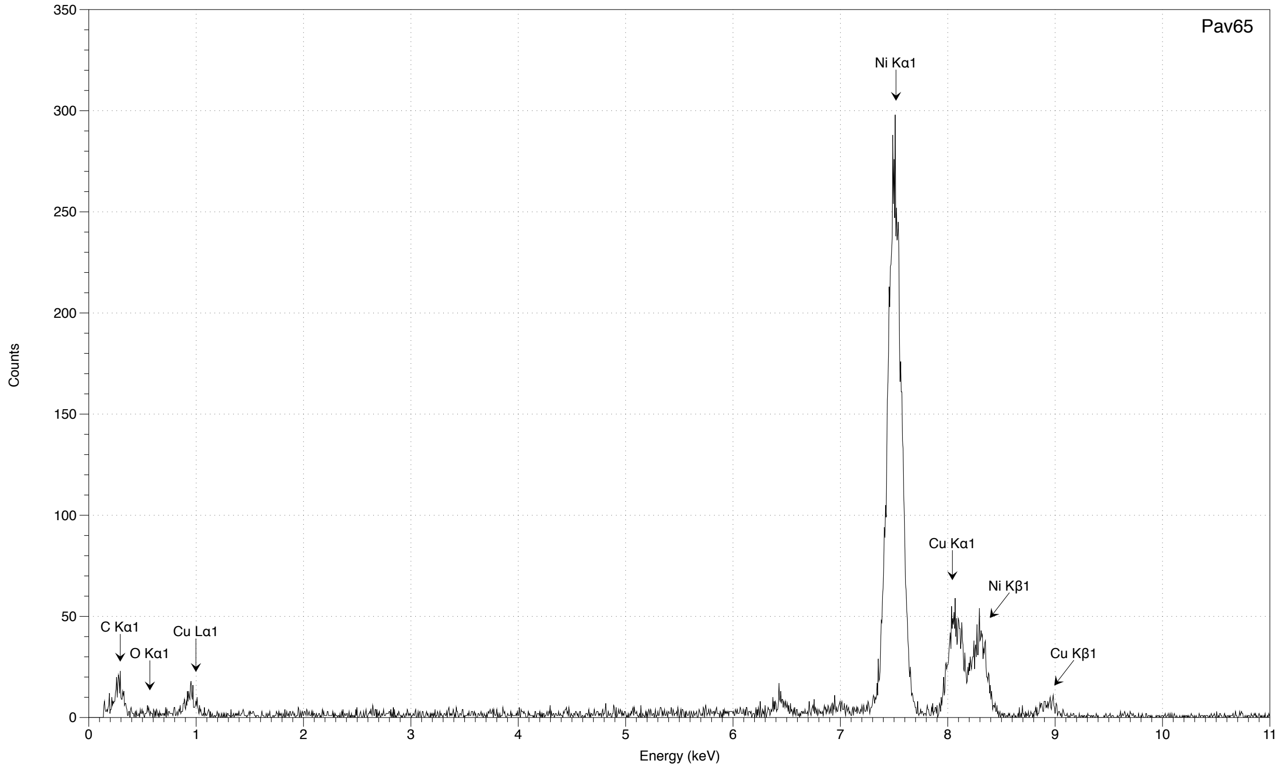

Figure S12c Representative narrow beam ED spectrum

Cu/PMMA120 13(reaction pav100)

$Cu(OAc)_2$ (90.81 mg, 0.50 mmol) and PMMA120 (average M_w = 120000, 300 mg, 3.00 mmol) were dissolved in THF (40 ml) under Ar and the mixture was stirred for 2.5 h at 40°C. The mixture was heated to reflux and $NaBH_4$ (37.83 mg, 1.0 mmol) in EtOH (10 ml) was added. The reaction was allowed to run to completion over 90 min to give a crude NP dispersion, an aliquot of which was purified by extraction using excess ethanol (1:10) over not more than 240 min. After sedimentation of the particles, the supernatant was decanted and the remaining suspension centrifuged, upon removal of the solvent layer, the precipitate was resuspended in THF.

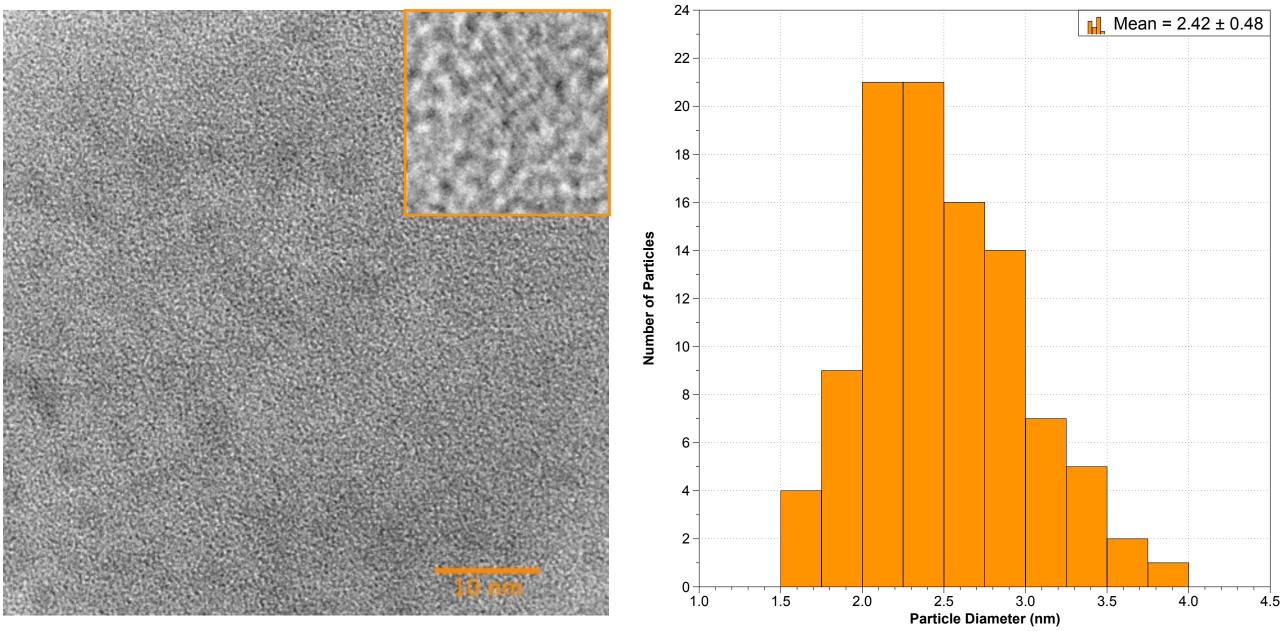

Figure S13a Representative TEM image of catalyst 13 at x300k with a magnified insert *(left)* and particle size distribution *(right)*

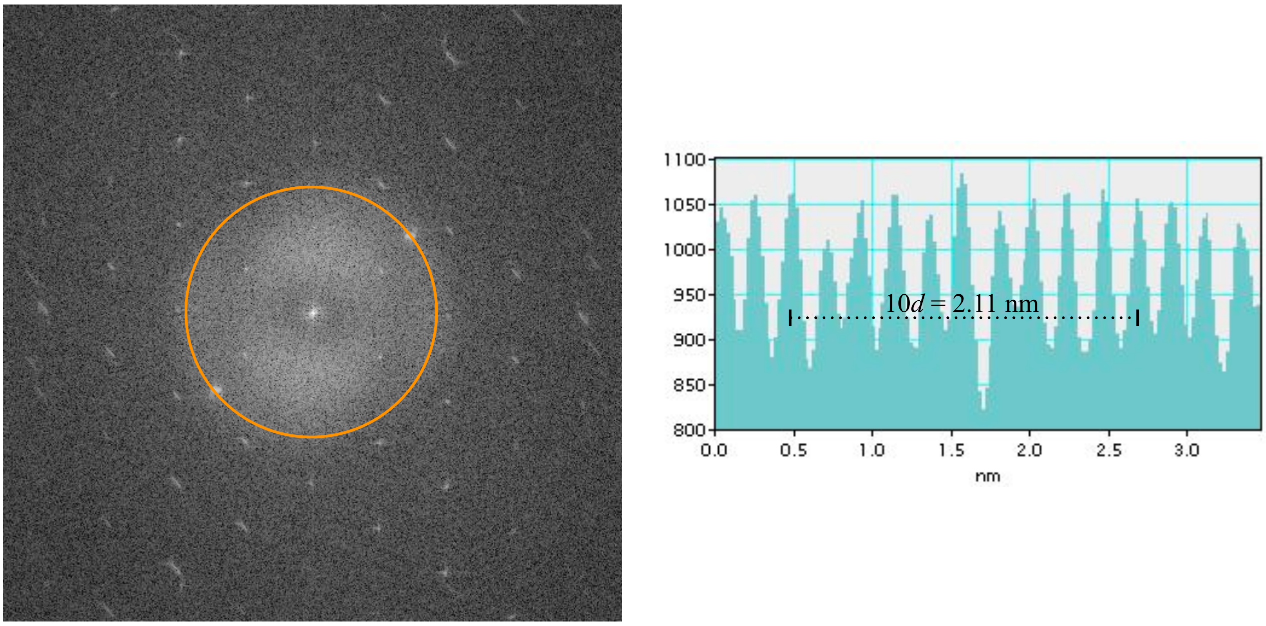

Figure 13b Representative Fourier transform image and fringe space analysis for catalyst 13 demonstrate an average *d* spacing of 2.11 Å corresponding to Cu (111)

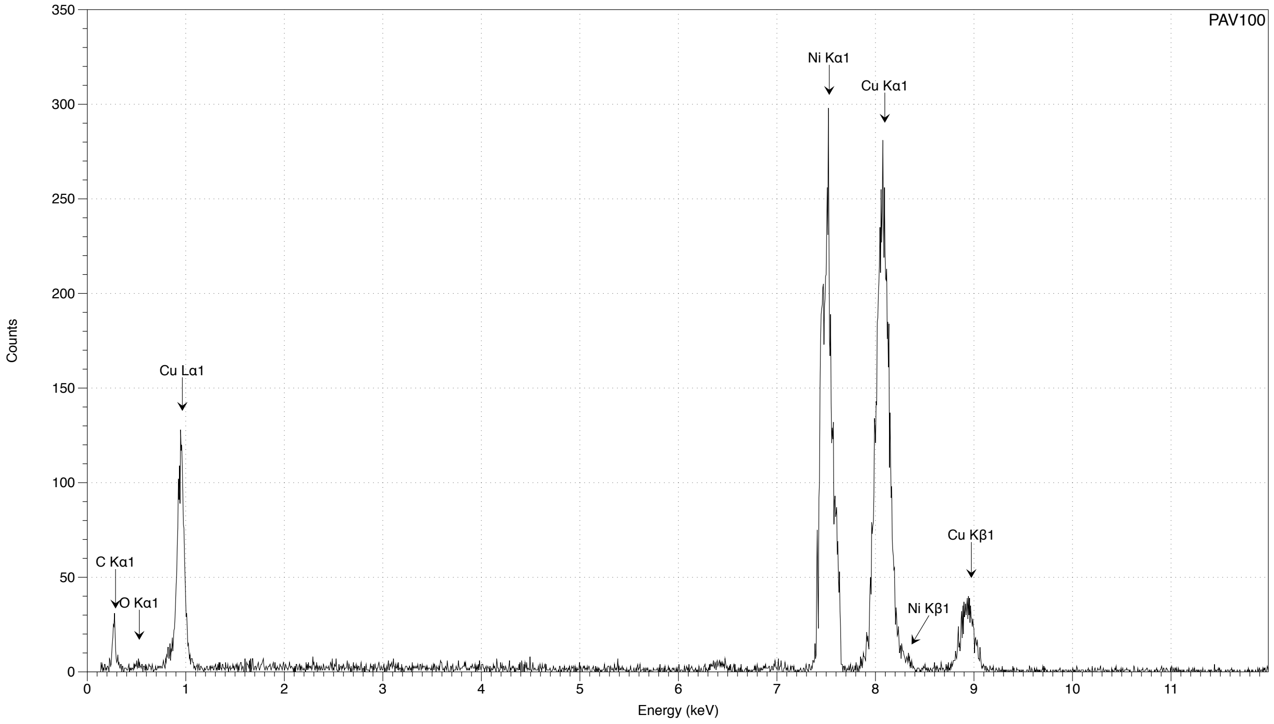

Figure S13c Representative narrow beam ED spectrum

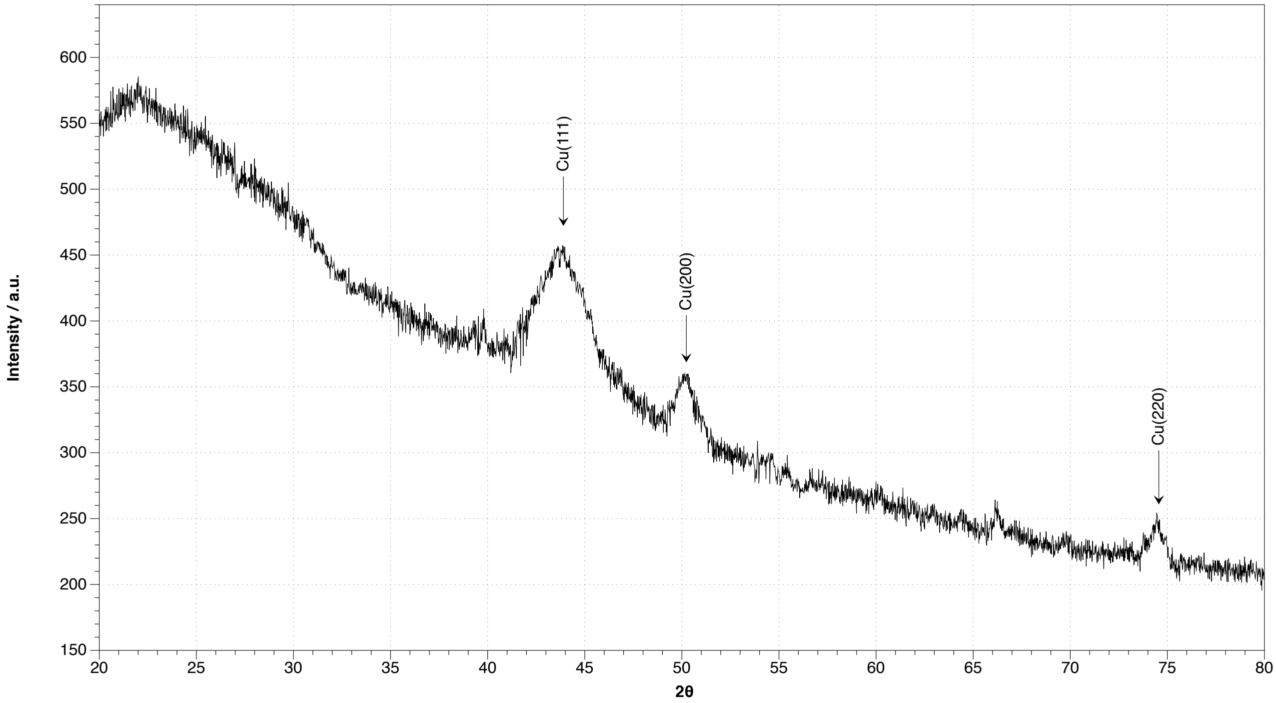

Figure S13d XRPD pattern of freshly synthesized catalyst 13 clearly points to metallic Cu only

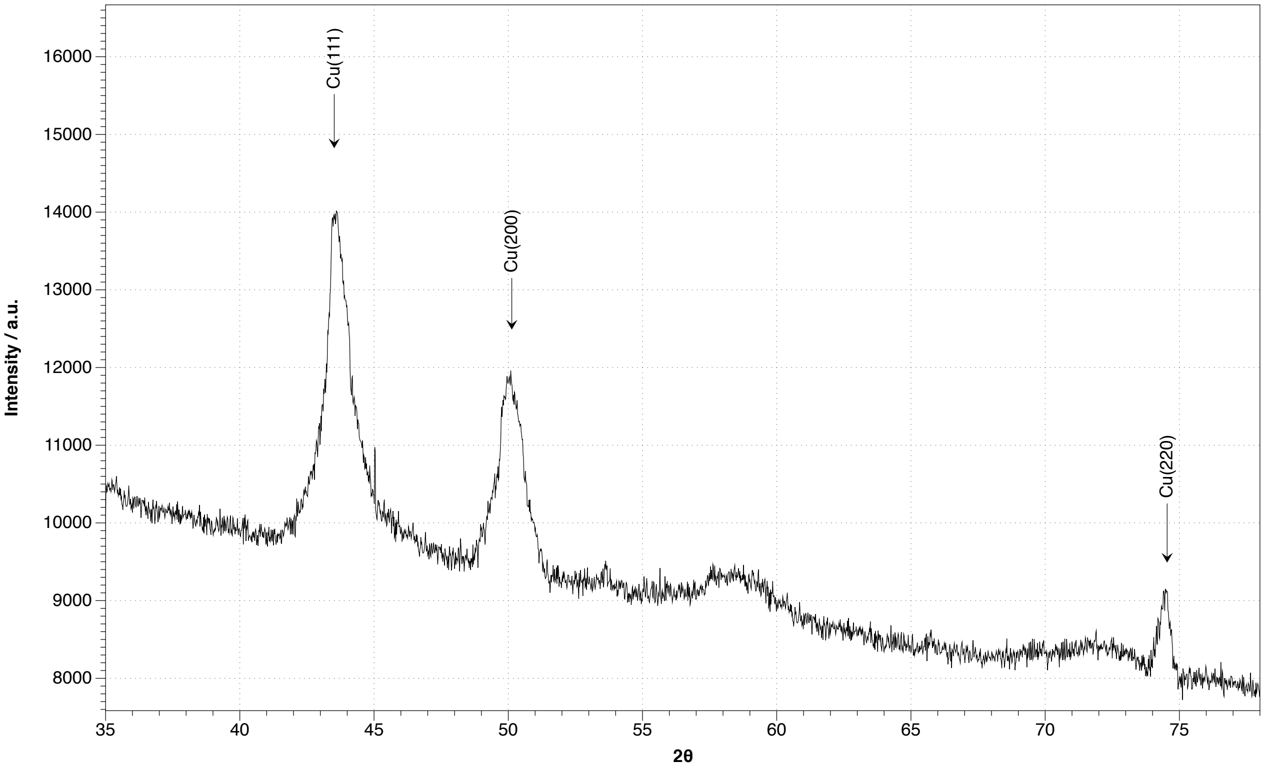

Figure S13e XRPD pattern of catalyst 13 after 14 days of exposure to air demonstrates the presence of Cu

Cu/PMMA120 14(reaction pav131)

$Cu(OAc)_2$ (90.81 mg, 0.50 mmol) and PMMA120 (300 mg, 3.00 mmol) were dissolved in THF:EtOH (20:20 ml) under Ar and the mixture was stirred for 2.5 h at 40°C. The mixture was heated to reflux and $NaBH_4$ (37.83 mg, 1.00 mmol) in EtOH (10 ml) was added. The reaction was allowed to run to completion over 90 min to give a crude NP dispersion, an aliquot of which was purified and redispersed as for catalyst 13.

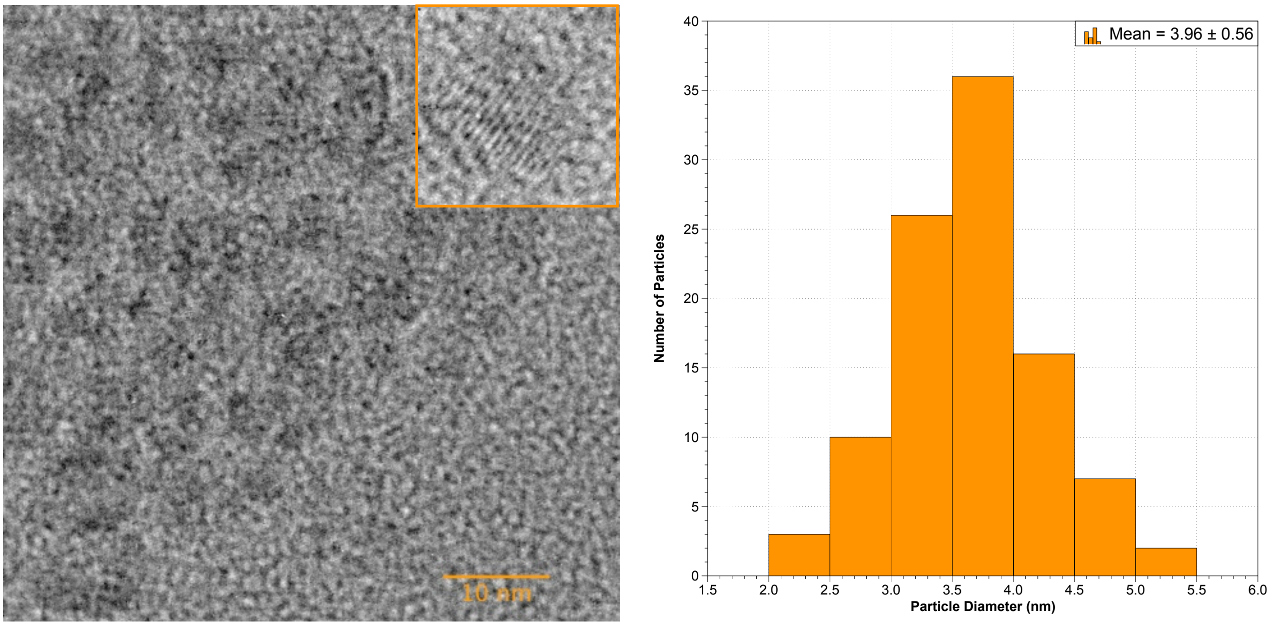

Figure S14a Representative TEM image of catalyst 14 at x300k with a magnified insert *(left)* and particle size distribution *(right)*

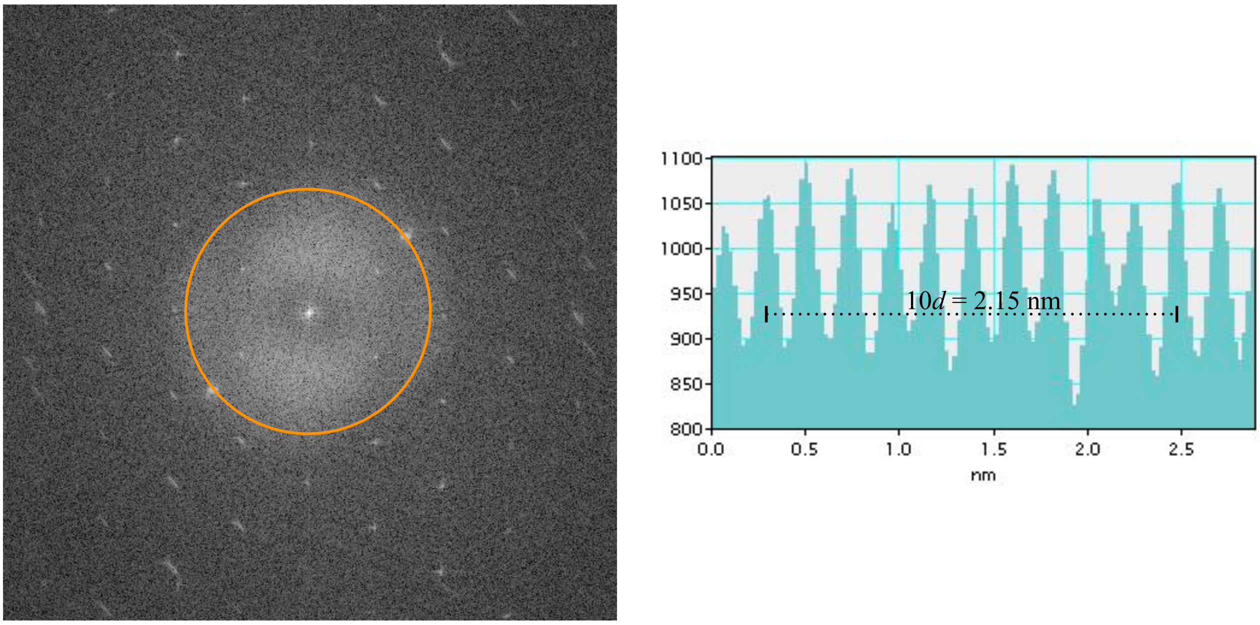

Figure 14b Representative Fourier transform image and fringe space analysis for catalyst 14 demonstrate an average *d* spacing of 2.15 Å corresponding to Cu (111)

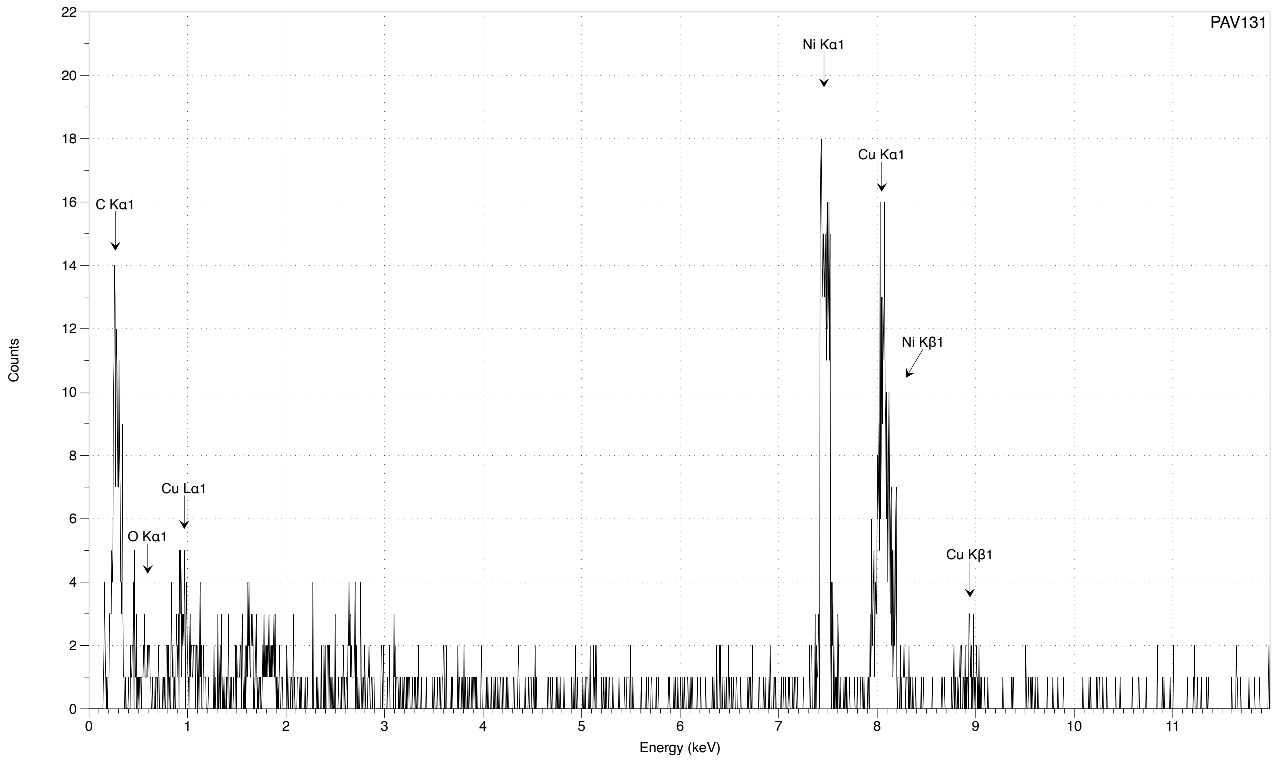

Figure S14c Representative narrow beam ED spectrum

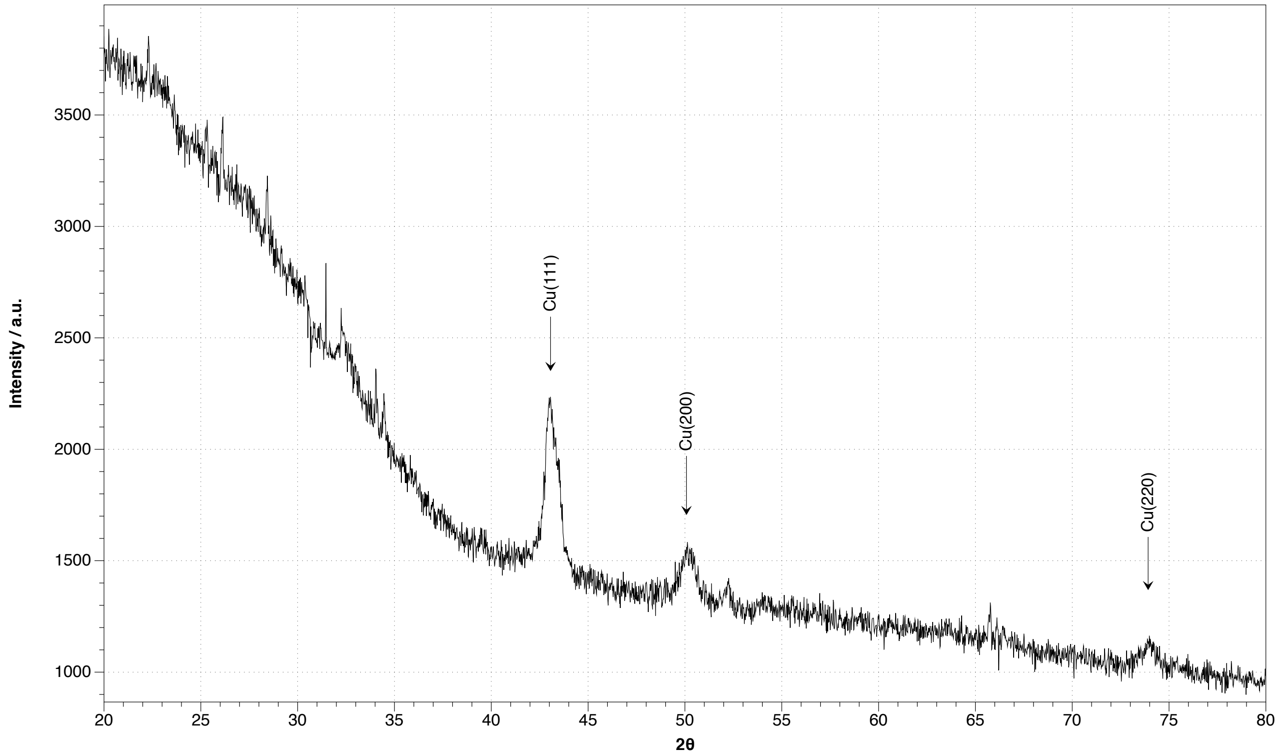

Figure S14d XRPD pattern clearly points to metallic Cu only

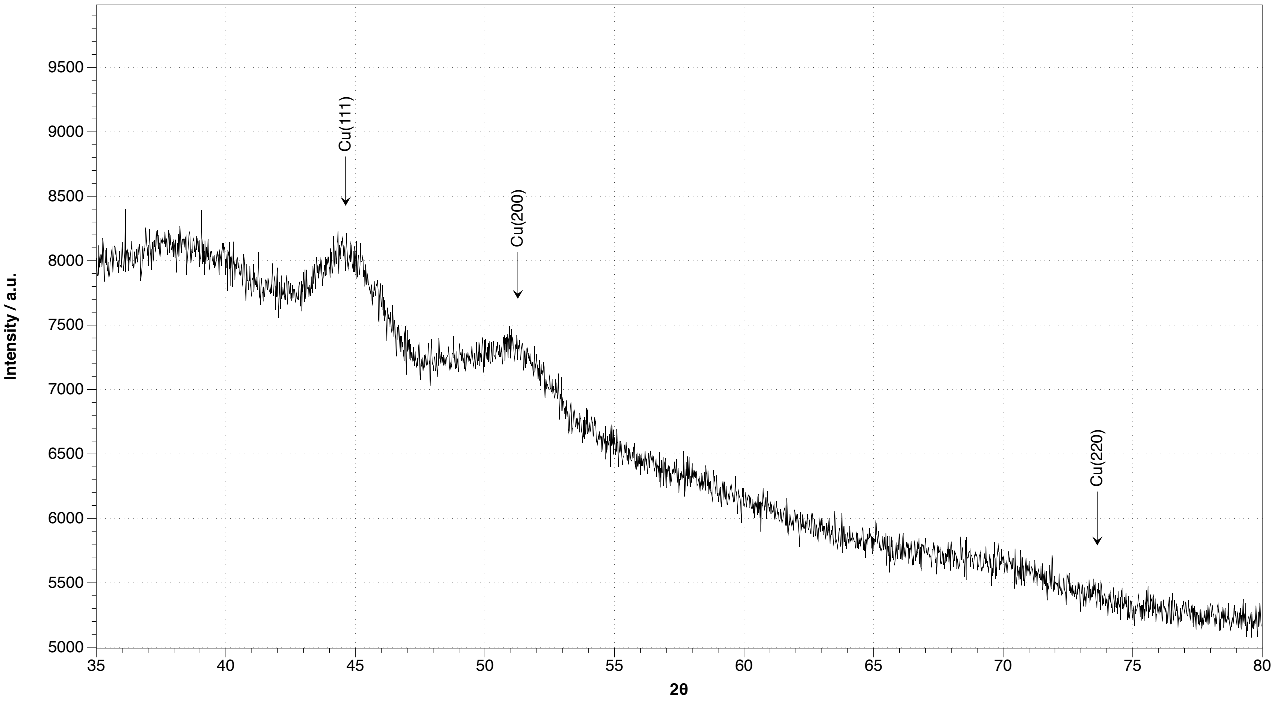

Figure S14f XRPD pattern of catalyst 14 after 14 days of exposure to air suggests the presence of metallic Cu

Cu/PMMA120 15(reaction pav205)

$Cu(OAc)_2$ (90.81 mg, 0.50 mmol) and PMMA120 (300 mg, 3.00 mmol) were dissolved in a 3:1 mixture of THF (30 ml) and EtOH (10 ml) under Ar and the mixture was stirred for 2.5 h at 40°C. The reaction was cooled to 25° and $NaBH_4$ (37.83 mg, 1.00 mmol) in EtOH (10 ml) was added. The reaction was allowed to run to completion over 90 min to give a crude NP dispersion, an aliquot of which was purified and redispersed as for catalyst 13.

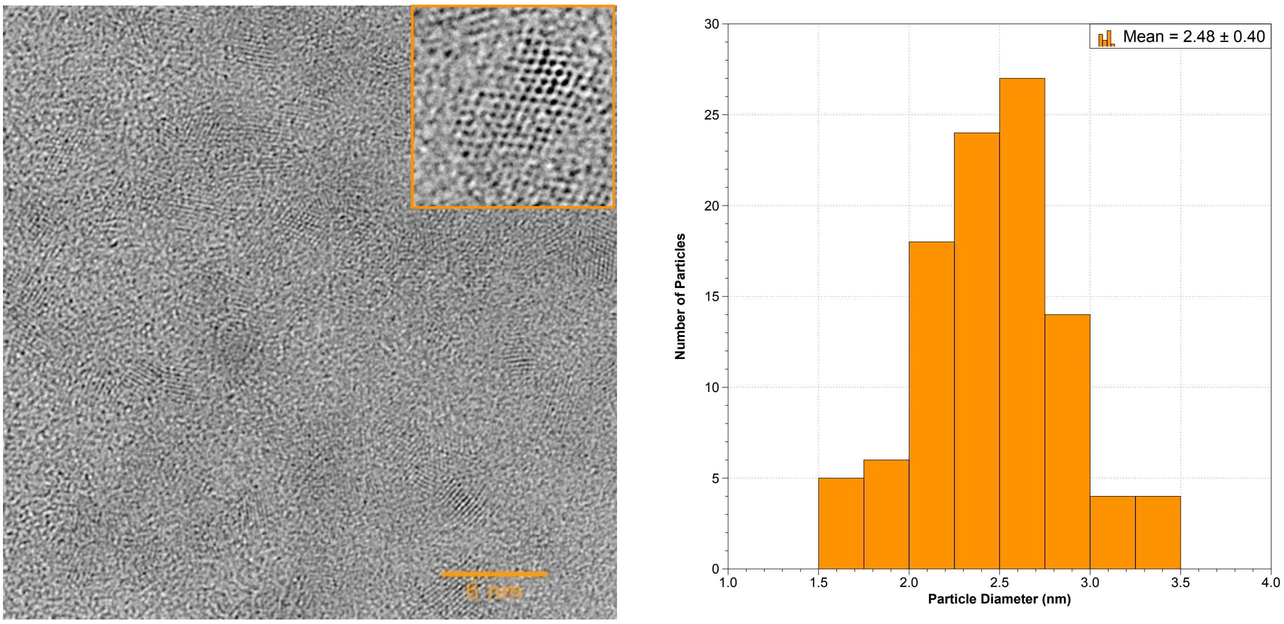

Figure S15a Representative TEM image of catalyst 15 at x620k with a magnified insert *(left)* and particle size distribution *(right)*

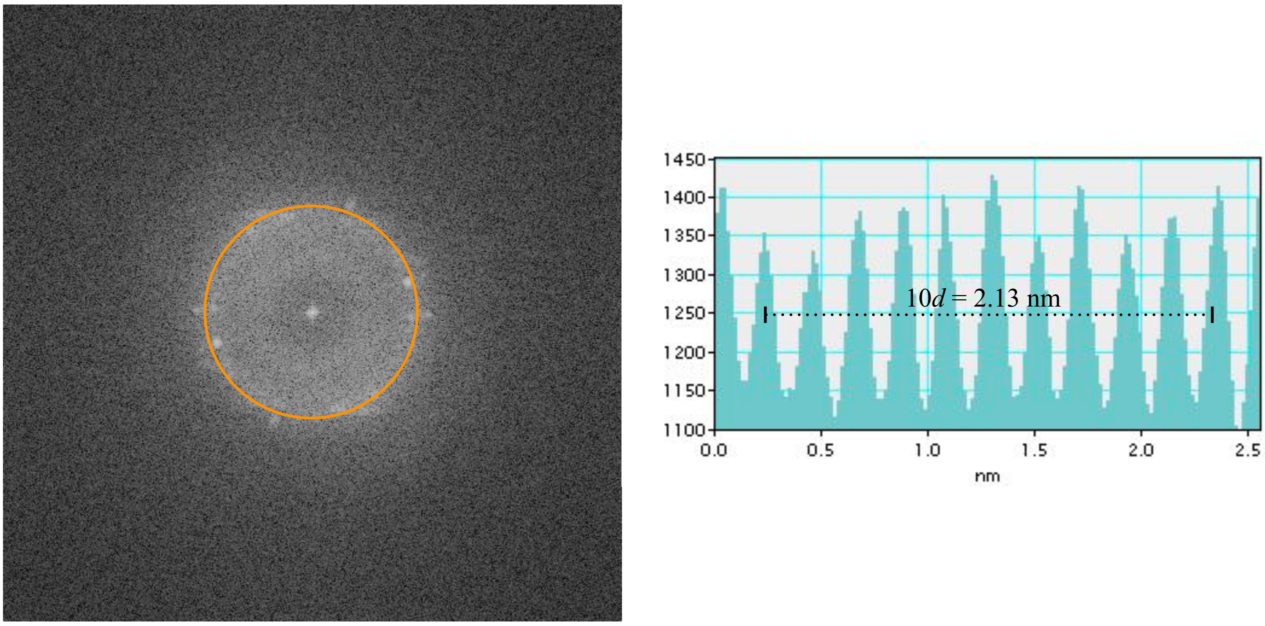

Figure 15b Representative Fourier transform image and fringe space analysis for catalyst 15 demonstrate an average *d* spacing of 2.13 Å corresponding to Cu (111)

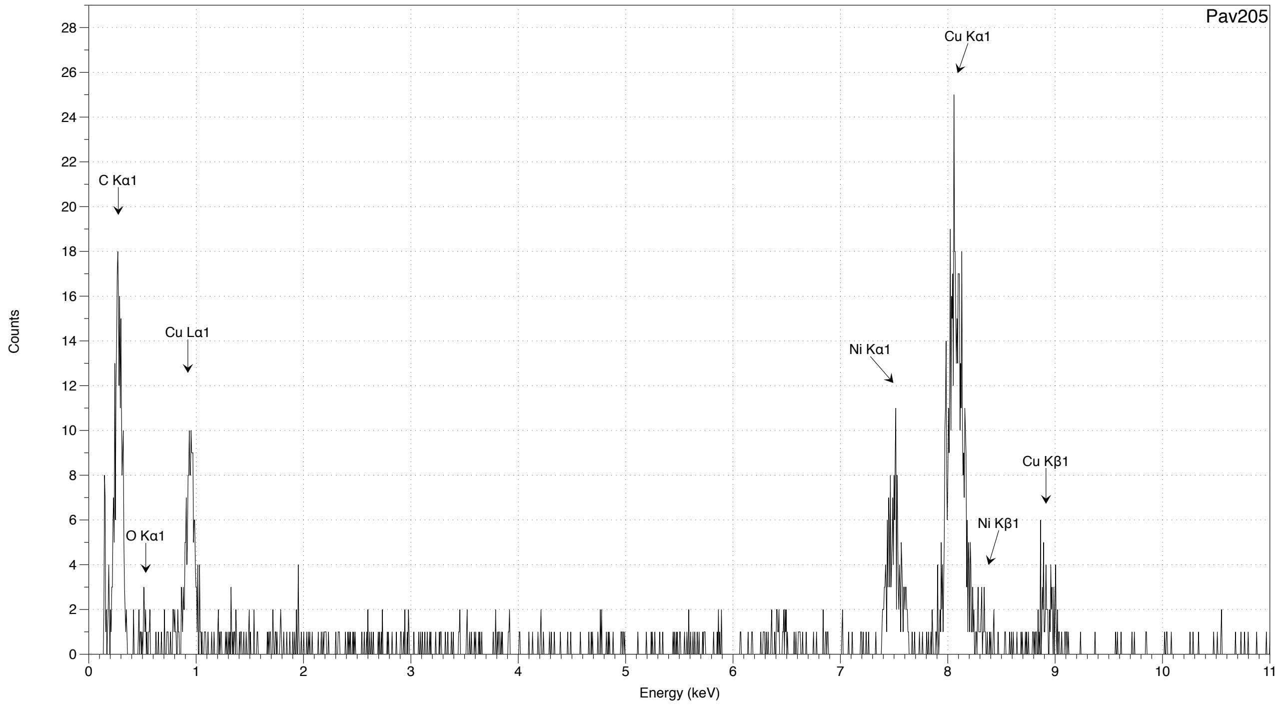

Figure S15c Representative narrow beam ED spectrum

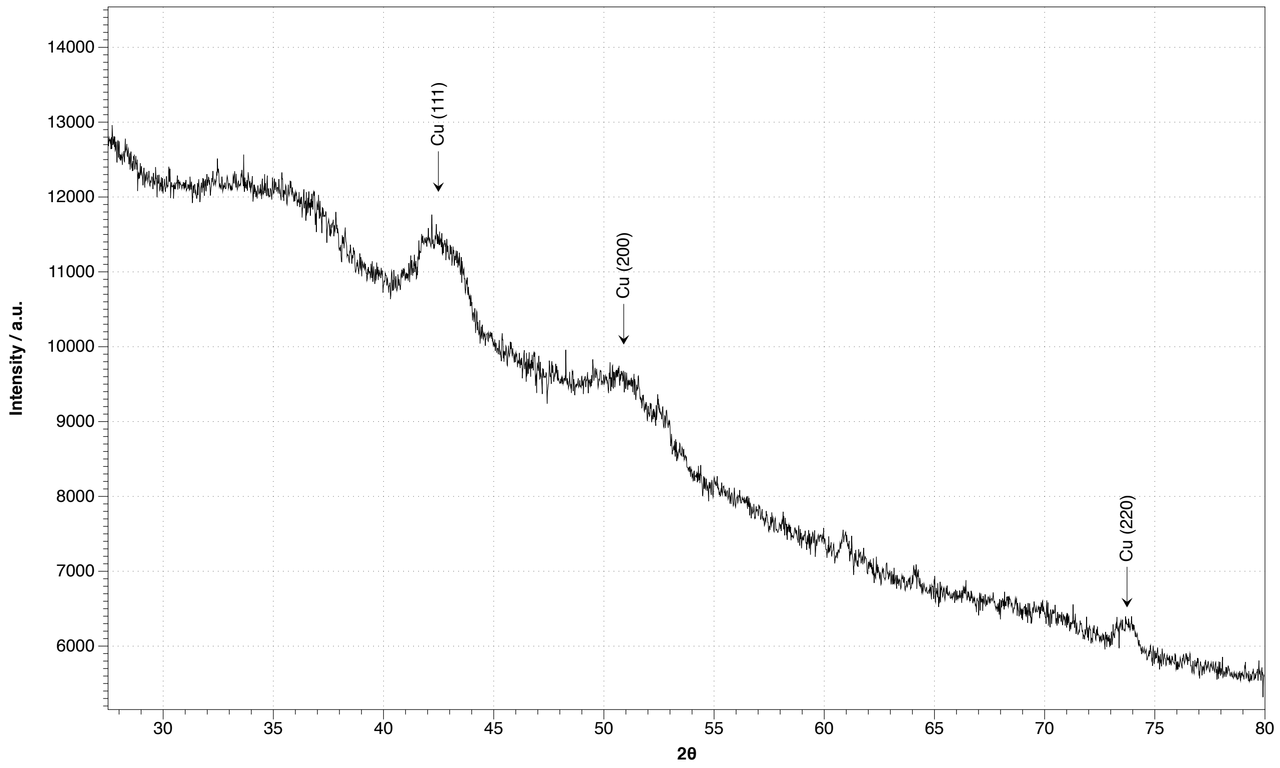

Figure S15d XRPD pattern of fresh catalyst 15 demonstrates the presence of metallic Cu only

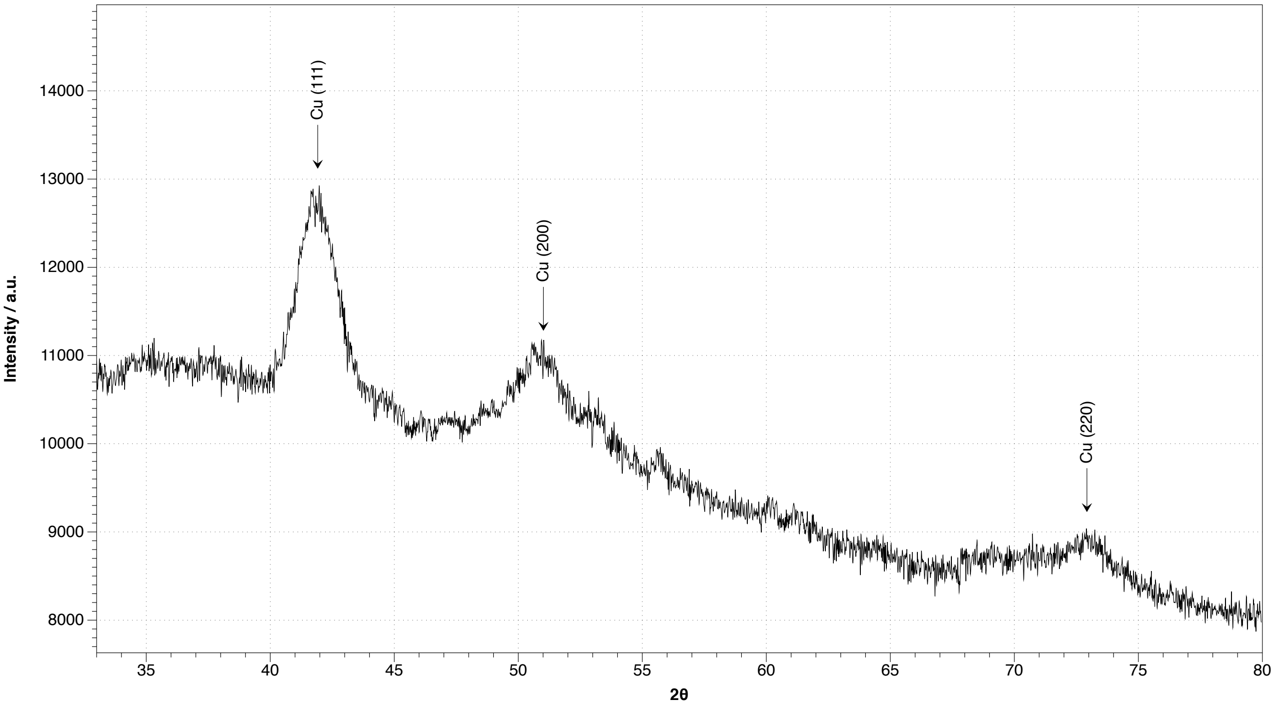

Figure S15e XRPD pattern of catalyst 15 after 14 days of exposure to air demonstrates the presence of metallic Cu only

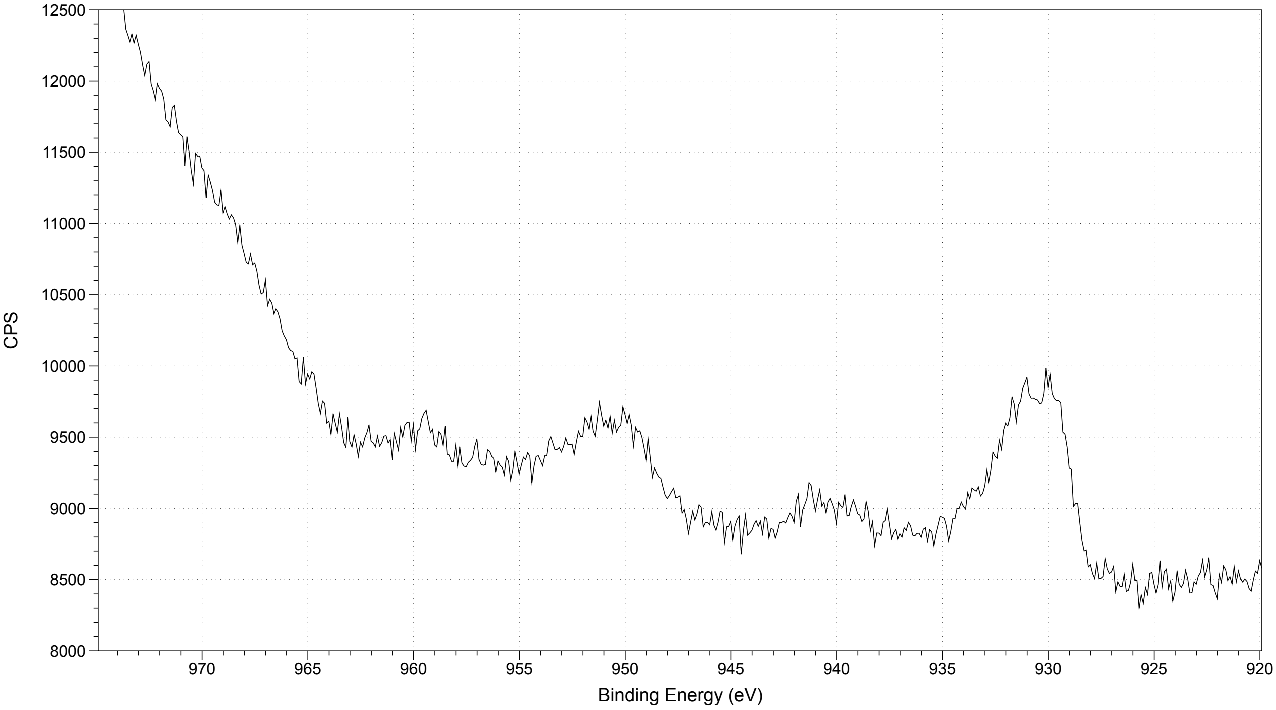

S15f XPS data Cu $2p_{1/2}$ and $2p_{3/2}$ region shows Cu_2O and Cu signals at 932.5 eV and 930 eV respectively

Cu/PMMA120 16(reaction pav136)

$Cu(OAc)_2$ (90.81 mg, 0.50 mmol) and PMMA120 (300 mg, 3.00 mmol) were dissolved in THF (40 ml) under Ar and the mixture was stirred for 2.5 h at 40°C. A The mixture was heated to reflux after which a stock solution of N_2H_4 (1M in THF, 1.00 ml, 1.00 mmol) was added. The reaction was allowed to run to completion over 120 min to give a crude NP dispersion, an aliquot of which was purified and redispersed as for catalyst 13.

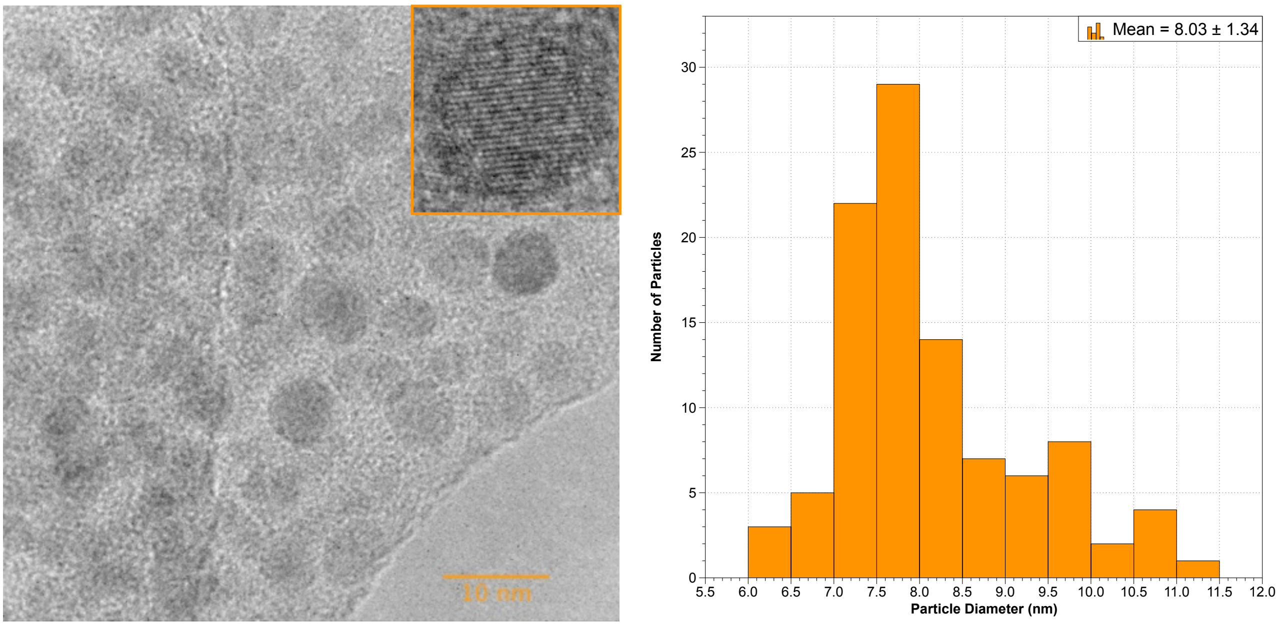

Figure S16a Representative TEM image of catalyst 16 at x300k with a magnified insert *(left)* and particle size distribution *(right)*

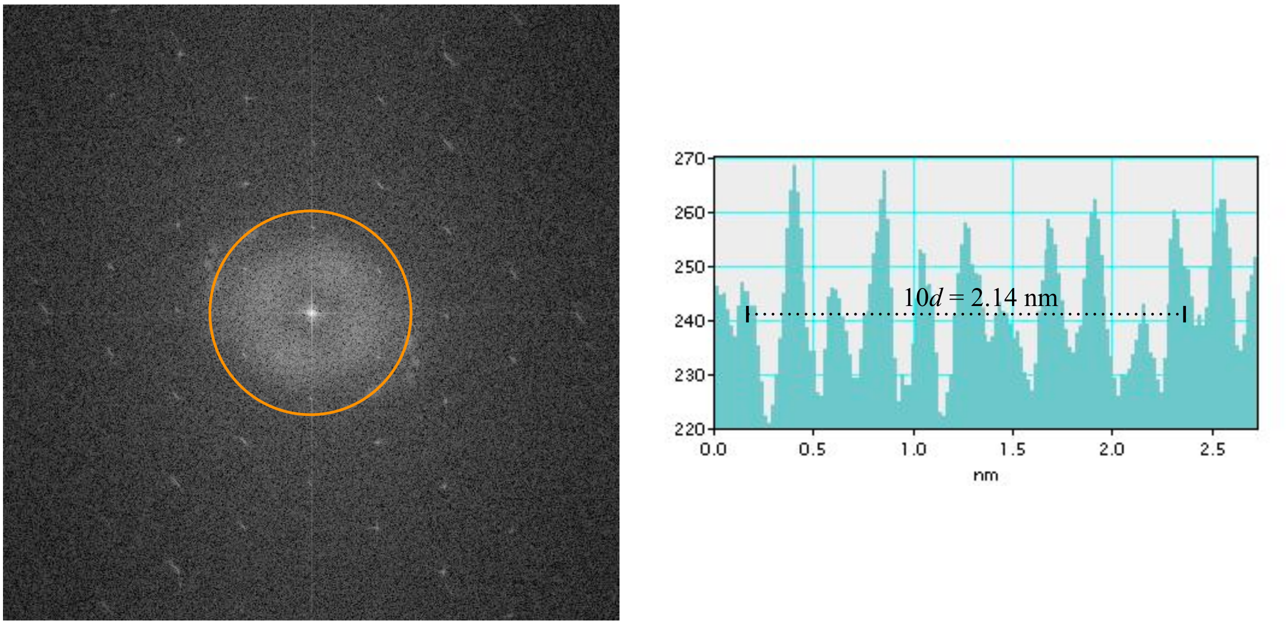

Figure 16b Representative Fourier transform image and fringe space analysis for catalyst 16 demonstrate an average *d* spacing of 2.14 Å corresponding to Cu (111)

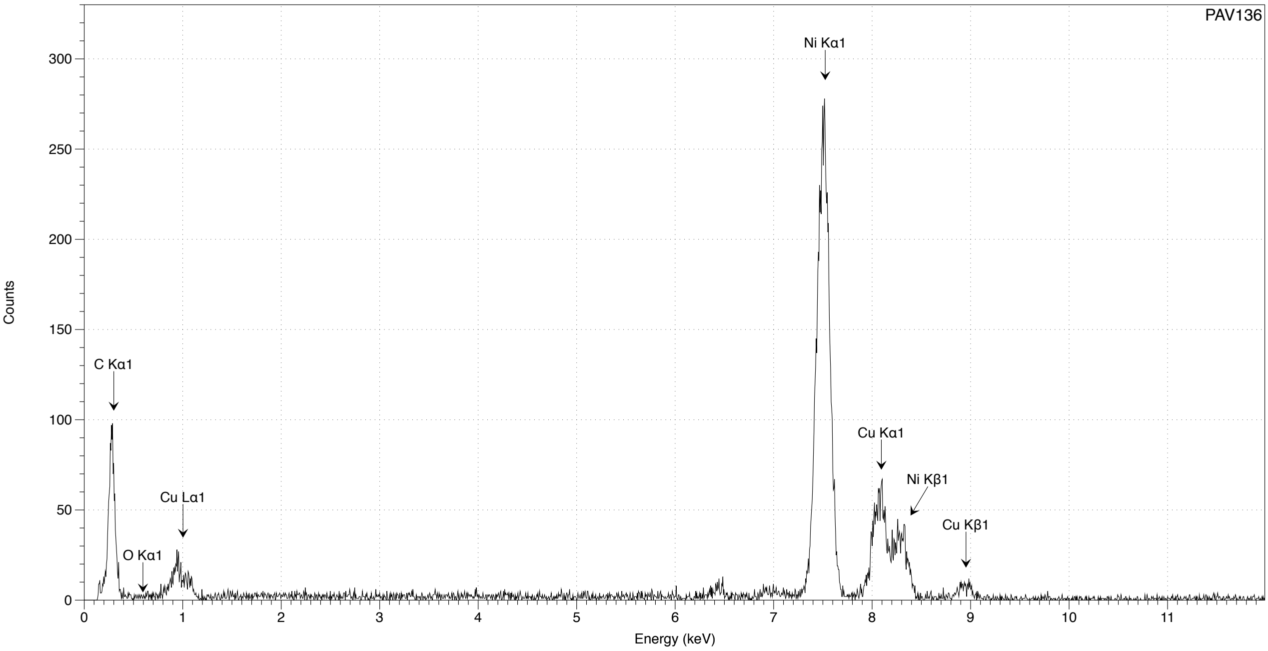

Figure S16c Representative narrow beam ED spectrum

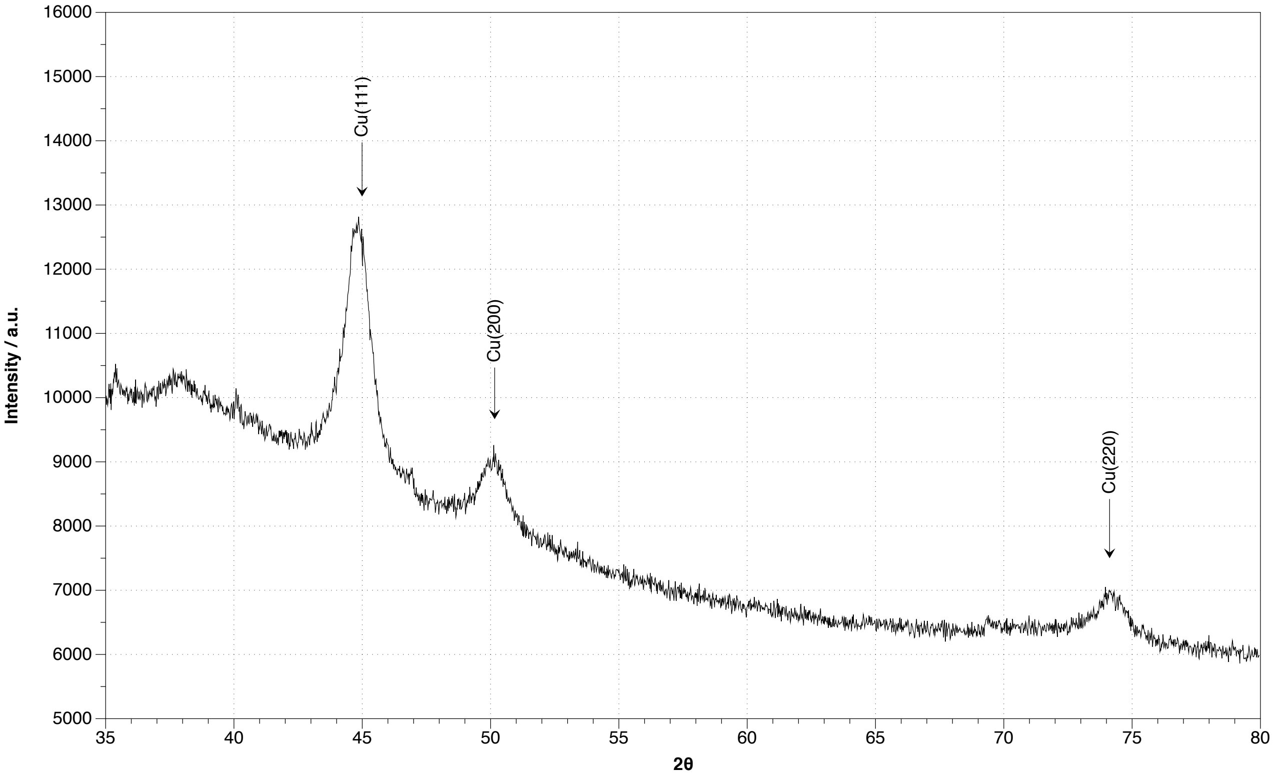

Figure S16d XRPD pattern of catalyst 16 after 14 days of exposure to air demonstrates the presence of metallic Cu only

Cu/PMMA120 17(reaction pav155)

Cu(OAc)$_2$ (90.81 mg, 0.50 mmol) and PMMA120 (300 mg, 3.00 mmol) were dissolved in THF (40 ml) under Ar and the mixture was stirred for 2.5 h at 40°C. With reaction temperature set 40°C a stock solution of N_2H_4 (1M in THF, 1.00 ml, 1.00 mmol) was added. The reaction was allowed to run to completion over 120 min to give a crude NP dispersion, an aliquot of which was purified and redispersed as for catalyst 13.

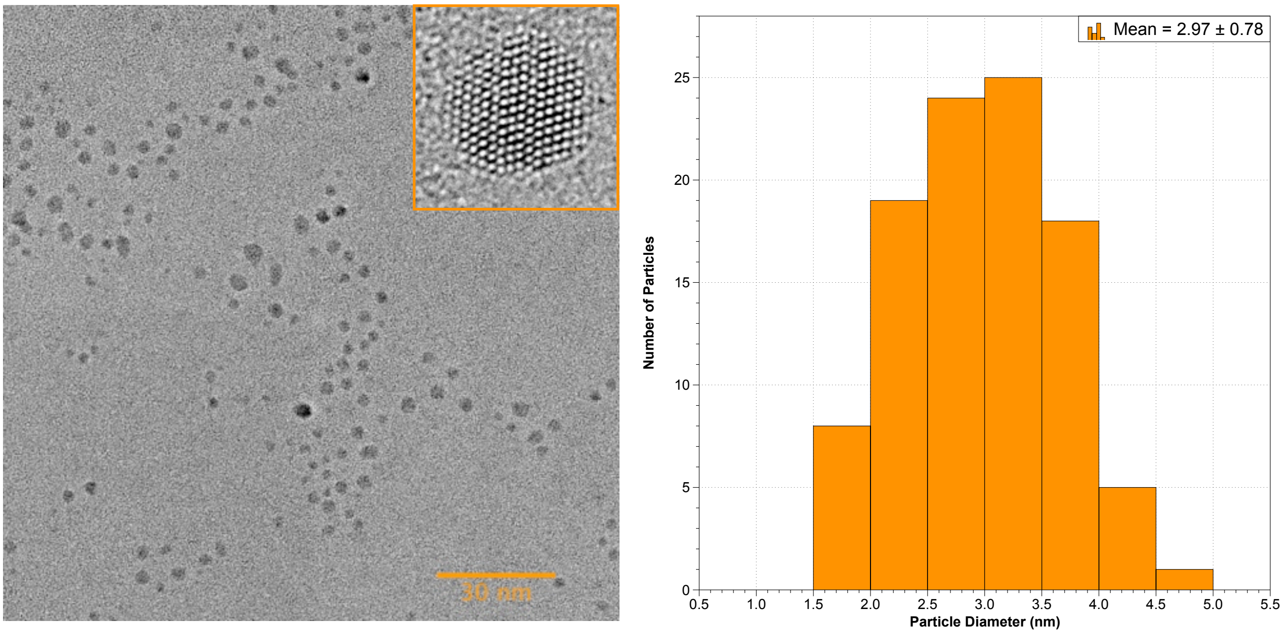

Figure S17a Representative TEM image of catalyst 17 at x145k with a magnified insert *(left)* and particle size distribution *(right)*

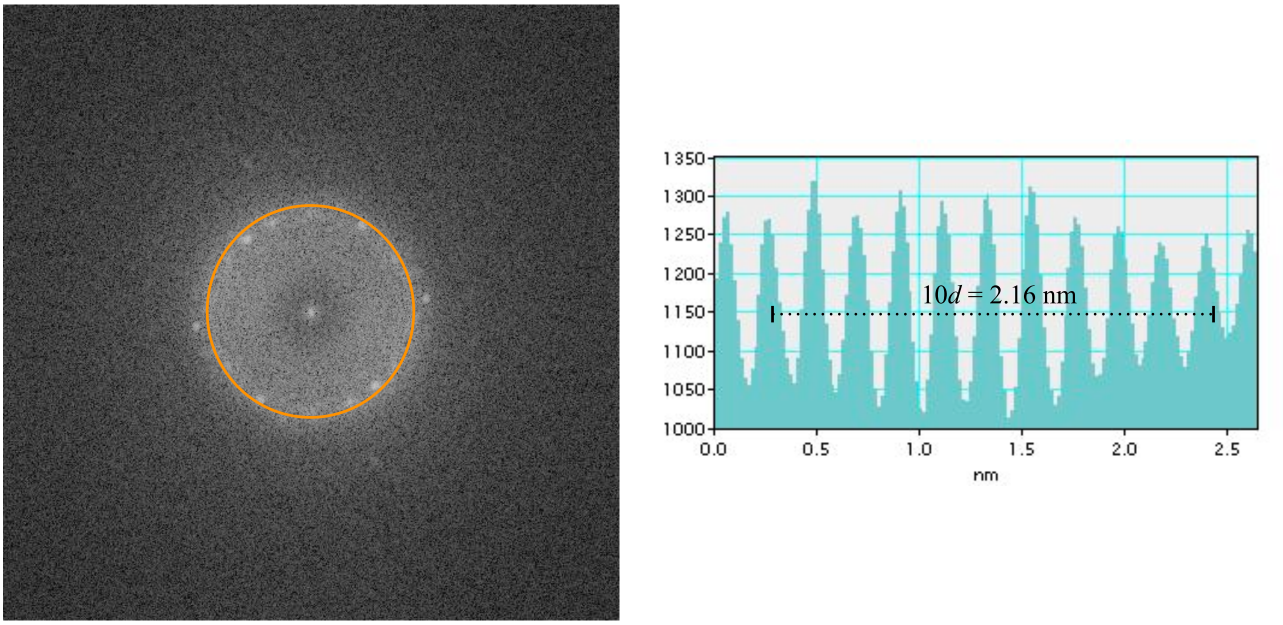

Figure 17b Representative Fourier transform image and fringe space analysis for catalyst 17 demonstrate an average *d* spacing of 2.16 Å corresponding to Cu (111)

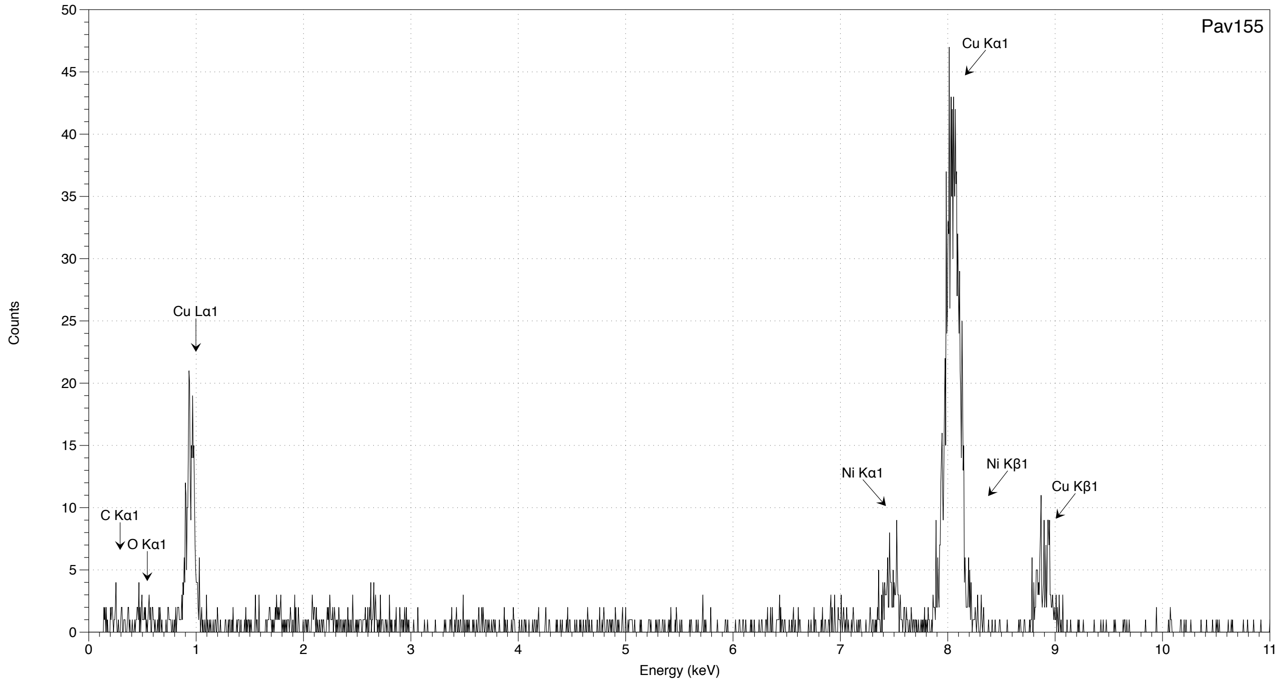

Figure S17c Representative narrow beam ED spectrum.

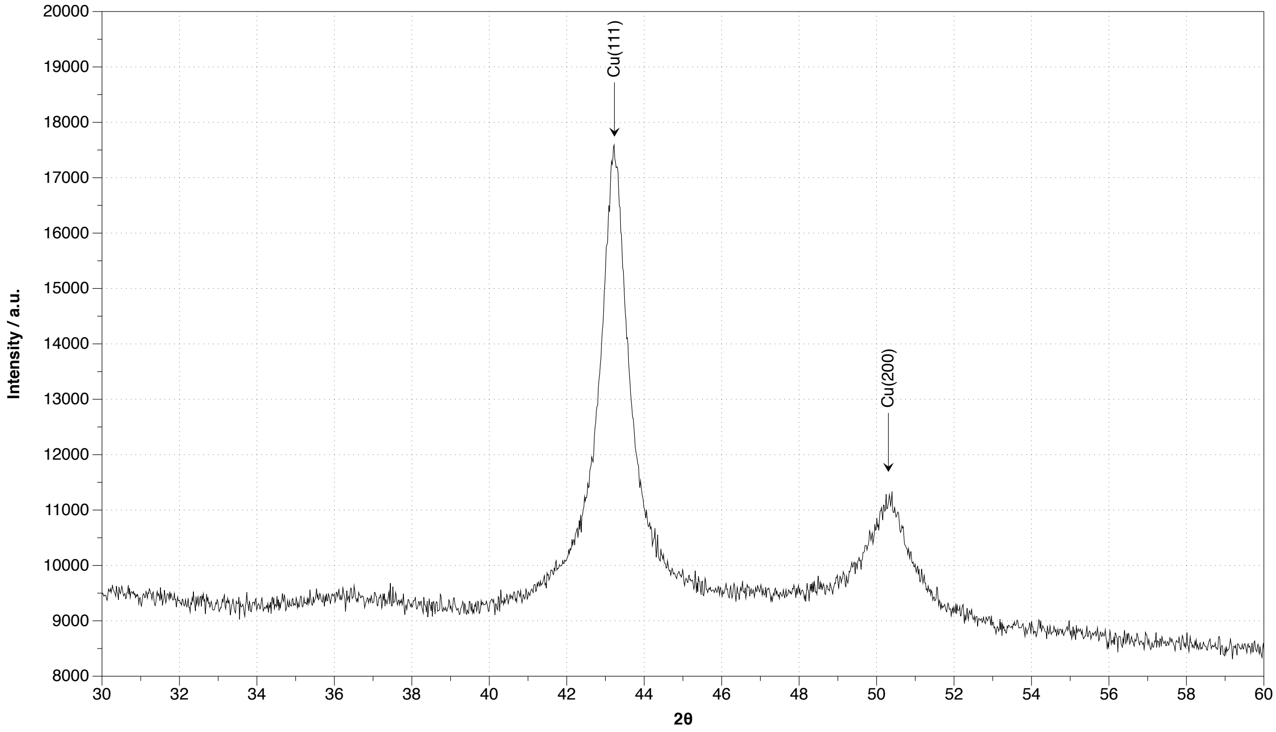

Figure S17d XRPD pattern clearly points to unoxidized Cu only for fresh 17

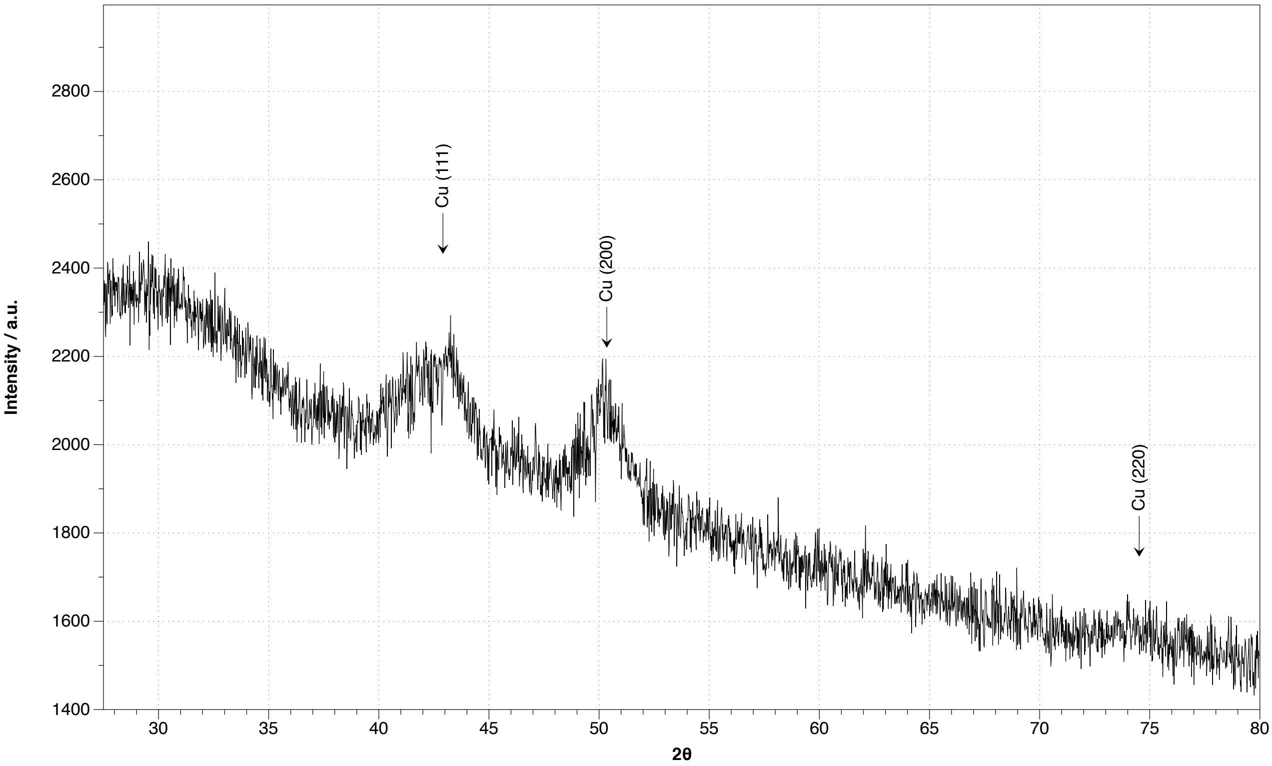

Figure S17e XRPD pattern of catalyst 17 clearly points to unoxidized Cu after 14 days of exposure to air

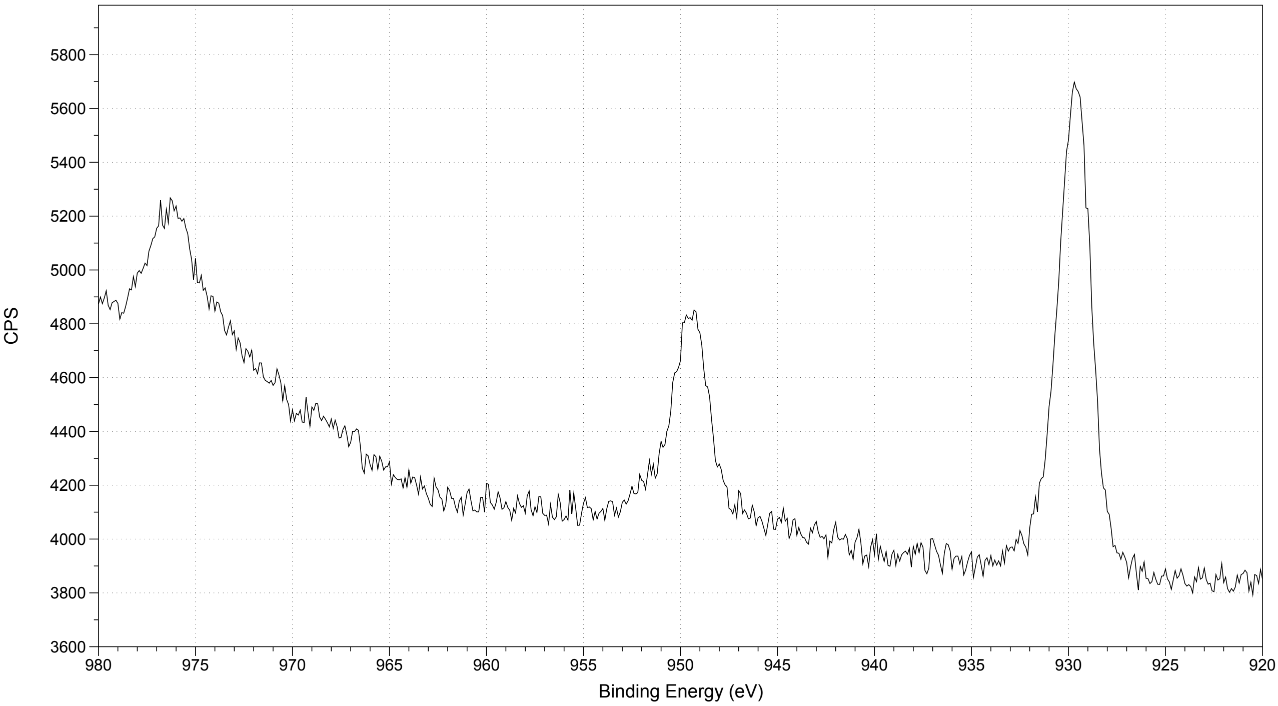

Figure S17f XPS data Cu $2p_{1/2}$ and $2p_{3/2}$ region shows a strong signal at 929.5 eV corresponding to Cu and no evidence of Cu_2O at 932.5 eV

Cu/PMMA120 18(reaction pav101)

$CuCl_2$ (67.22 mg, 0.50 mmol) and PMMA120 (300 mg, 3.00 mmol) were dissolved in THF (40 ml) under Ar and the mixture was stirred for 2.5 h at 40°C. The mixture was heated to reflux and $NaBH_4$ (37.83 mg, 1.0 mmol) in EtOH (10 ml) was added. The reaction was allowed to run to completion over additional 90 min to give a crude NP dispersion, an aliquot of which was purified and redispersed as for catalyst 13.

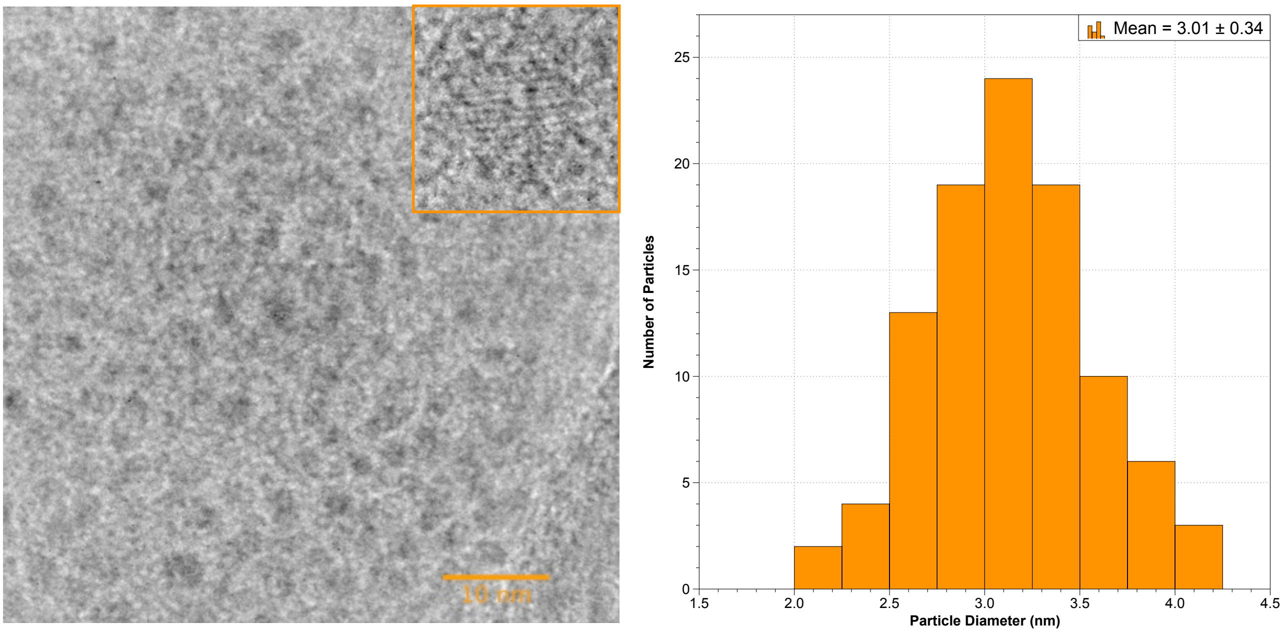

Figure S18a Representative TEM image of catalyst 10 at x300k with a magnified insert *(left)* and particle size distribution *(right)*

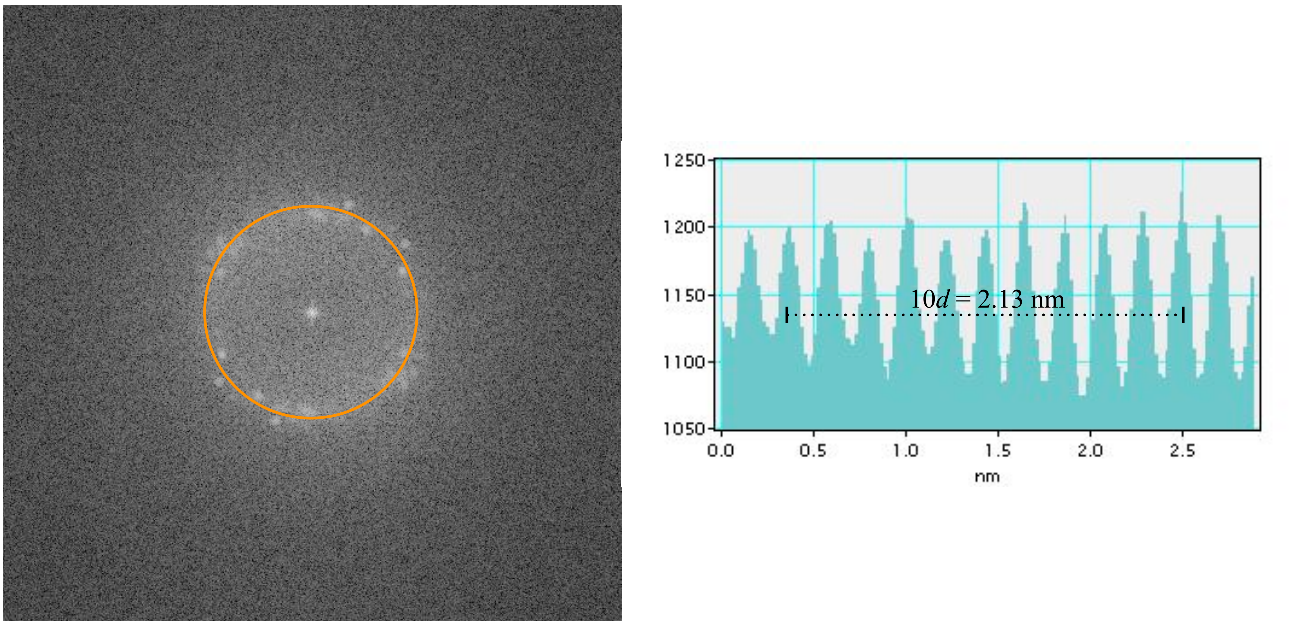

Figure 18b Representative Fourier transform image and fringe space analysis for catalyst 18 demonstrate an average *d* spacing of 2.13 Å corresponding to Cu (111)

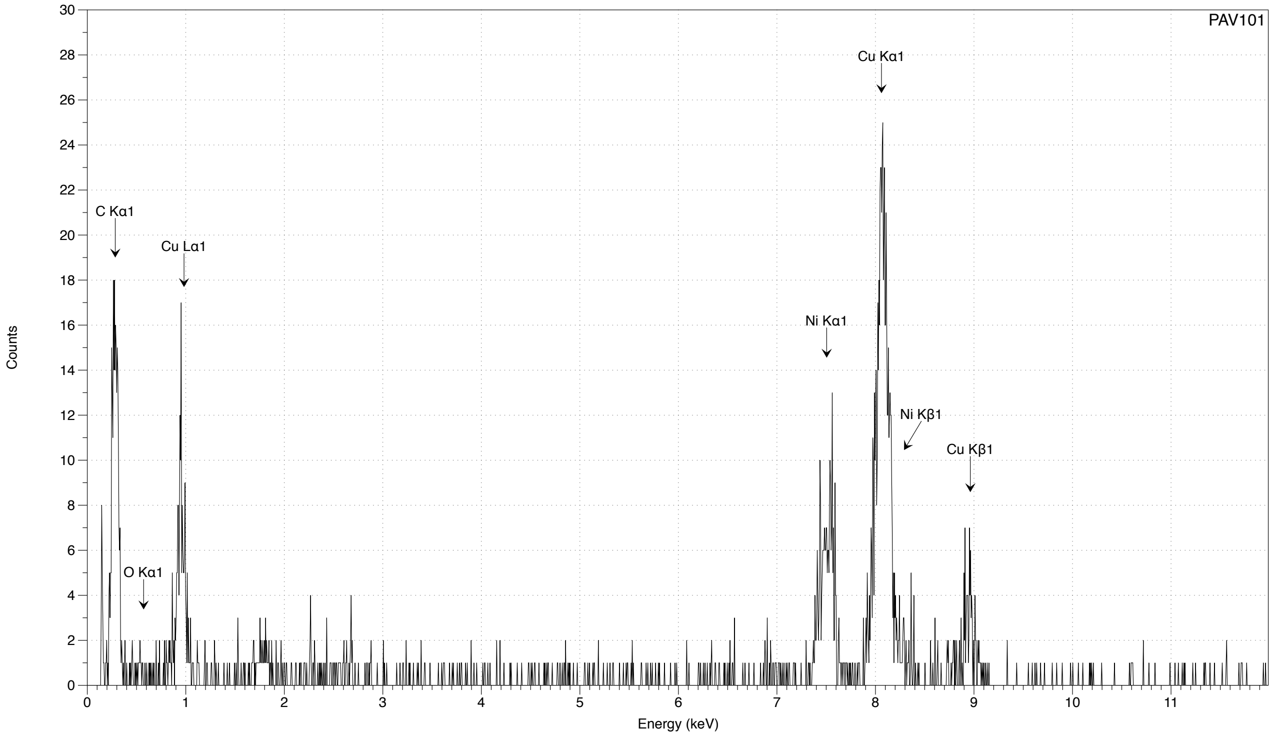

Figure S18c Representative narrow beam ED spectrum

Cu/PMMA120 19(reaction pav132)

$CuCl_2$ (67.22 mg, 0.50 mmol) and PMMA120 (300 mg, 3.0 mmol) were dissolved in THF:EtOH (20:20 ml) under Ar and the mixture was stirred for 2.5 h at 40°. The mixture was heated to reflux and $NaBH_4$ (37.83 mg, 1.00 mmol) in EtOH (10 ml) was added. The reaction was allowed to run to completion over 90 min to give a crude NP dispersion, an aliquot of which was purified and redispersed as for catalyst 13.

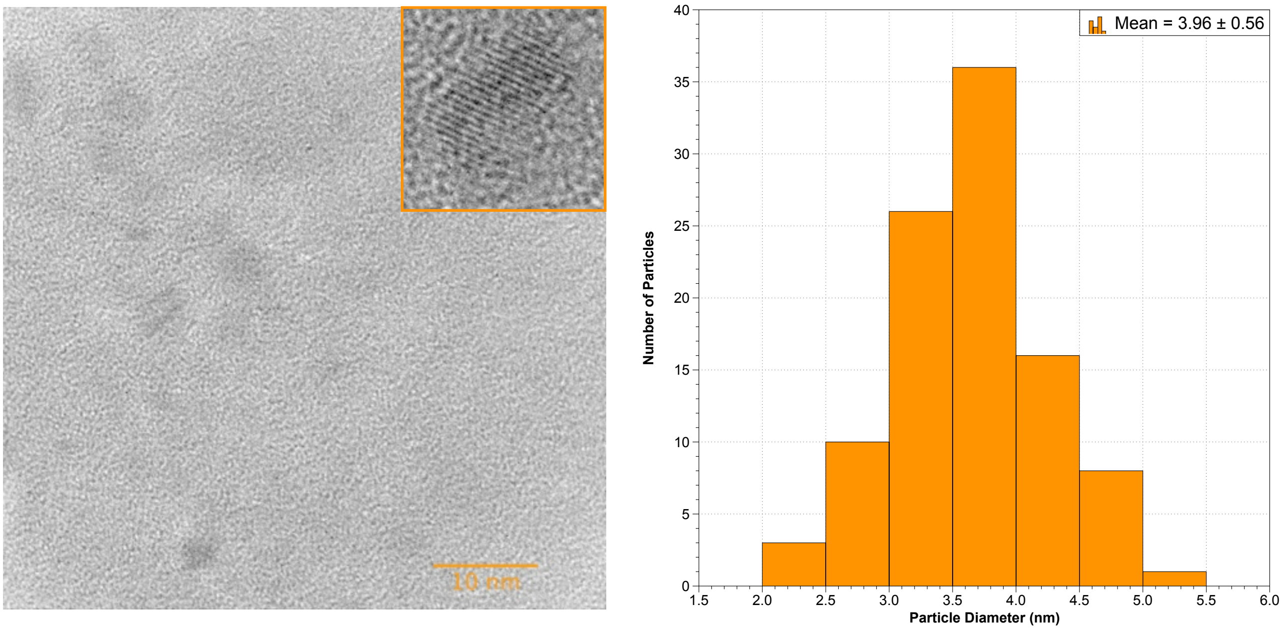

Figure S19a Representative TEM image of catalyst 90 at x300k with a magnified insert *(left)* and particle size distribution *(right)*

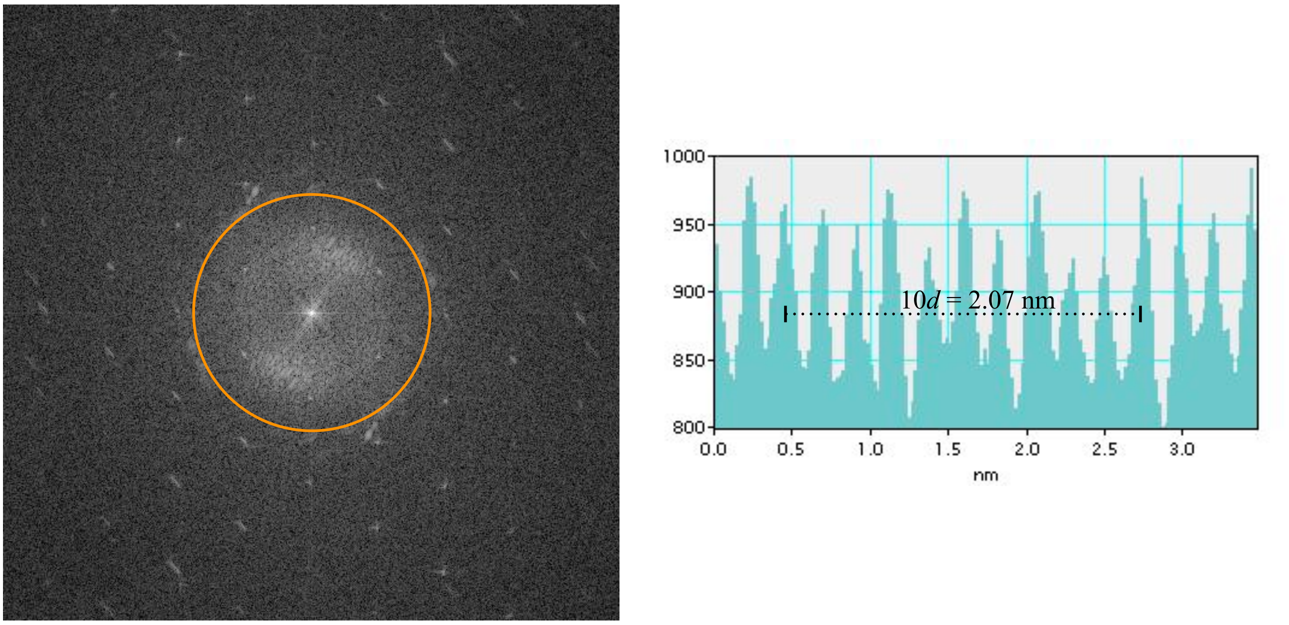

Figure 19b Representative Fourier transform image and fringe space analysis for catalyst 19 demonstrate an average *d* spacing of 2.07 Å corresponding to Cu (111)

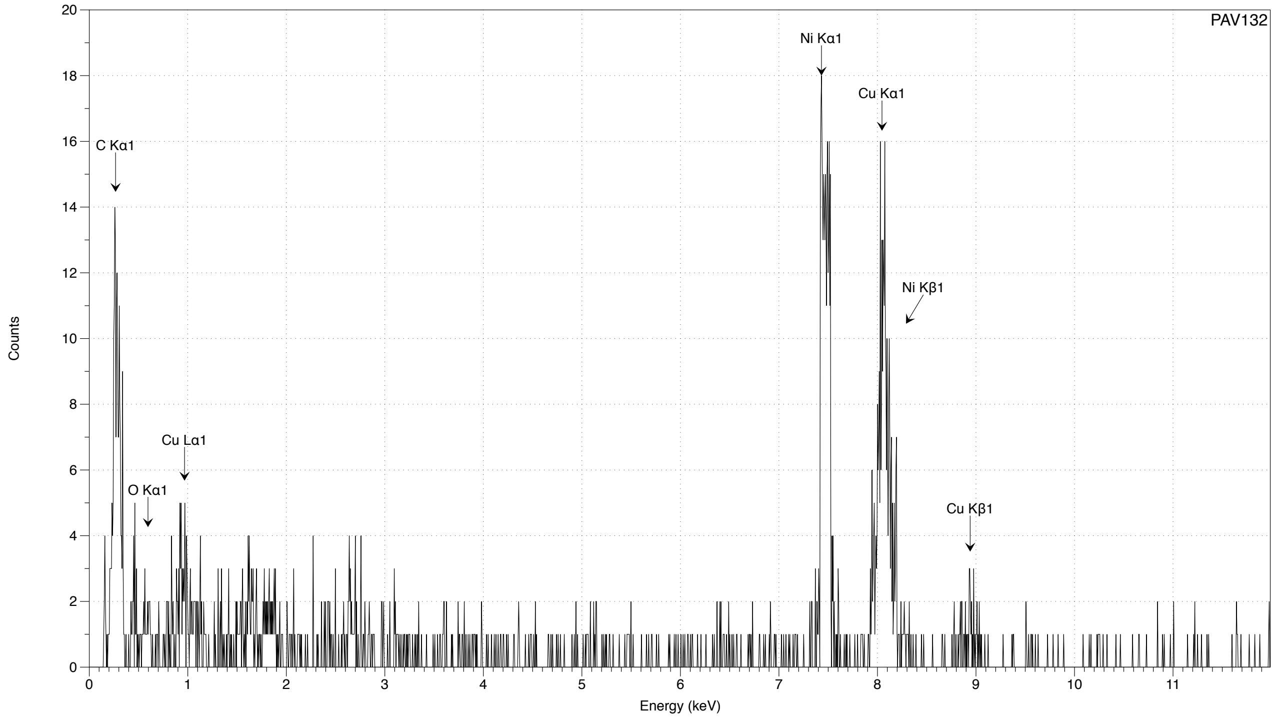

Figure S19c Representative narrow beam ED spectrum

Cu/PMMA120 20(reaction pav137)

$CuCl_2$ (67.22 mg, 0.50 mmol) and PMMA120 (300 mg, 3.00 mmol) were dissolved in THF (40 ml) under Ar and the mixture was stirred for 2.5 h at 40°C. The reaction mixture was heated to reflux after which a stock solution of N_2H_4 (1M in THF) (1.00 ml, 1.00 mmol) was added. The reaction was allowed to run to completion over 90 min to give a crude NP dispersion, an aliquot of which was purified and redispersed as for catalyst 13.

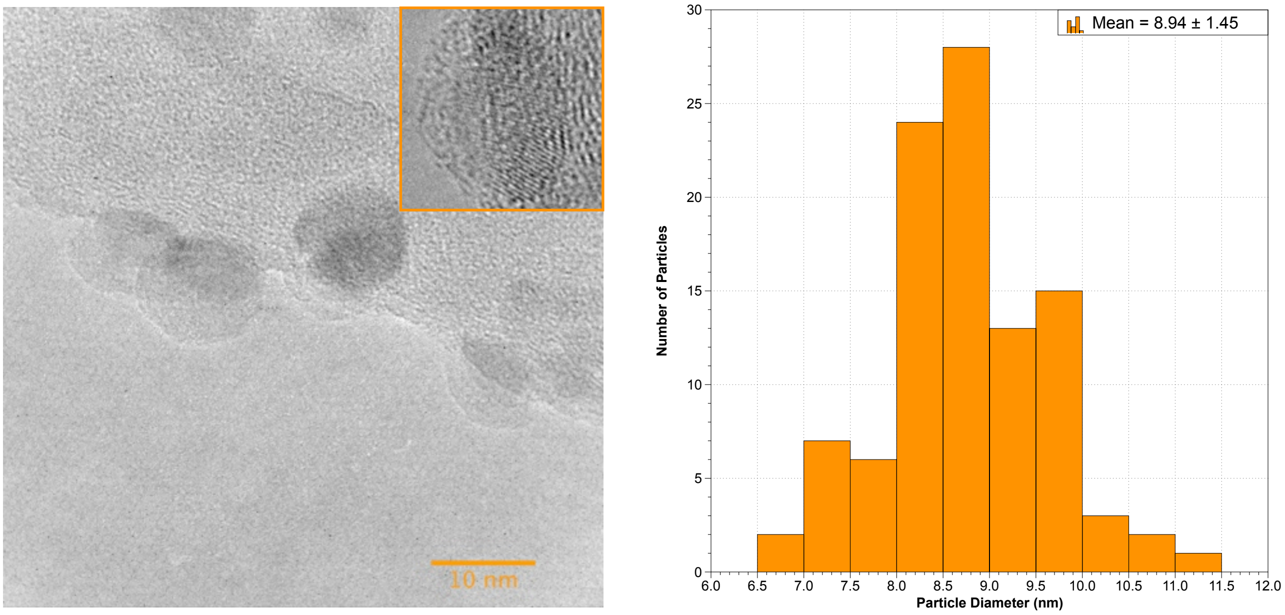

Figure S20a Representative TEM image of catalyst 20 at x300k with a magnified insert *(left)* and particle size distribution *(right)*

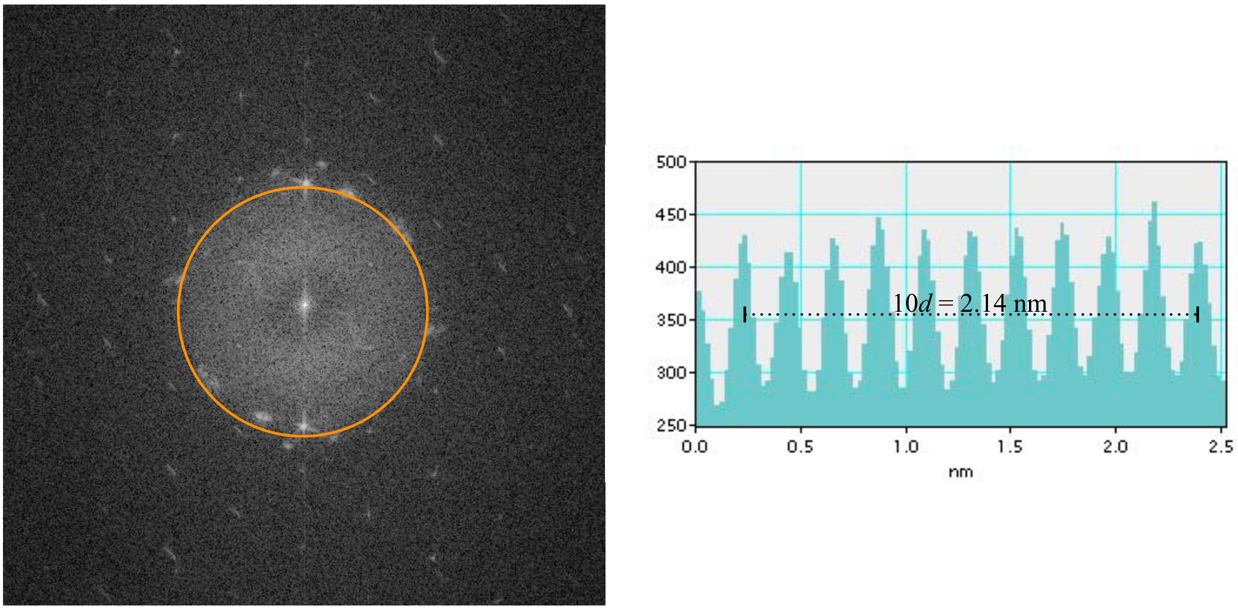

Figure 20b Representative Fourier transform image and fringe space analysis for catalyst 20 demonstrate an average *d* spacing of 2.14 Å corresponding to Cu (111)

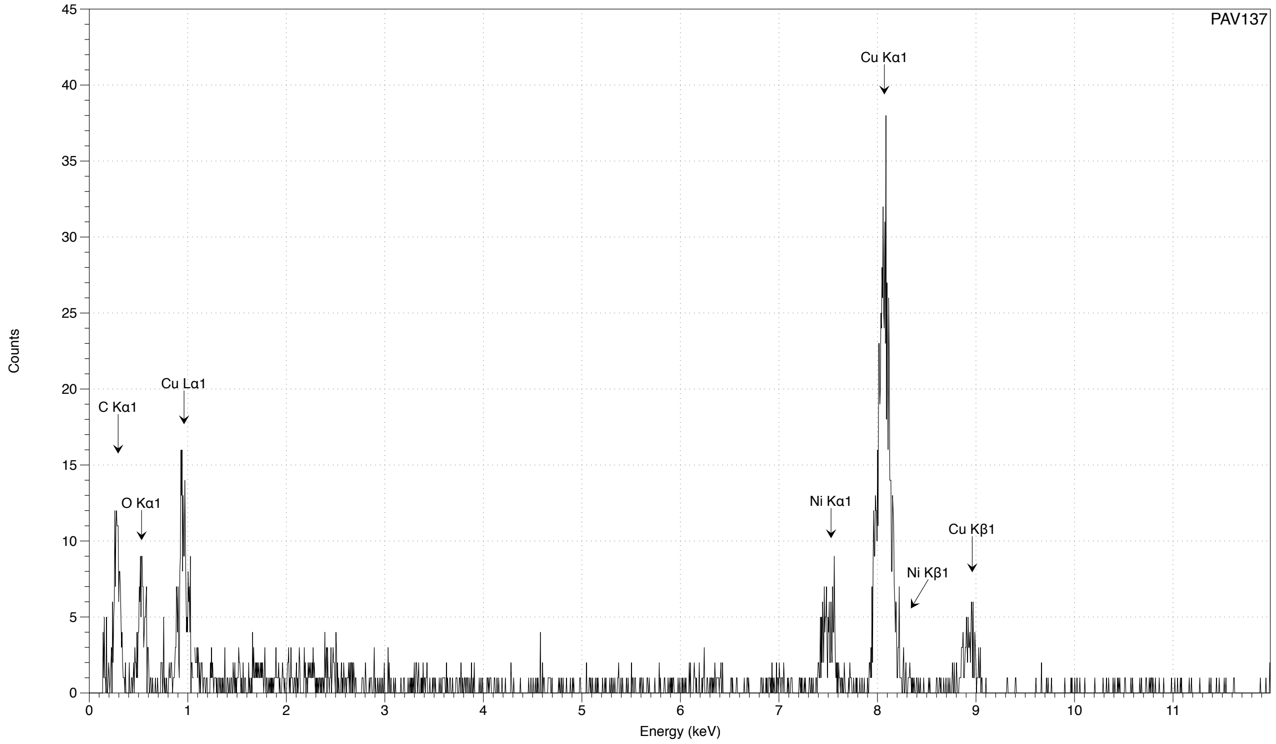

Figure S20c Representative narrow beam ED spectrum

Cu/PMMA120 21(reaction pav102)

$CuSO_4$ (79.81 mg, 0.50 mmol) and PMMA120 (300 mg, 3.00 mmol) were dissolved in THF (40 ml) under Ar and the mixture was stirred for 2.5 h at 40°C. The mixture was heated to reflux after which $NaBH_4$ (37.83 mg, 1.00 mmol) in EtOH (10 ml) was added. The reaction was allowed to run to completion over 90 min to give a crude NP dispersion, an aliquot of which was purified and redispersed as for catalyst 13.

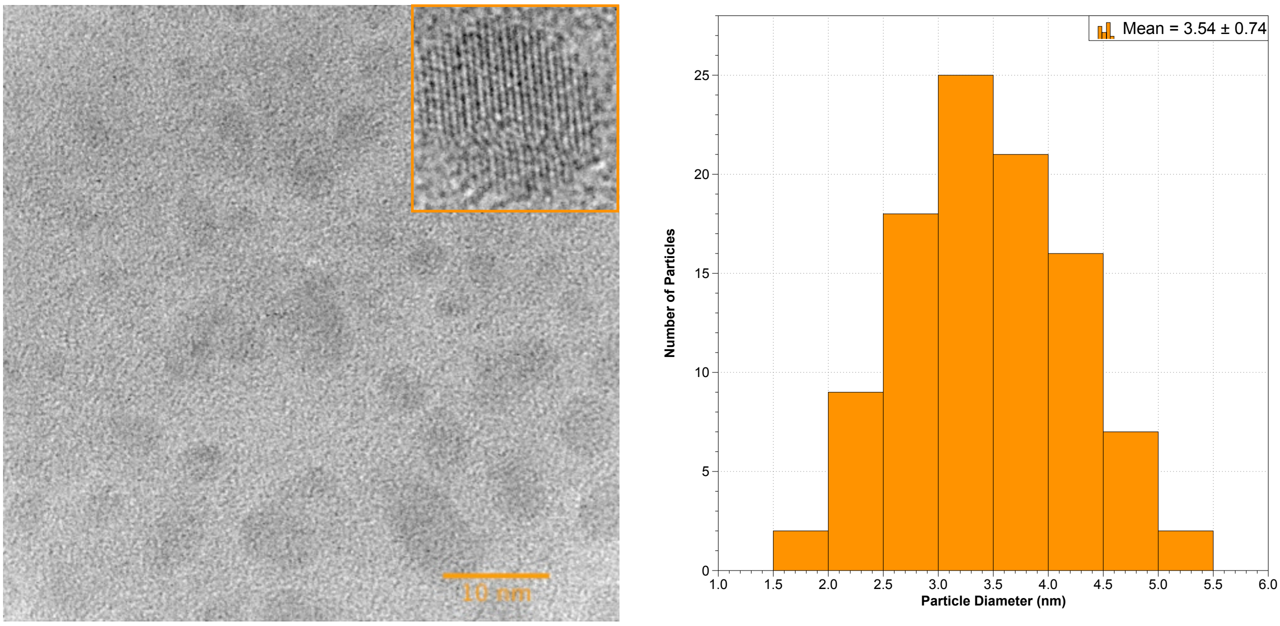

Figure S21a Representative TEM image of catalyst 21 at x300k with a magnified insert *(left)* and particle size distribution *(right)*

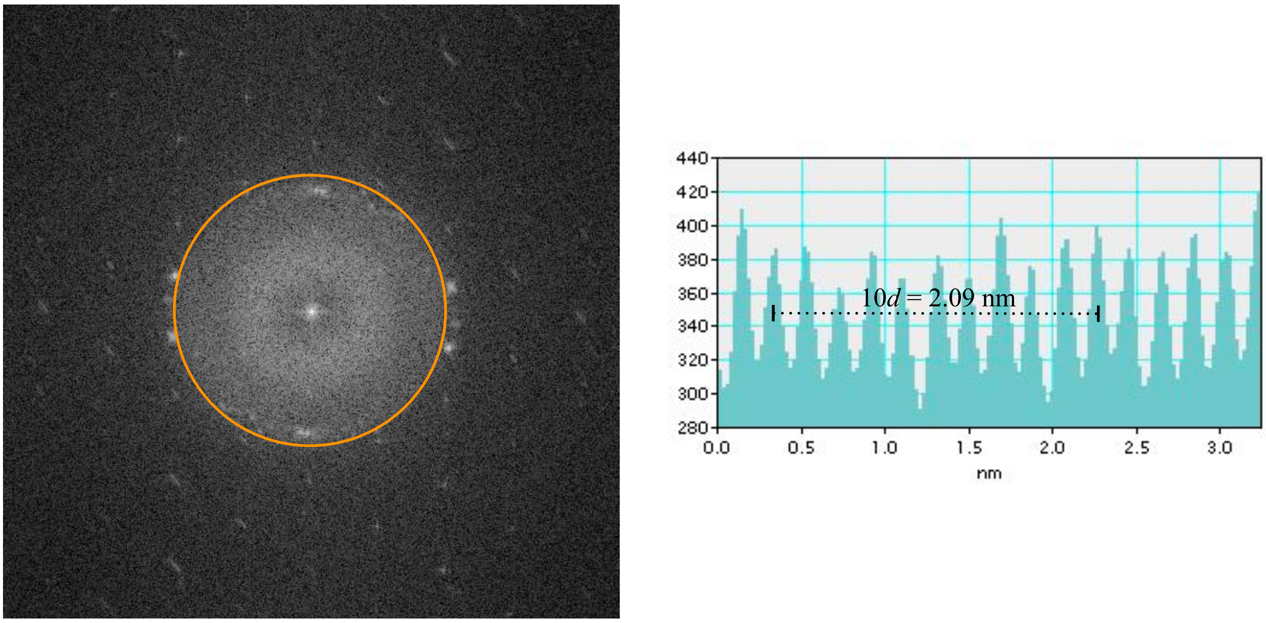

Figure 21b Representative Fourier transform image and fringe space analysis for catalyst 21 demonstrate an average d spacing of 2.09 Å corresponding to Cu (111)

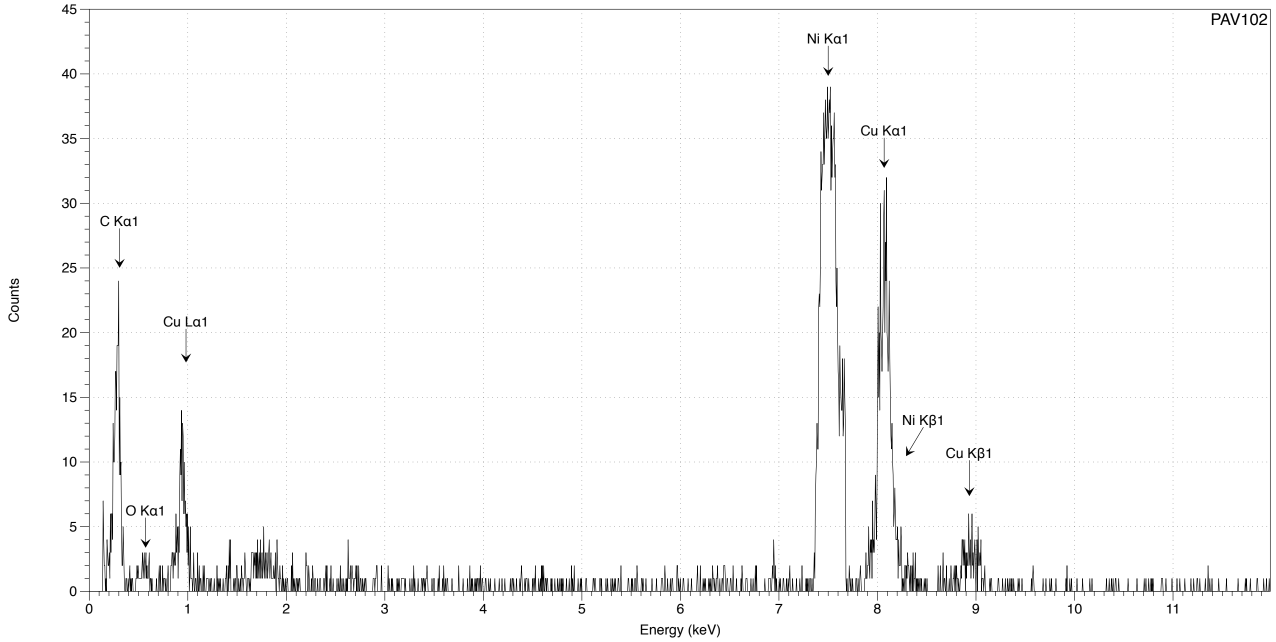

Figure S21c Representative narrow beam ED spectrum

25:75 CuZn/PVP29 22(reaction pav58)

$CuSO_4{\bullet}5H_2O$ (62.42 mg, 0.25 mmol) and PVP29 (1.11 g, 10.00 mmol) were dissolved in ethylene glycol (120 ml) under Ar and the mixture was stirred for 2 h at 80°C. This solution was cooled to 0°C and $ZnCl_2$ (102.23 mg, 0.75 mmol) in H_2O (MiliQ, 2 ml) was added. The pH of the resulting mixture was adjusted to *ca*. 10 by adding NaOH (aq) (1 M, 5 ml). The mixture was stirred for 15 min after which $NaH_2PO_2{\bullet}H_2O$ (211.98 mg, 2 mmol) in deionized water (2 ml) was added. The reaction was stirred at 140°C for 90 min to give a crude NP dispersion, an aliquot of which was purified and redispersed as for catalyst 1.

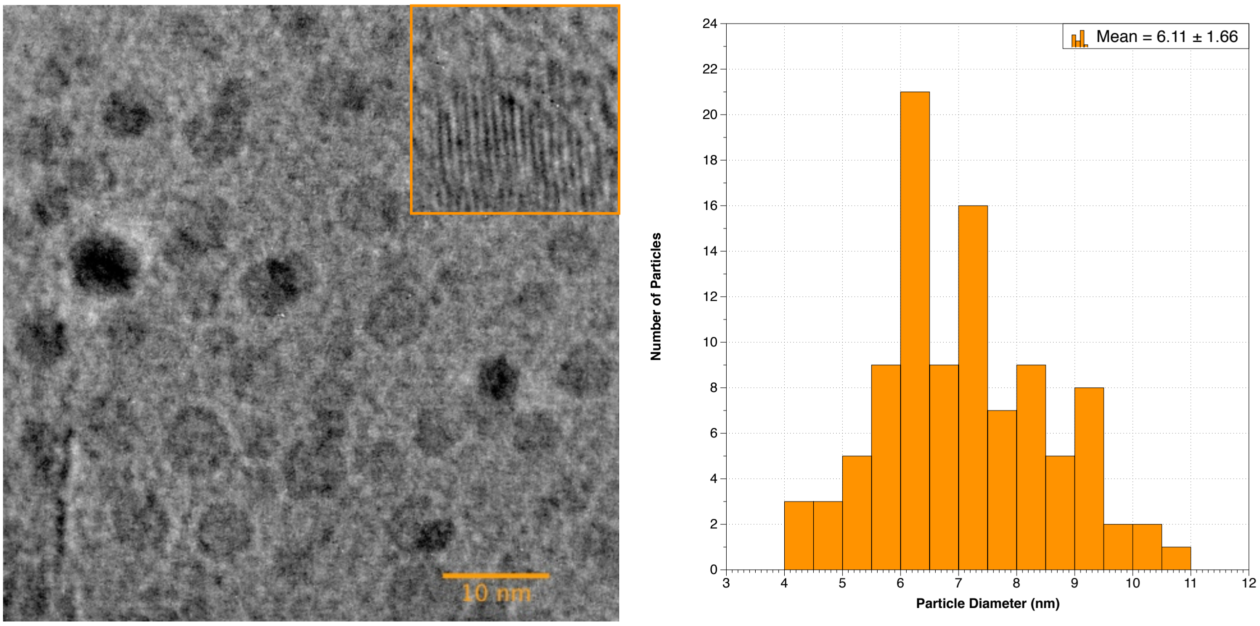

Figure S22a Representative TEM image of catalyst 22 at x300k with a magnified insert *(left)* and particle size distribution *(right)*

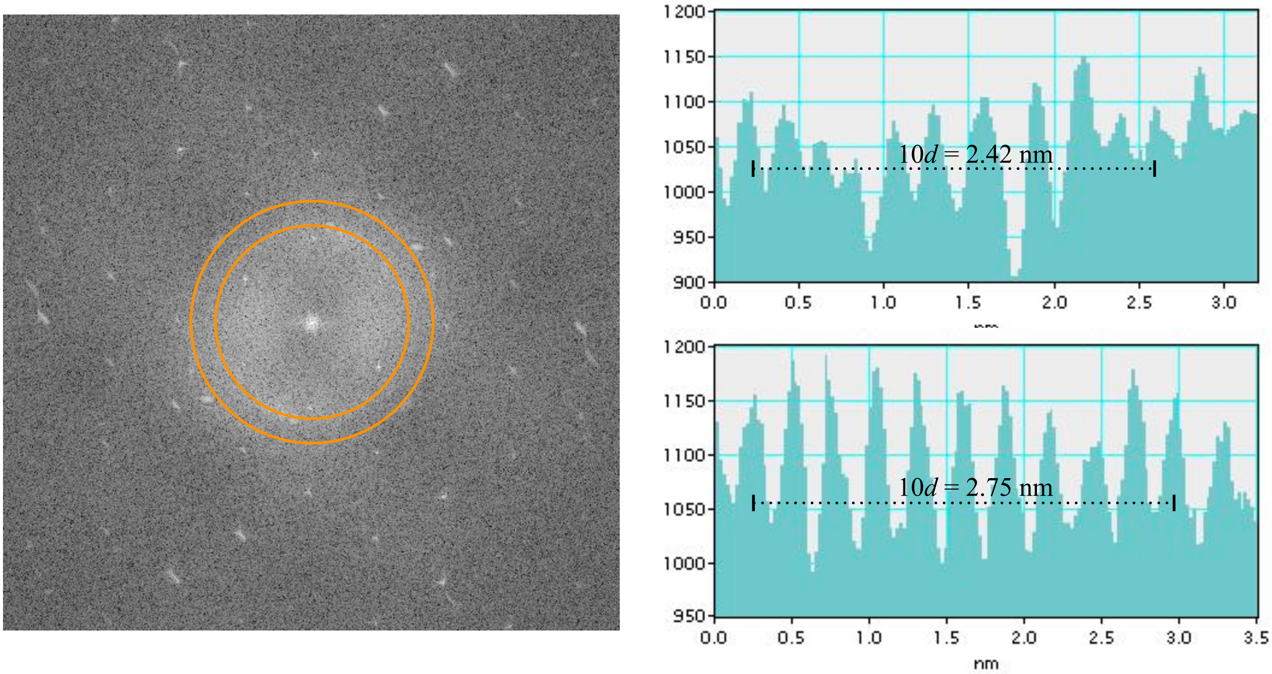

Figure 22b Representative Fourier transform image and fringe space analysis for catalyst 22 demonstrate average *d* spacings of 2.42 Å and 2.75 Å corresponding to Cu_2O (111) and ZnO (100), respectively

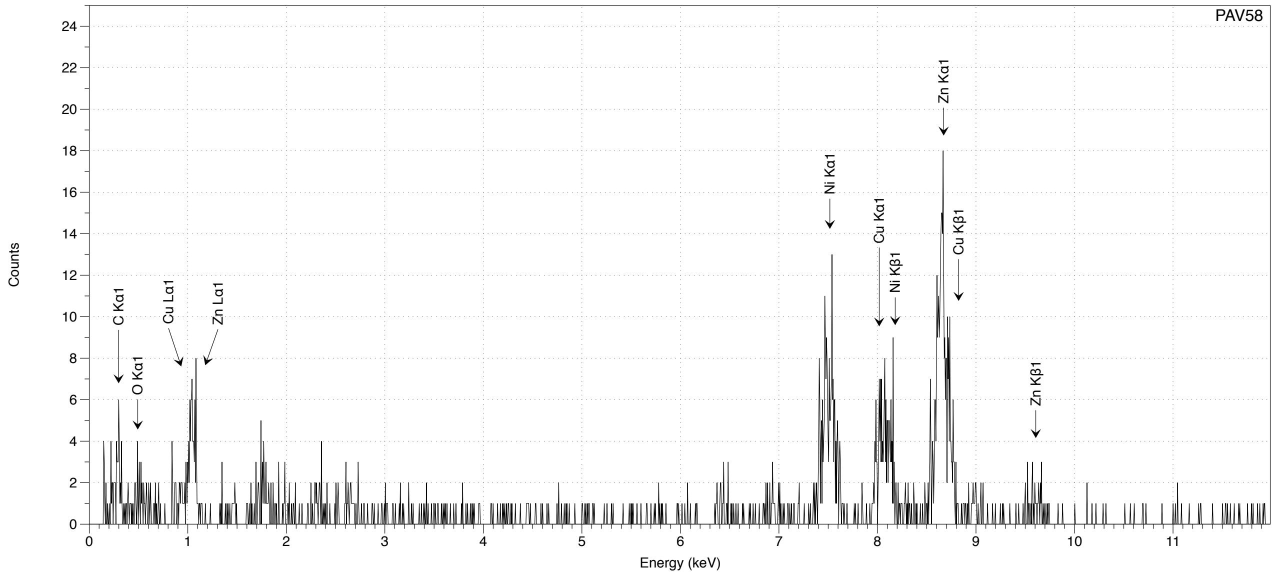

Figure S22c Representative narrow beam ED spectrum reveals emission lines for Cu and stronger lines for Zn. Peak integration and background subtraction reveals the actual approximate Cu:Zn ratio for this region to be 0.26

50:50 CuZn/PVP29 23(reaction pav56)

$CuSO_4$•$5H_2O$ (124.85 mg, 0.50 mmol) and PVP29 (1.11 mg, 10.0 mmol) were dissolved in ethylene glycol (120 ml) under Ar and the mixture was stirred for 2 h at 80°C. This solution was cooled to 0°C and $ZnCl_2$ (68.15 mg, 0.5 mmol) in H_2O (MiliQ, 2 ml) was added. The pH of the resulting mixture was adjusted to *ca*. 10 by adding NaOH (aq) (1M, 5 ml). The mixture was stirred for 15 min after which NaH_2PO_2•H_2O (211.98 mg, 2 mmol) in deionized water (2 ml) was added. The reaction was stirred at 140°C for 90 min to give a crude NP dispersion, an aliquot of which was purified and redispersed as for catalyst 1.

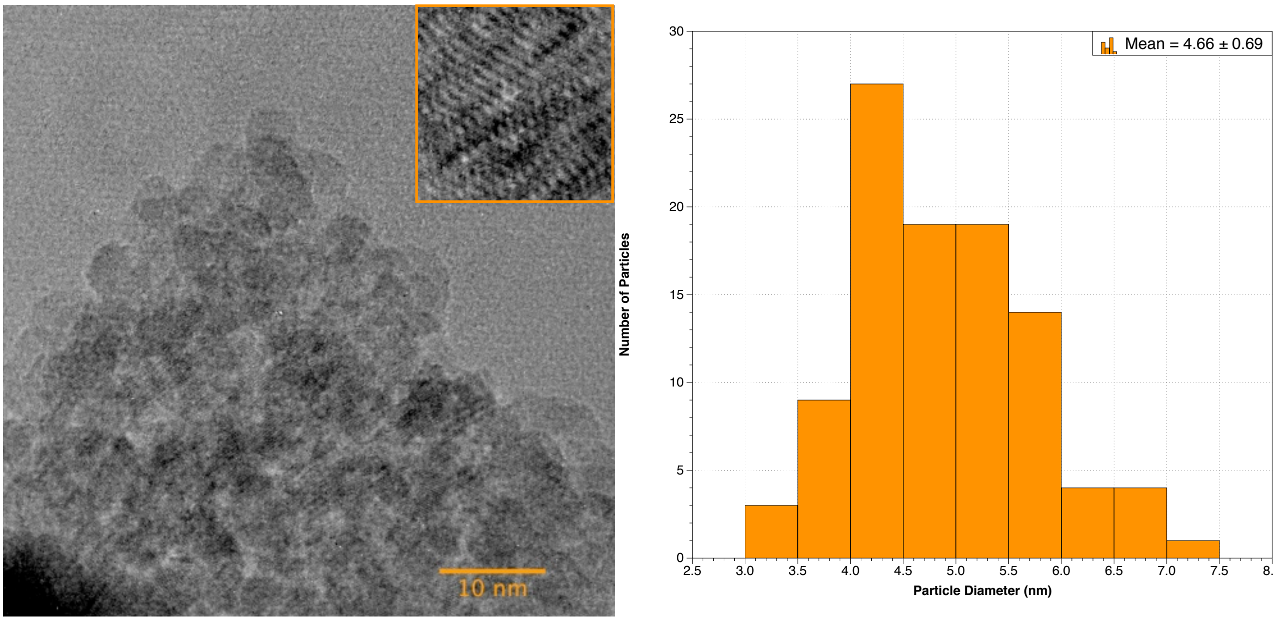

Figure S23a Representative TEM image of catalyst 23 at x300k with a magnified insert *(left)* and particle size distribution *(right)*

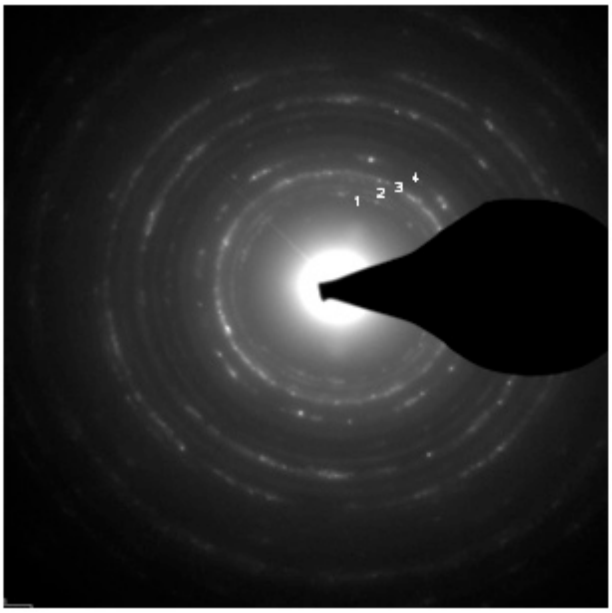

Lattice spacing / Å	Phase
3.02	Cu_2O (110)
2.82	ZnO (100)
2.48	Cu_2O (111)/ ZnO(110)
2.14	Cu_2O (200)

Figure S23b Electron diffraction pattern demonstrates the presence of Cu_2O and ZnO

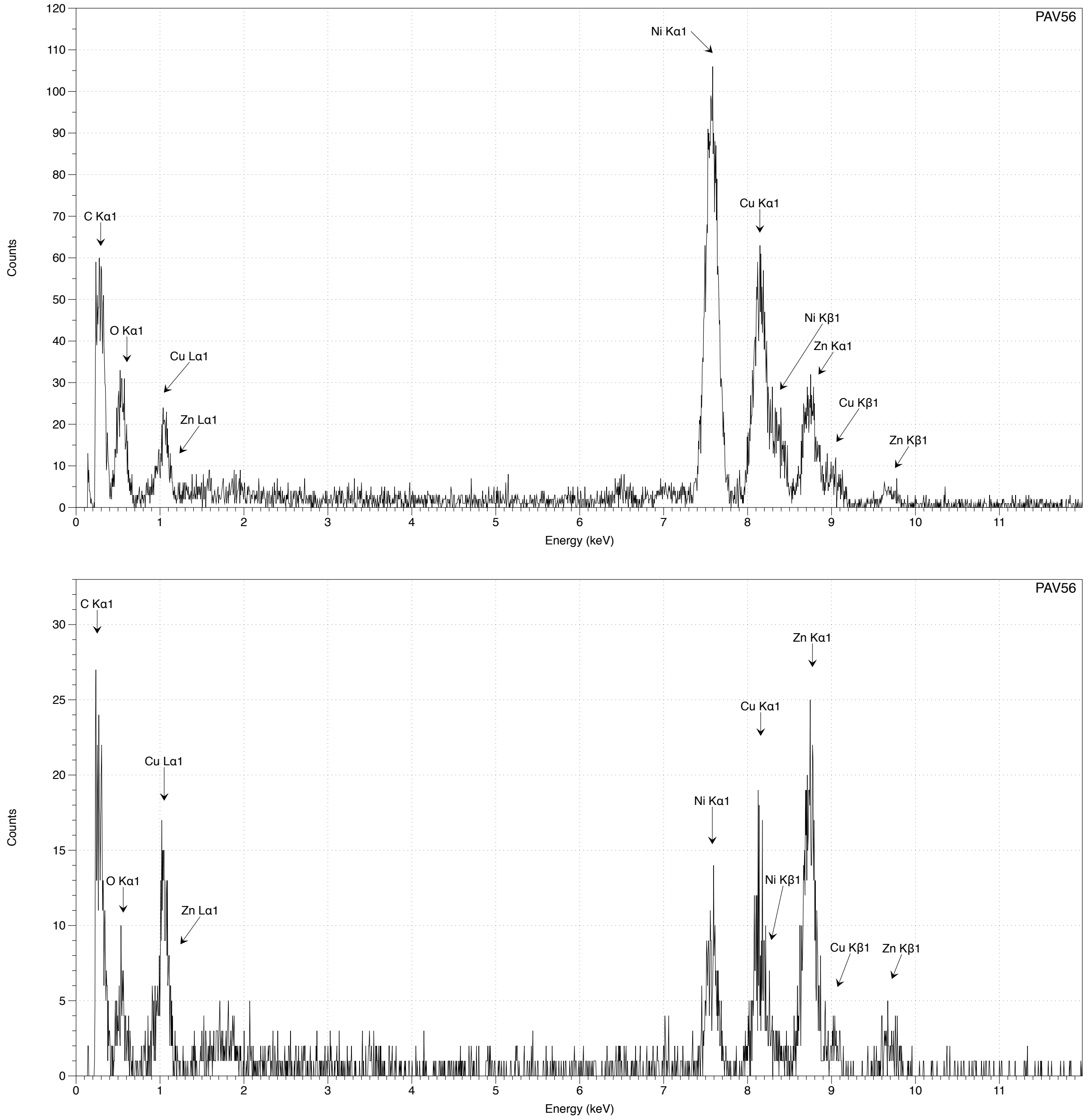

Figure S23c Representative narrow beam ED spectra reveal emission lines for Cu and Zn, suggesting the presence of Cu-rich *(top)* and Zn-rich *(bottom)* regions and pointing to segregation of the metals (consistent with the formation of ZnO). Peak integration and background subtraction reveals the actual approximate Cu:Zn ratio for these regions to be 1.84 and 0.61 respectively

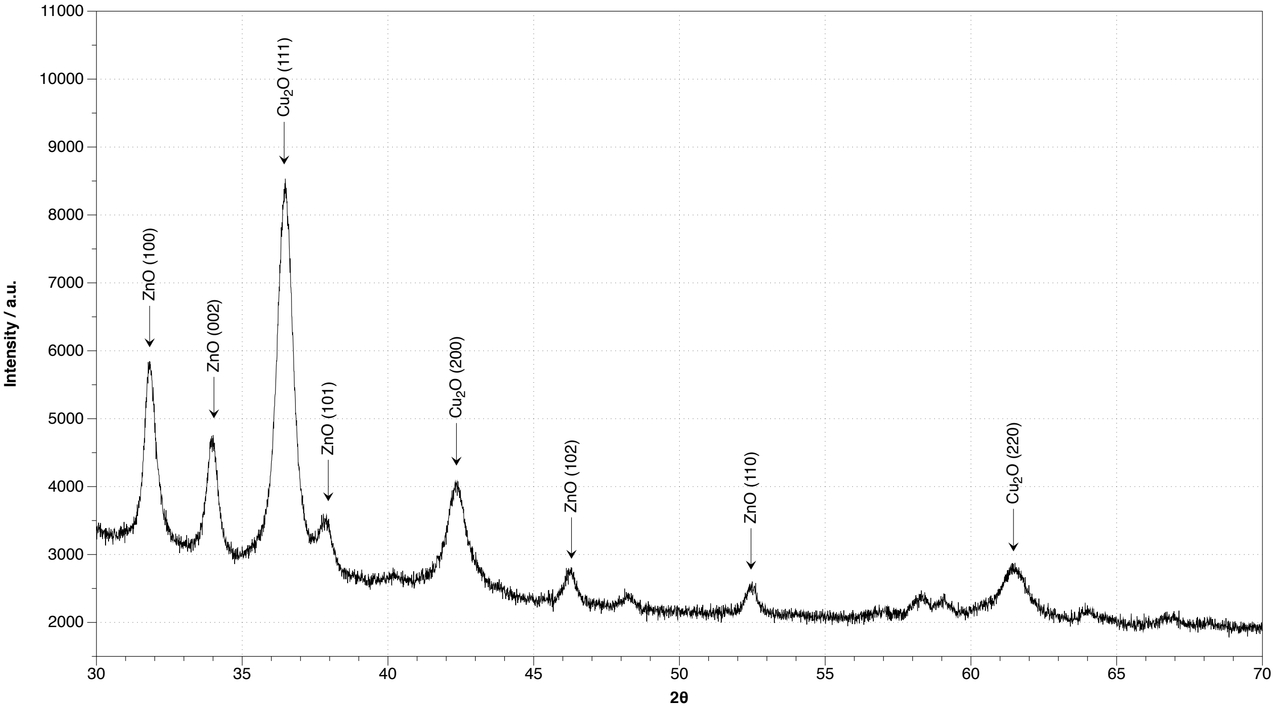

Figure S23d XRPD pattern of fresh catalyst 23 demonstrates the presence of Cu_2O and ZnO

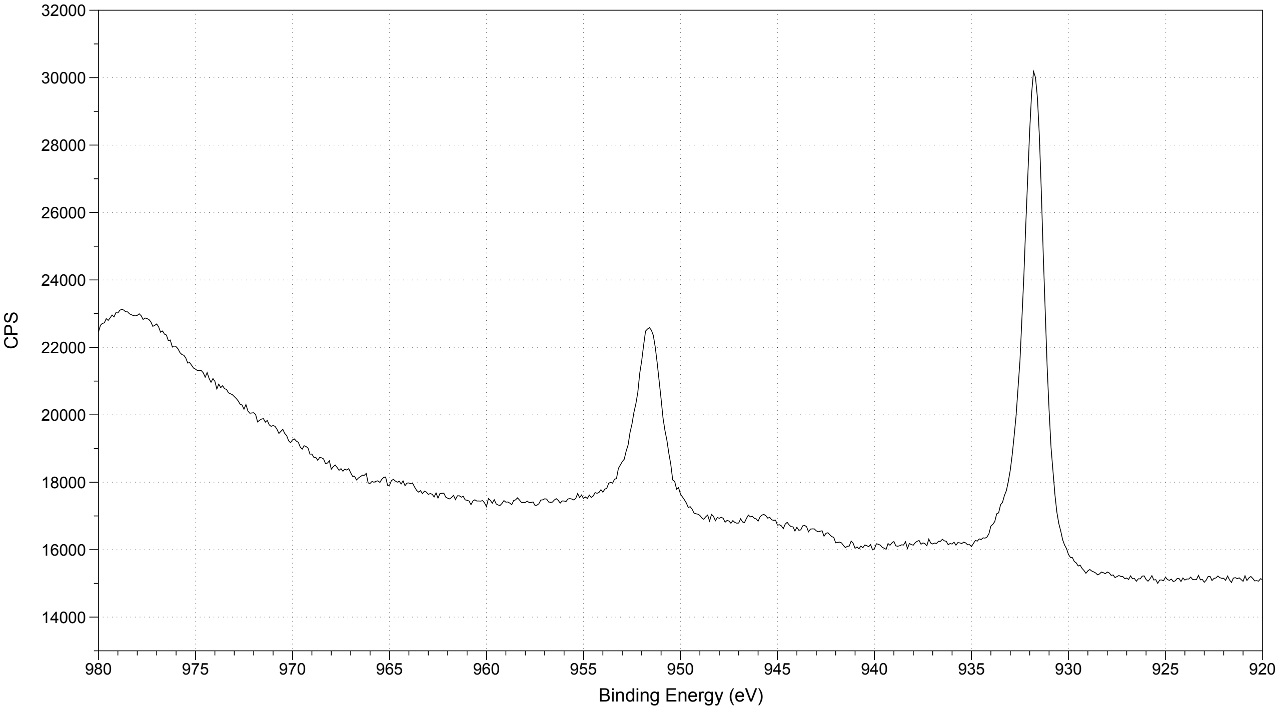

Figure S23e XPS data Cu $2p_{1/2}$ and $2p_{3/2}$ region shows Cu_2O signal at 932.5 eV

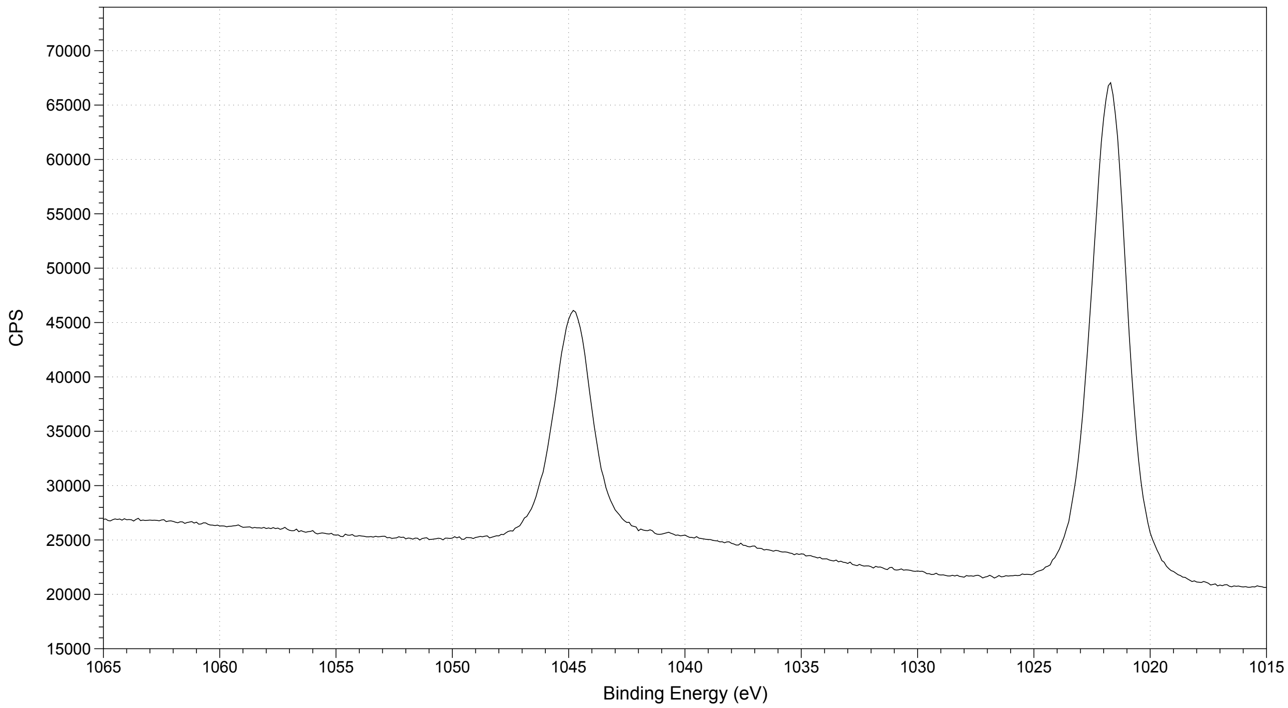

Figure S23f XPS data Zn $2p_{1/2}$ and $2p_{3/2}$ region shows peaks at 1044.6 eV and 1021.4 eV consistent with ZnO

75:25 CuZn/PVP29 24(reaction pav57)

$CuSO_4$•$5H_2O$ (187.27 mg, 0.75 mmol) and PVP29 (1.11 g, 10.0 mmol) were dissolved in ethylene glycol (120 ml) under Ar and the mixture was stirred for 2 h at 80°C. This solution was cooled to 0°C and $ZnCl_2$ (31.57 mg, 0.25 mmol) in H_2O (MiliQ, 2 ml) was added. The pH of the resulting mixture was adjusted to *ca*. 10 by adding 1 M NaOH (aq). The mixture was stirred for 15 min after which NaH_2PO_2•H_2O (211.98 mg, 2 mmol) in deionized water (2 ml) was added. The reaction was stirred at 140°C for 90 min to give a crude NP dispersion, an aliquot of which was purified and redispersed as for catalyst 1.

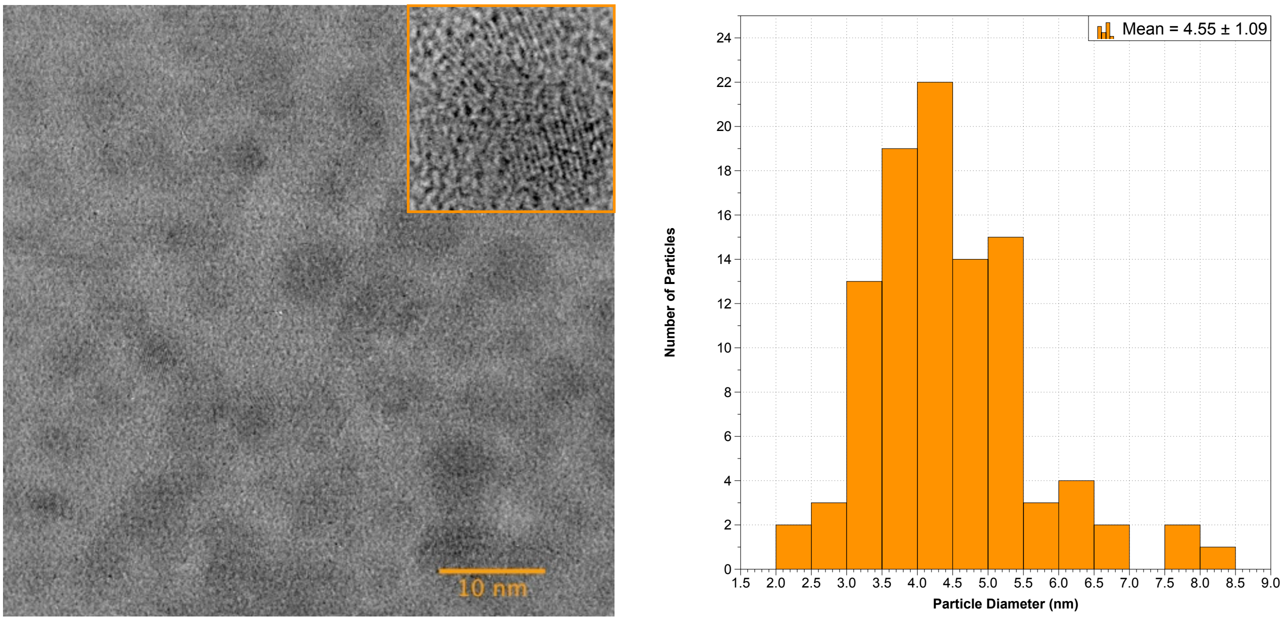

Figure S24a Representative TEM image of catalyst 23 at x300k with a magnified insert *(left)* and particle size distribution *(right)*

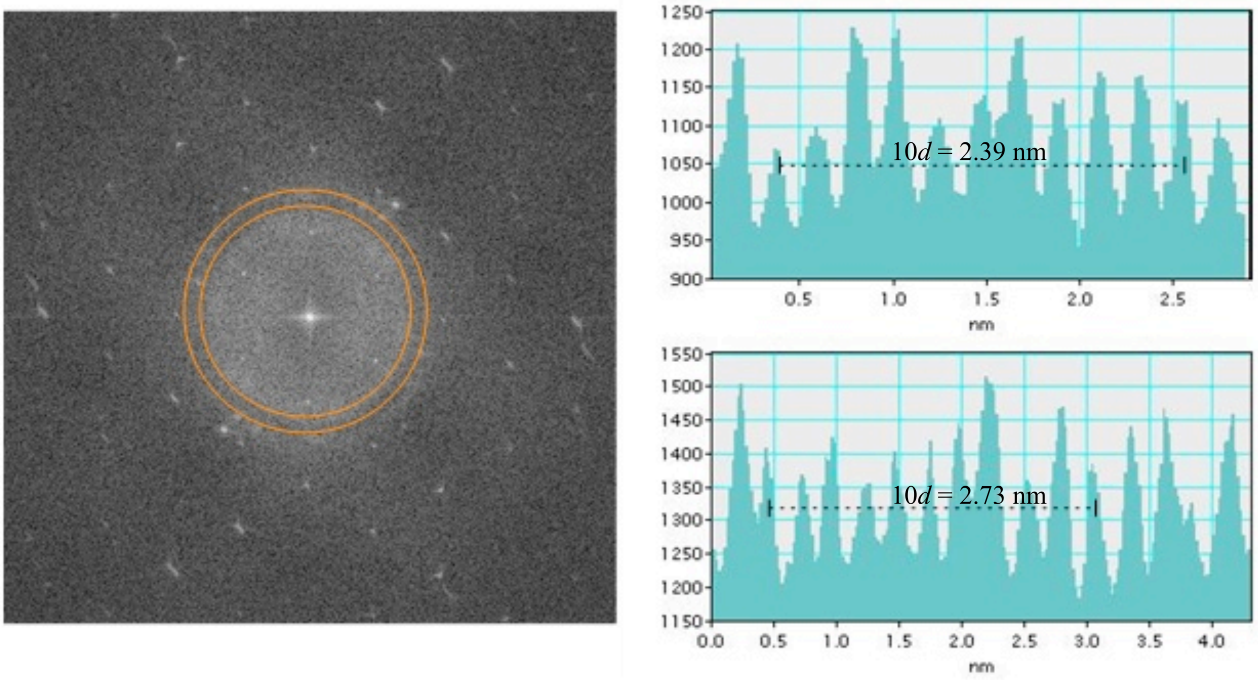

Figure 24b Representative Fourier transform image and fringe space analysis for catalyst 24 demonstrate average *d* spacings of 2.39 Å and 2.73 Å corresponding to Cu_2O (111) and ZnO (100), respectively

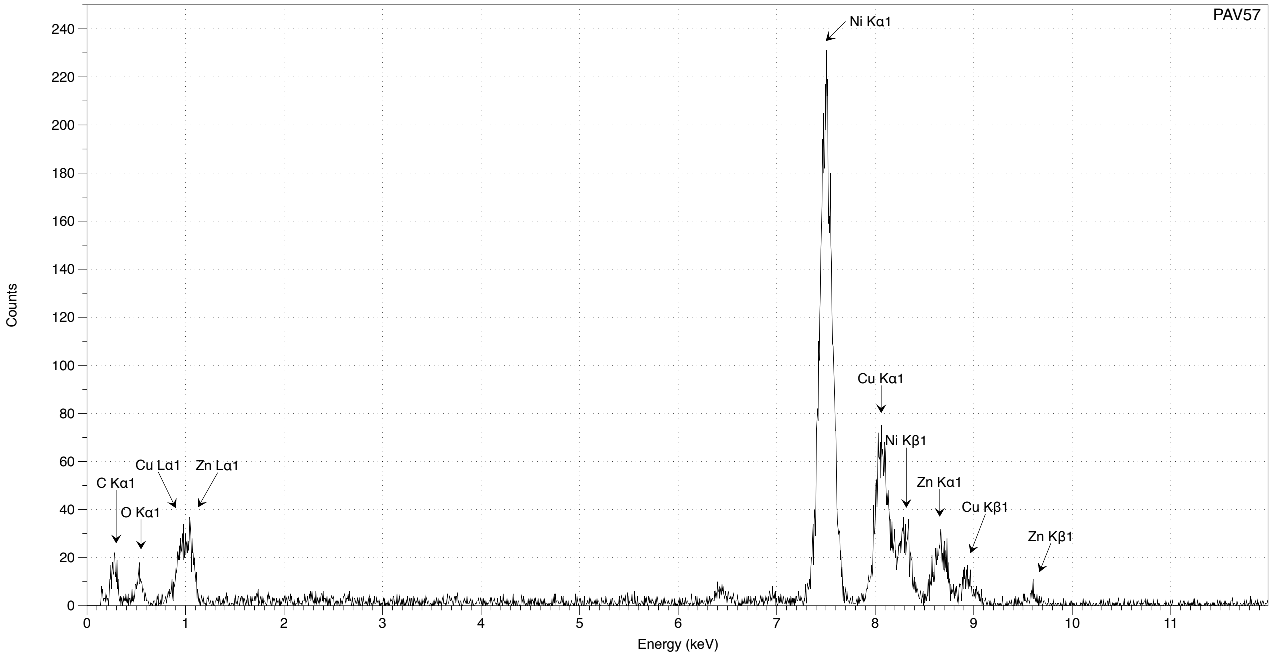

Figure S24c Representative narrow beam ED spectrum reveals strong emission lines for Cu and weak lines for Zn. Peak integration and background subtraction reveals the actual approximate Cu:Zn ratio for this region to be 4.16

25:75 CuZn/PVP29 25(reaction pav63)

$CuSO_4$ (39.90 mg, 0.25 mmol) and PVP29 (1.11 g, 10.00 mmol) were dissolved in anhydrous ethylene glycol (120 ml) under Ar and the mixture was stirred for 2 h at 80°C. This solution was cooled to 0°C and $ZnCl_2$ (102.23 mg, 0.75 mmol) in ethylene glycol (7 ml) was added. The pH was adjusted to *ca*. 10 by adding NaOH (1M in ethylene glycol, 5ml). The mixture was stirred for 15 min after which NaH_2PO_2 (175.96mg, 2 mmol) in ethylene glycol (5 ml) was added. The reaction was heated to 140°C for 90 min to give a crude NP dispersion, an aliquot of which was purified and redispersed as for catalyst 1.

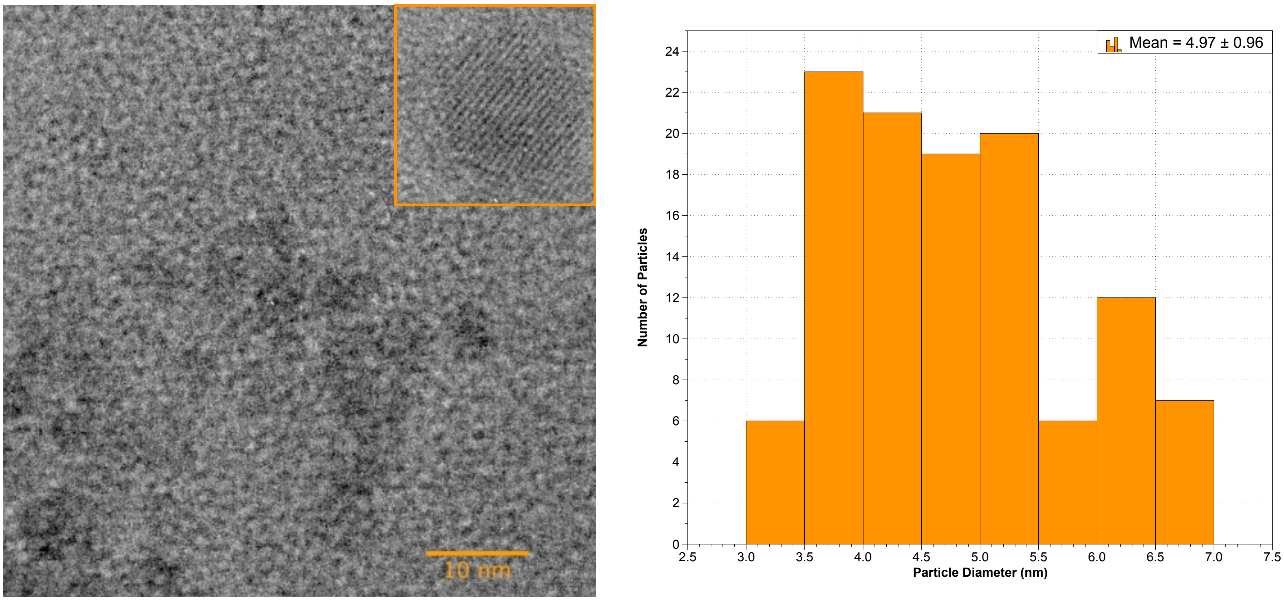

Figure S25a Representative TEM image of catalyst 25 at x300k with a magnified insert *(left)* and particle size distribution *(right)*

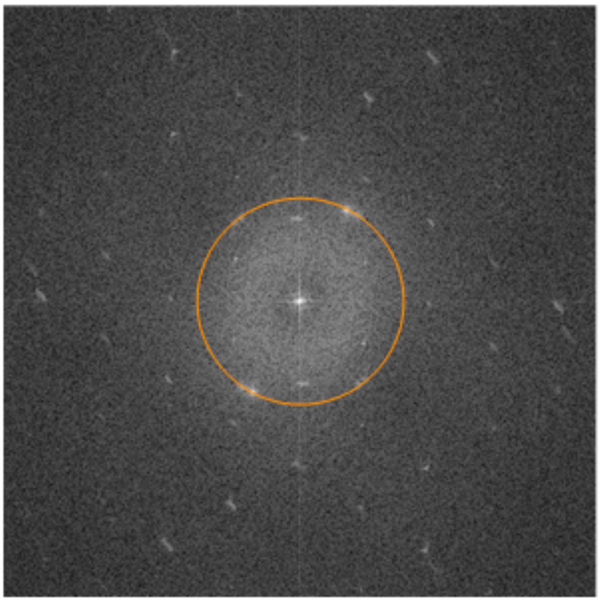

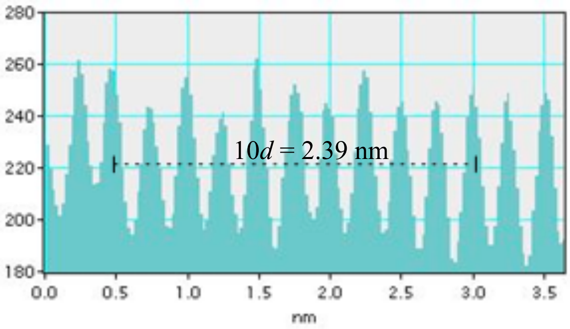

Figure 25b Fourier transform image and fringe space analysis for catalyst 25 demonstrate an average *d* spacing of 2.39 Å corresponding to Cu_2O (111)

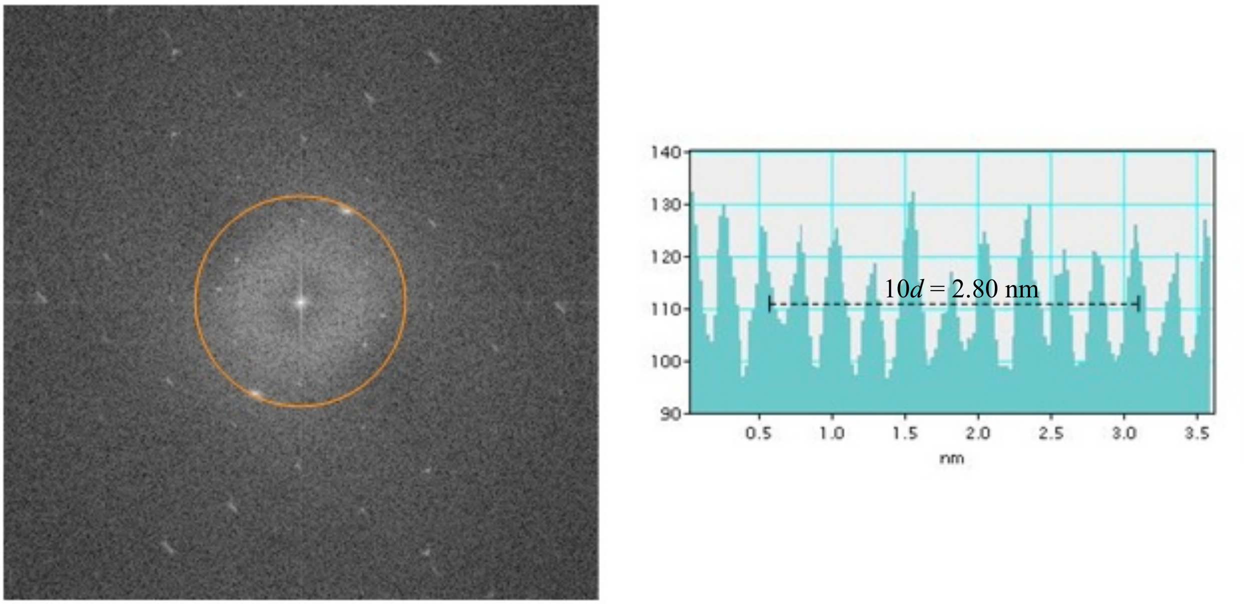

Figure 25c Fourier transform image and fringe space analysis for catalyst 25 demonstrate an average *d* spacing of 2.80 Å corresponding to ZnO (100)

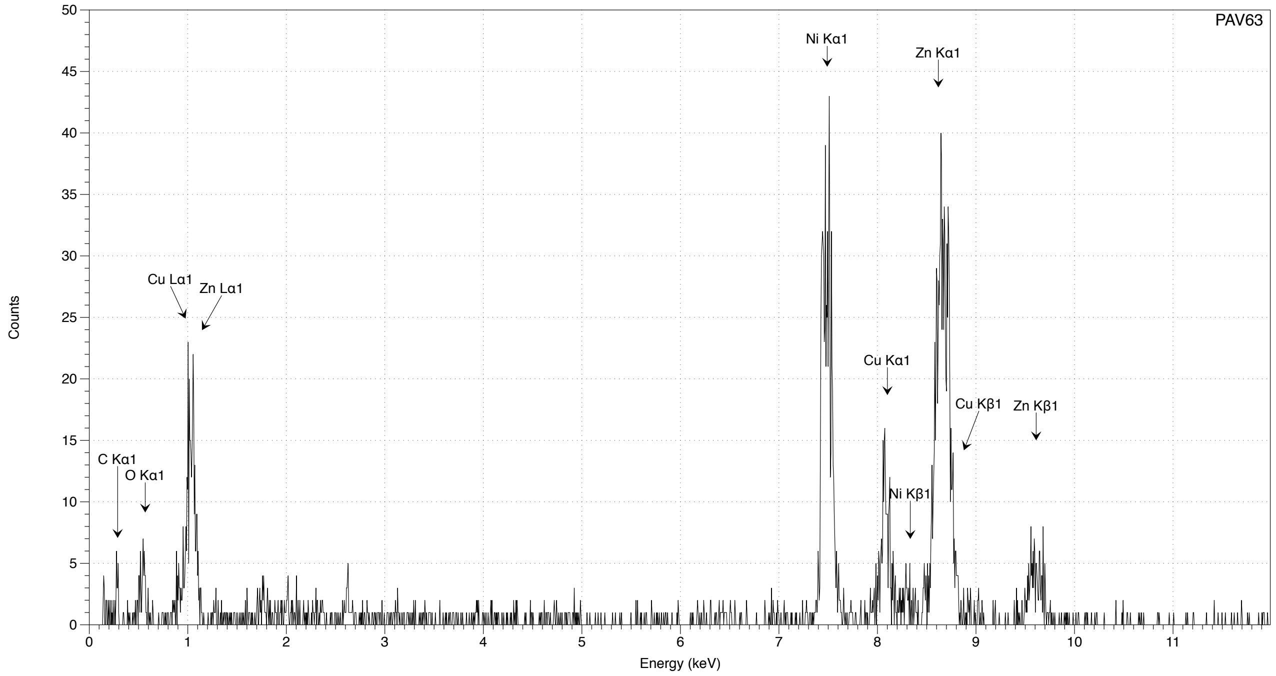

Figure S25d Representative narrow beam ED spectrum reveals weak emission lines for Cu and strong lines for Zn. Peak integration and background subtraction reveals the actual approximate Cu:Zn ratio for this region to be 0.63

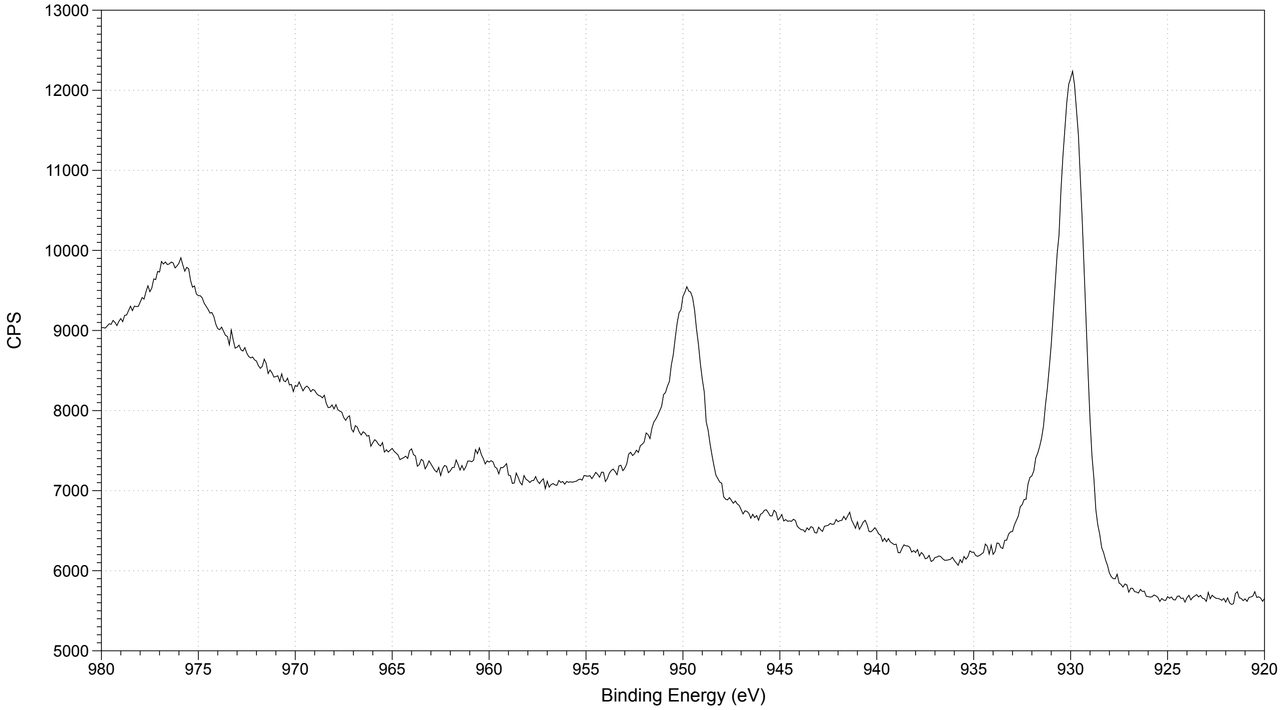

Figure S25e XPS data Cu $2p_{1/2}$ and $2p_{3/2}$ region shows major signal at 929.5 eV corresponding to Cu and evidence of a minor Cu_2O signal at 932.5 eV

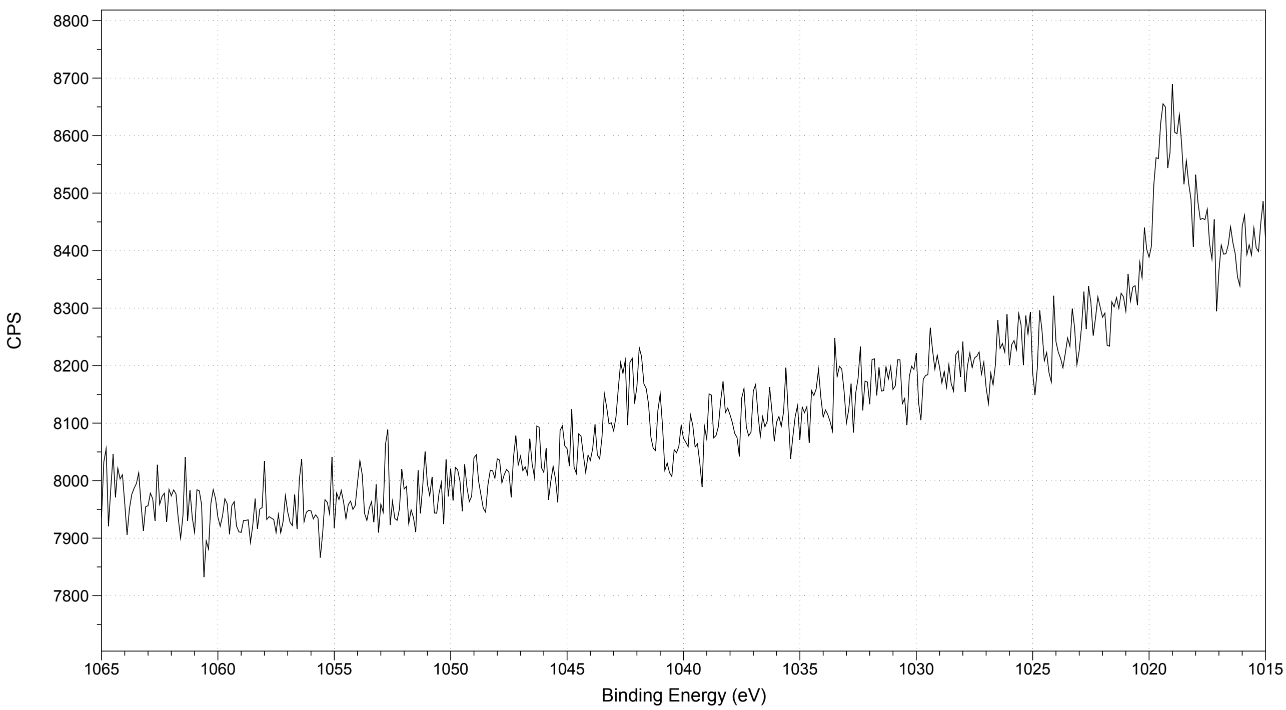

Figure S25f XPS data Zn $2p_{1/2}$ and $2p_{3/2}$ region shows peaks at 1042.5 eV and 1019.3 eV consistent with ZnO

50:50 CuZn/PVP29 26(reaction pav61)

$CuSO_4$ (79.81 mg, 0.50 mmol) and PVP29 (1.11 g, 10.00 mmol) were dissolved in anhydrous ethylene glycol (120 ml) under Ar and the mixture was stirred for 2 h at 80°C. This solution was cooled to 0°C and $ZnCl_2$ (68.15 mg, 0.5 mmol) in ethylene glycol (5 ml) was added. The pH was adjusted to *ca*. 10 by adding NaOH (1M in ethylene glycol, 5ml). The mixture was stirred for 15 min after which NaH_2PO_2 (175.96 mg, 2 mmol) in ethylene glycol (5 ml) was added. The reaction was heated to 140°C for 90 min to give a crude NP dispersion, an aliquot of which was purified and redispersed as for catalyst 1.

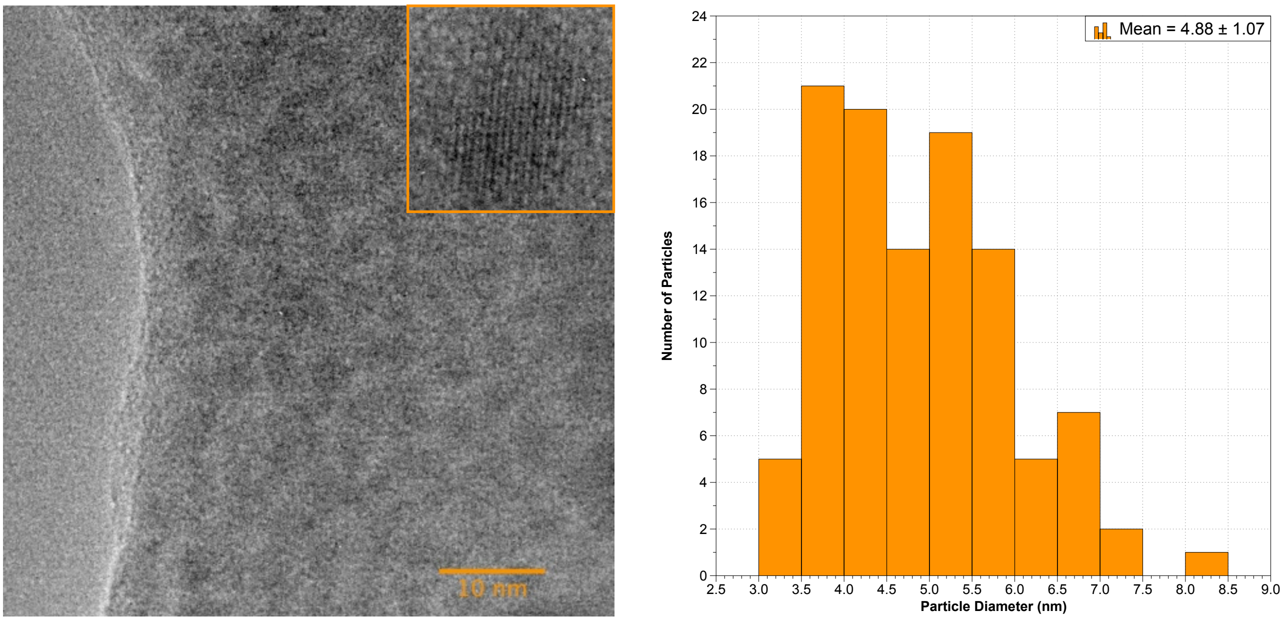

Figure S26a Representative TEM image of catalyst 26 at x300k with a magnified insert *(left)* and particle size distribution *(right)*

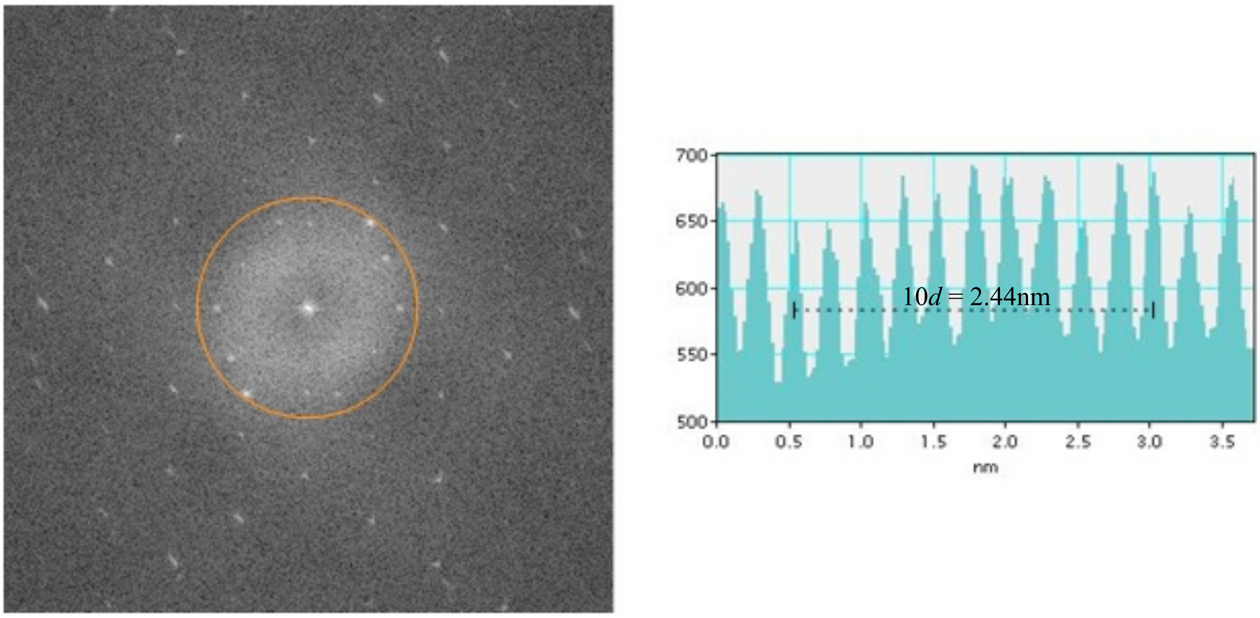

Figure 26b Fourier transform image and fringe space analysis for catalyst 26 demonstrate an average *d* spacing of 2.44 Å corresponding to Cu_2O (111)

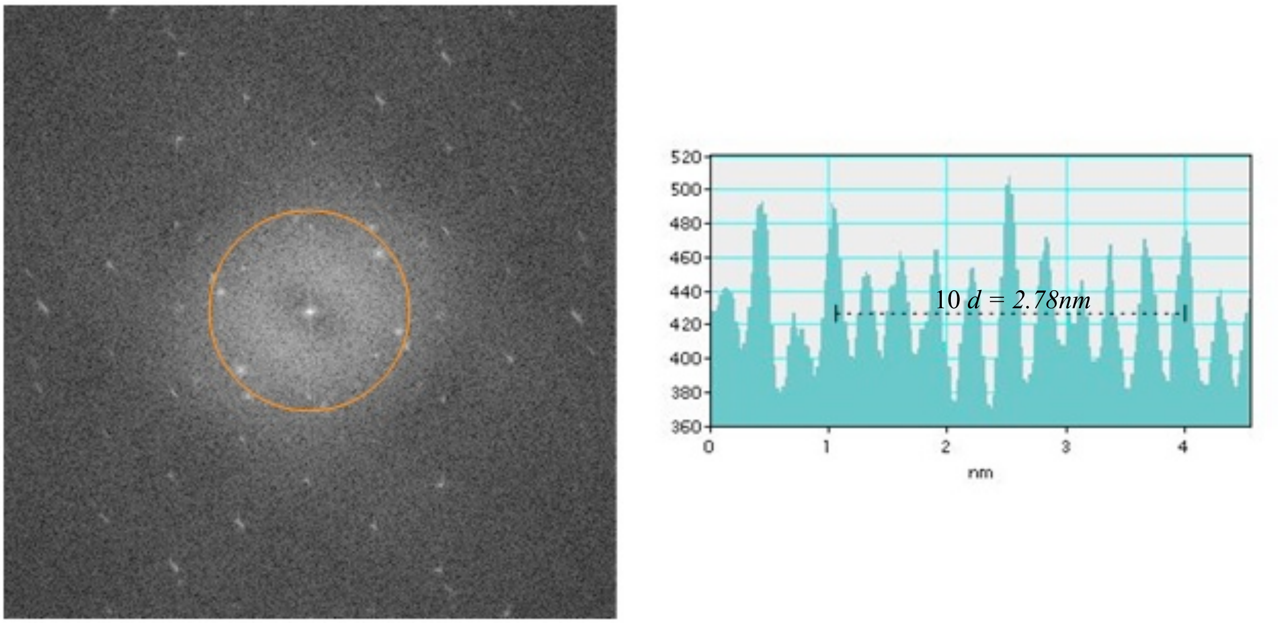

Figure 26c Fourier transform image and fringe space analysis for catalyst 26 demonstrate an average *d* spacing of 2.78 Å corresponding to ZnO (100)

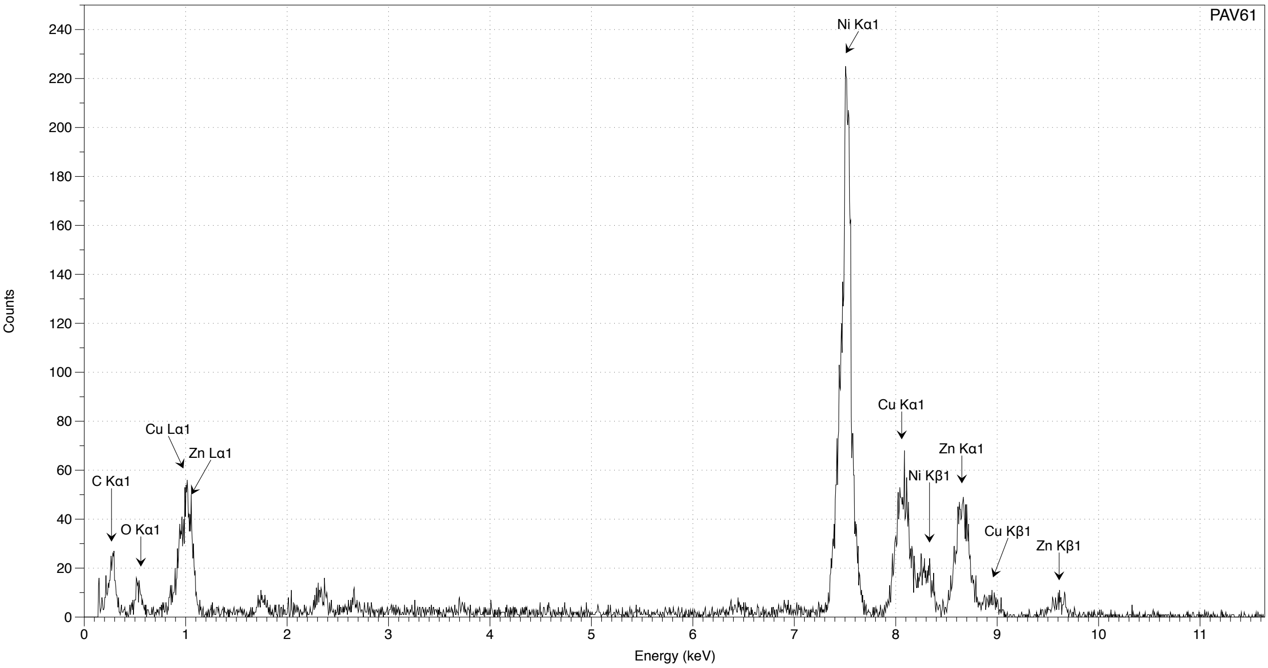

Figure S26d Representative narrow beam ED spectrum reveals emission lines for Cu and Zn. Peak integration and background subtraction reveals the actual approximate Cu:Zn ratio for this region to be 1.08

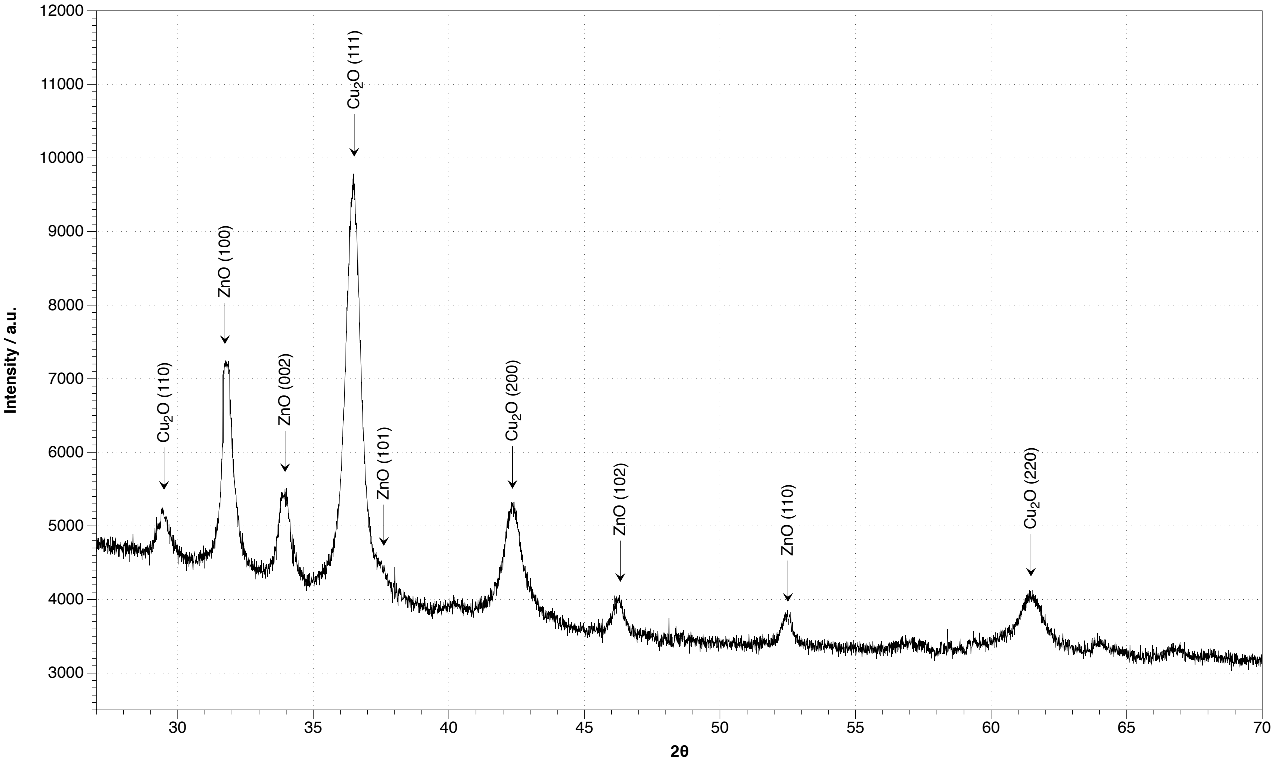

Figure S26e XRPD pattern demonstrates the presence of Cu$_2$O and ZnO

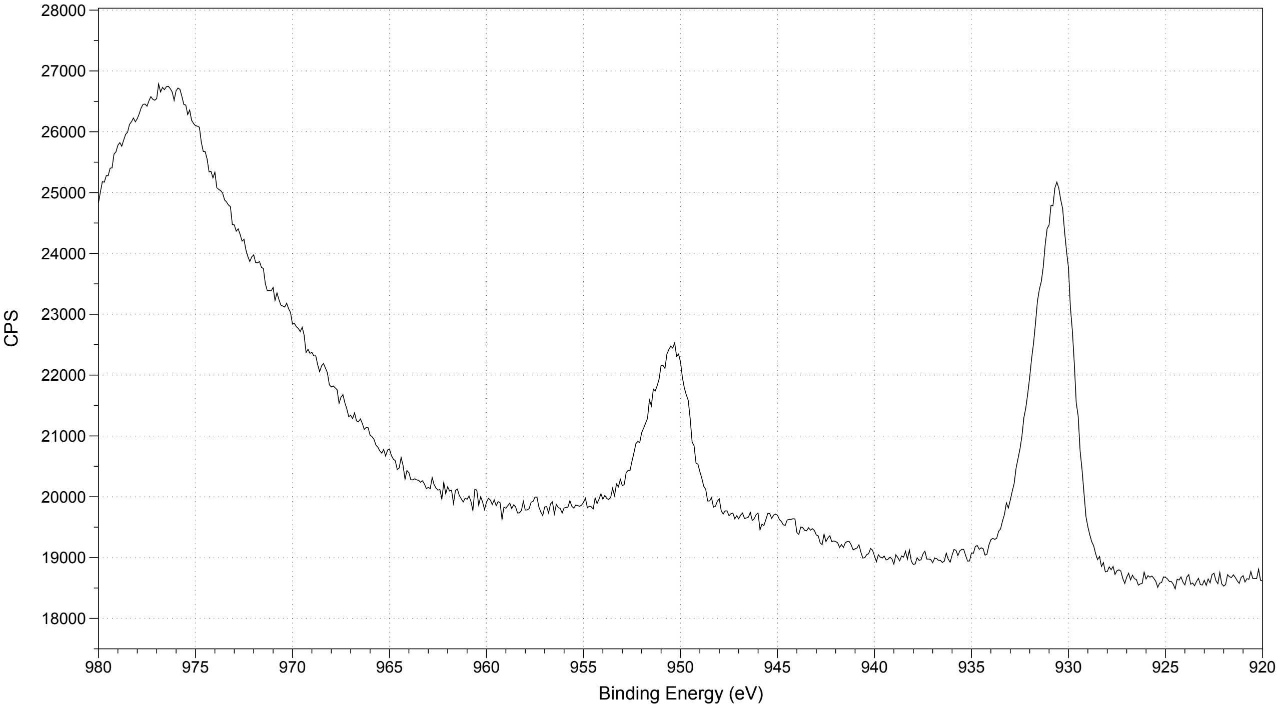

Figure S26f XPS data showing Cu $2p_{1/2}$ and $2p_{3/2}$ region demostrates a strong Cu$_2$O at 931.5 eV

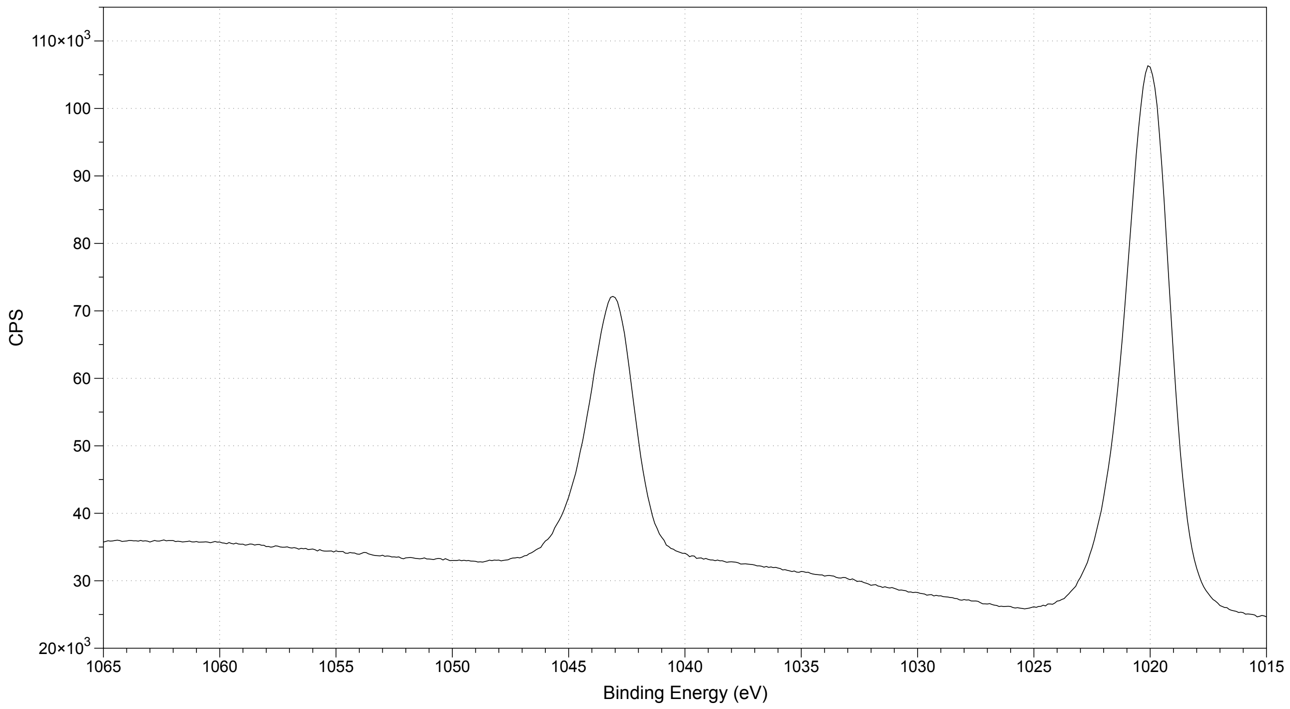

Figure S26g XPS data showing Zn $2p_{1/2}$ and $2p_{3/2}$ region demonstrates peaks at 1043.5 eV and 1020.6 eV consistent with ZnO

75:25 CuZn/PVP29 27(reaction pav62)

$CuSO_4$ (119.71 mg, 0.75 mmol) and PVP29 (1.11 g, 10.00 mmol) were dissolved in ethylene glycol (120 ml) under Ar and the mixture was stirred for 2 h at 80°C. This solution was cooled to 0°C and $ZnCl_2$ (34.07 mg, 0.25 mmol) in ethylene glycol (5 ml) was added. The pH was adjusted to *ca*. 10 by adding NaOH (1M in ethylene glycol, 5ml). The mixture was stirred for 15 min after which NaH_2PO_2 (175.96 mg, 2 mmol) in ethylene glycol (5 ml) was added. The reaction was heated to 140°C for 90 min to give a crude NP dispersion, an aliquot of which was purified and redispersed as for catalyst 1.

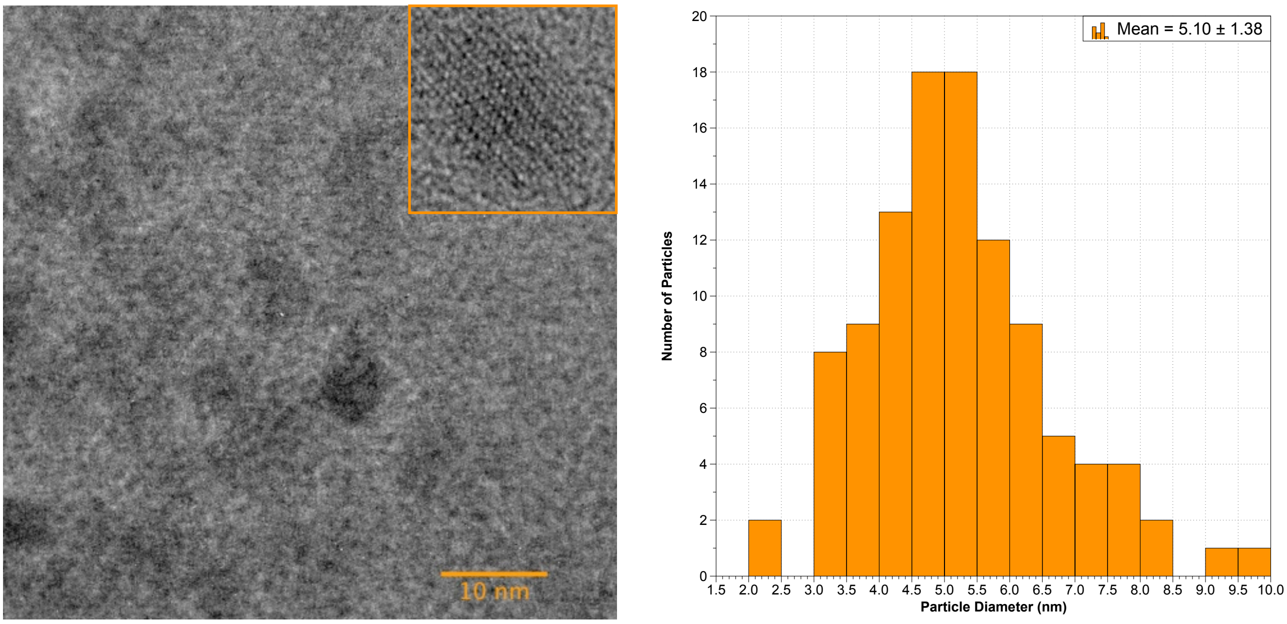

Figure S27a Representative TEM image of catalyst 27 at x300k with a magnified insert *(left)* and particle size distribution *(right)*

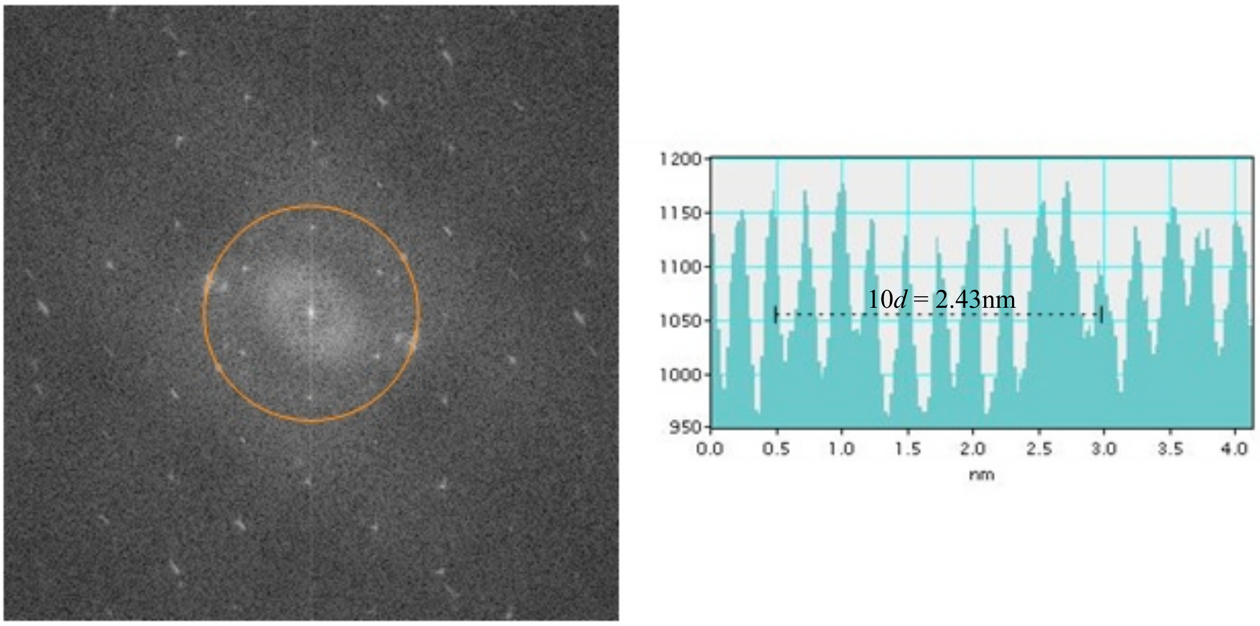

Figure 27b Fourier transform image and fringe space analysis for catalyst 27 demonstrate an average *d* spacing of 2.43 Å corresponding to Cu_2O (111)

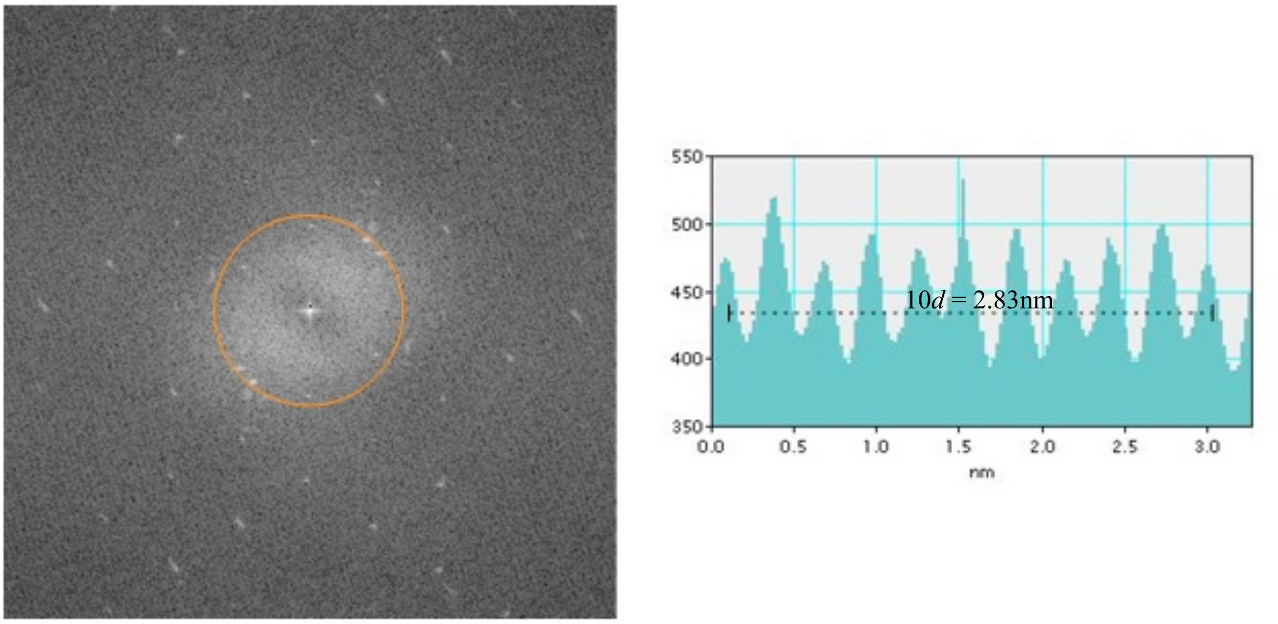

Figure 27c Fourier transform image and fringe space analysis for catalyst 27 demonstrate an average *d* spacing of 2.83 Å corresponding to ZnO (100)

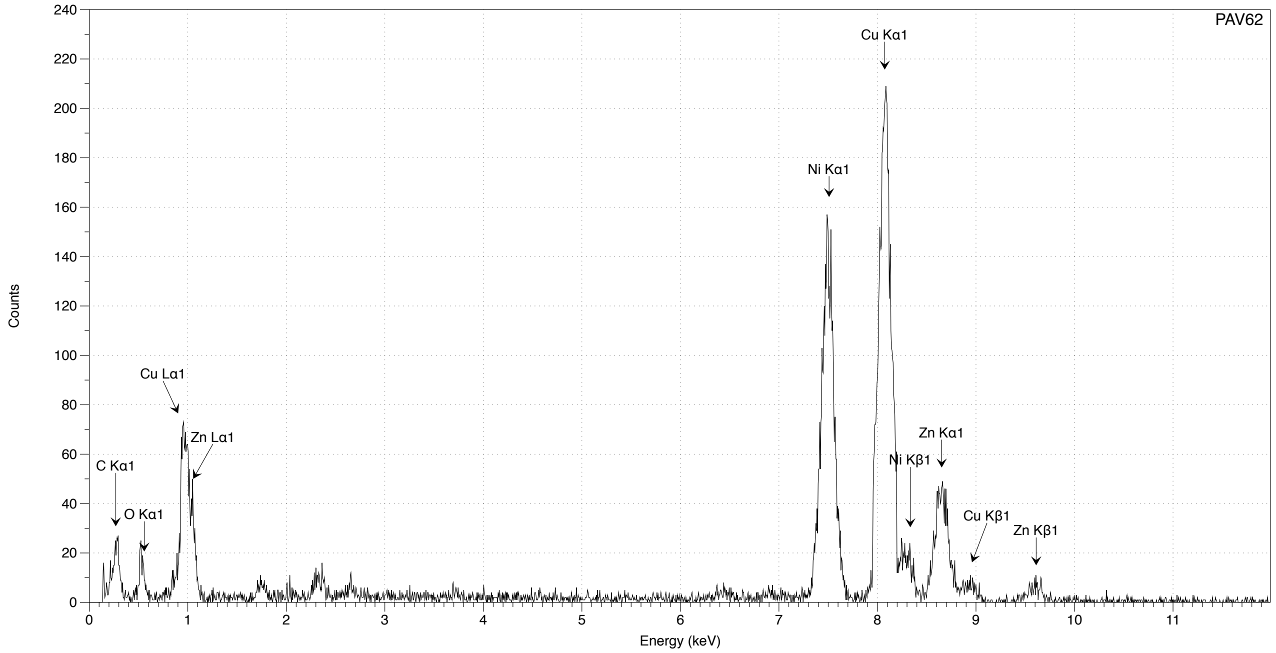

Figure S27d Representative narrow beam ED spectrum reveals strong emission lines for Cu and weak lines for Zn. Peak integration and background subtraction reveals the actual approximate Cu:Zn ratio for this region to be 2.37

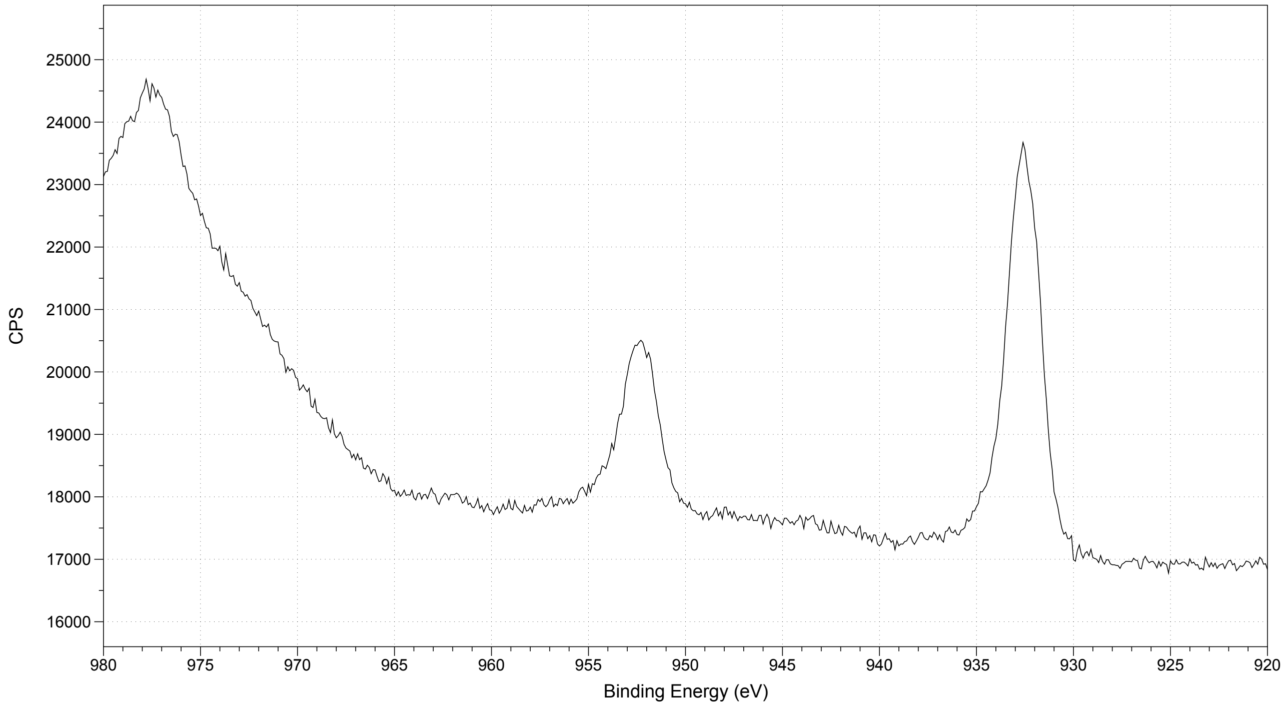

Figure S27e XPS data showing Cu $2p_{1/2}$ and $2p_{3/2}$ region reveal Cu_2O signal at 932.5 eV

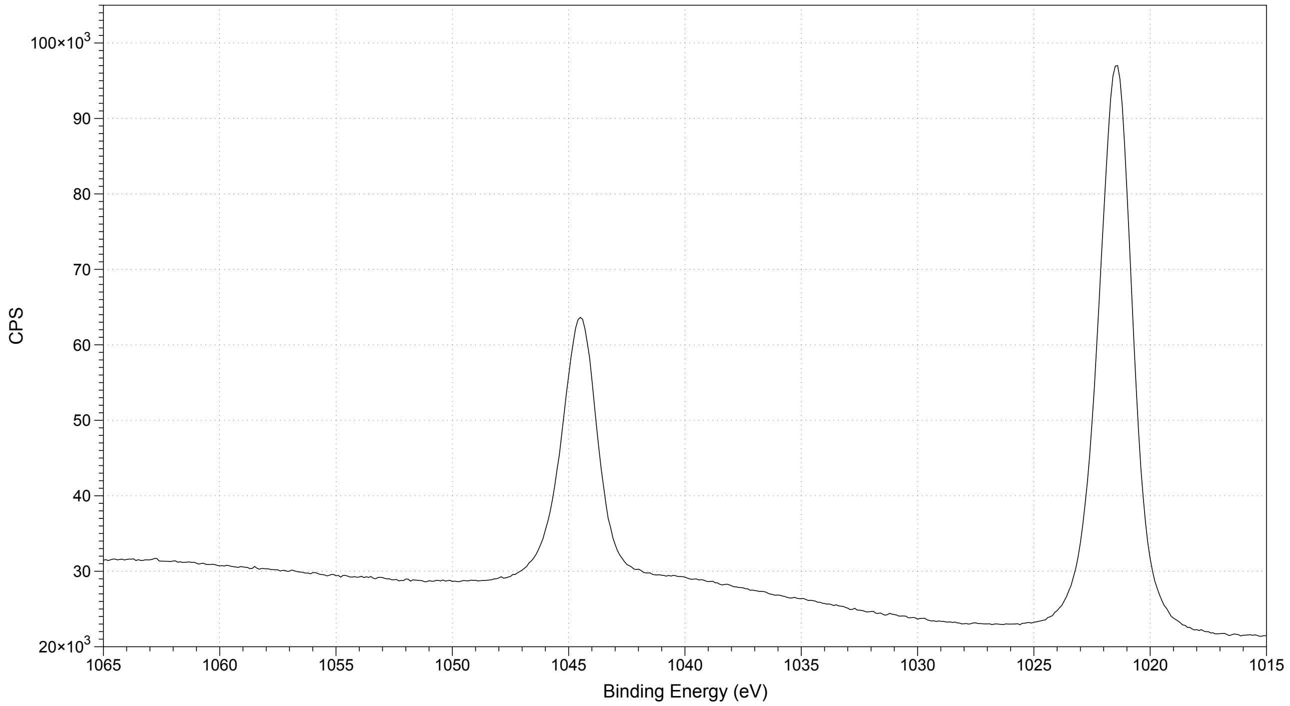

Figure S27f XPS data Zn $2p_{1/2}$ and $2p_{3/2}$ region shows peaks at 1044.6 eV and 1021.4 eV consistent with ZnO

25:75 CuZn/PVPy60 28(reaction pav68)

$CuSO_4$ (39.90 mg, 0.25 mmol) and PVPy60 (1.05 g, 10.00 mmol) were dissolved in ethylene glycol (120 ml) under Ar and the mixture was stirred for 2 h at 80°C. This solution was cooled to 0°C and $ZnCl_2$ (102.24 mg, 0.75 mmol) in ethylene glycol (10 ml) was added. The pH was adjusted to *ca*. 10 by addingNaOH (in ethylene glycol) (1M, 5ml). The mixture was stirred for 15 min after which NaH_2PO_2 (175.96 mg, 2.00 mmol) in ethylene glycol (10 ml) was added. The reaction was heated to 140°C for 90 min to give a crude NP dispersion, an aliquot of which was purified and redispersed as for catalyst 1.

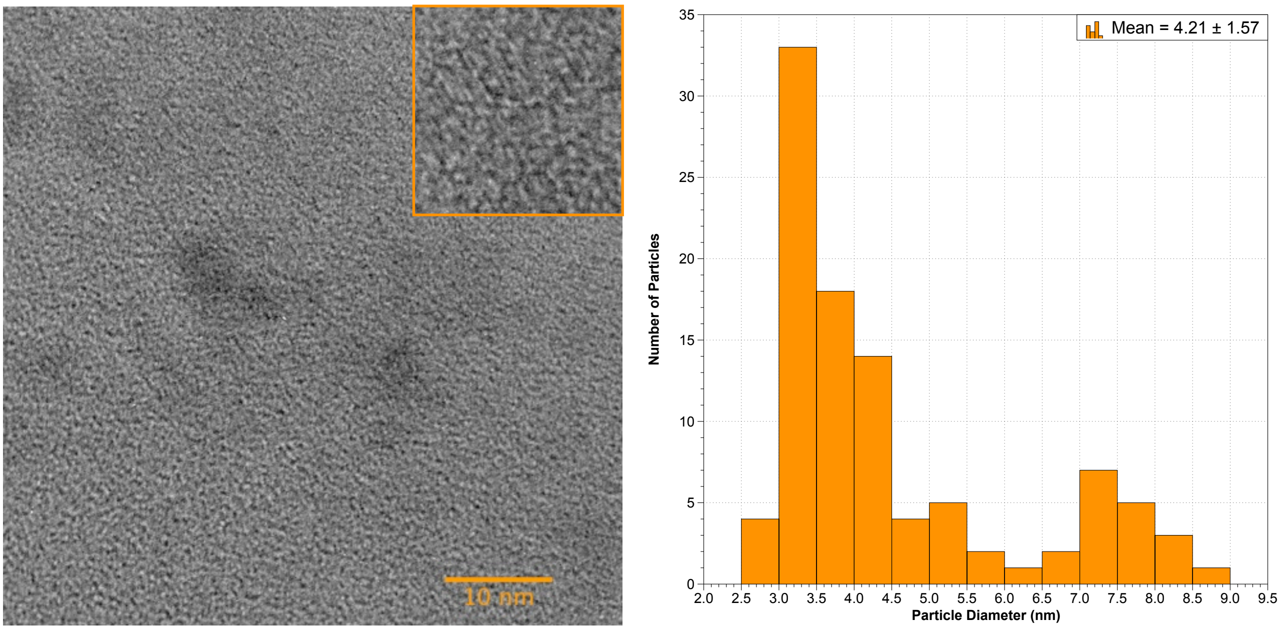

Figure S28a Representative TEM image of catalyst 28 at x300k with a magnified insert *(left)* and particle size distribution *(right)*

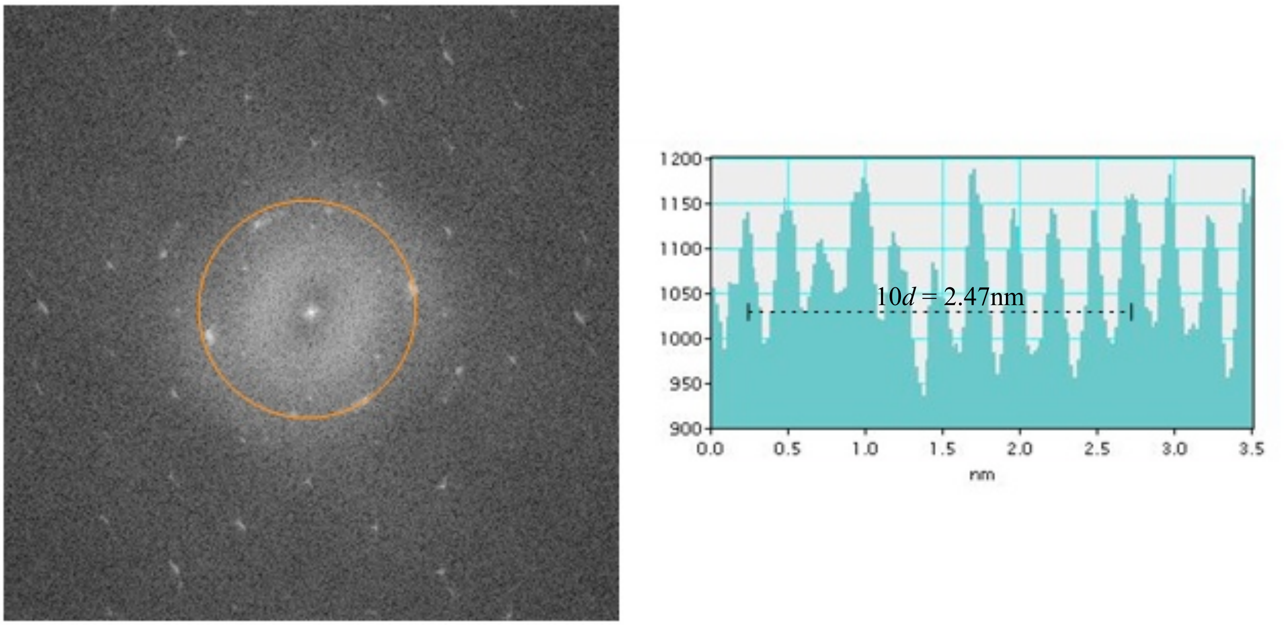

Figure 28b Fourier transform image and fringe space analysis for catalyst 28 demonstrate an average *d* spacing of 2.47 Å corresponding to Cu_2O (111)

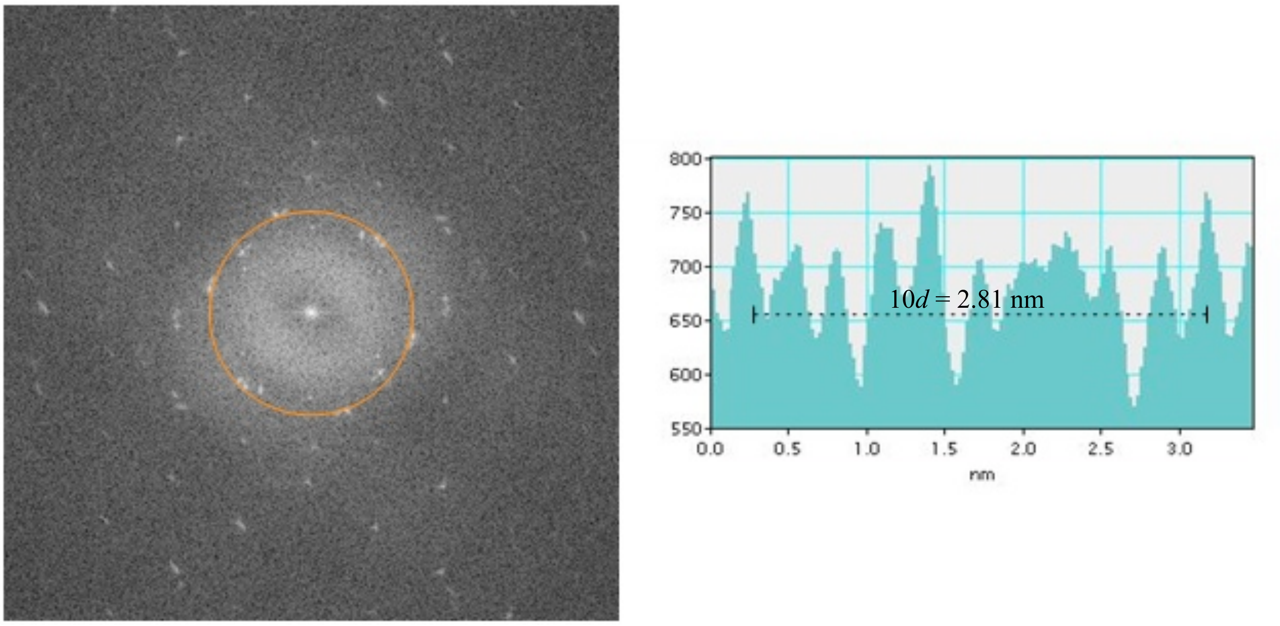

Figure 28c Fourier transform image and fringe space analysis for catalyst 28 demonstrate an average *d* spacing of 2.81 Å corresponding to ZnO(100)

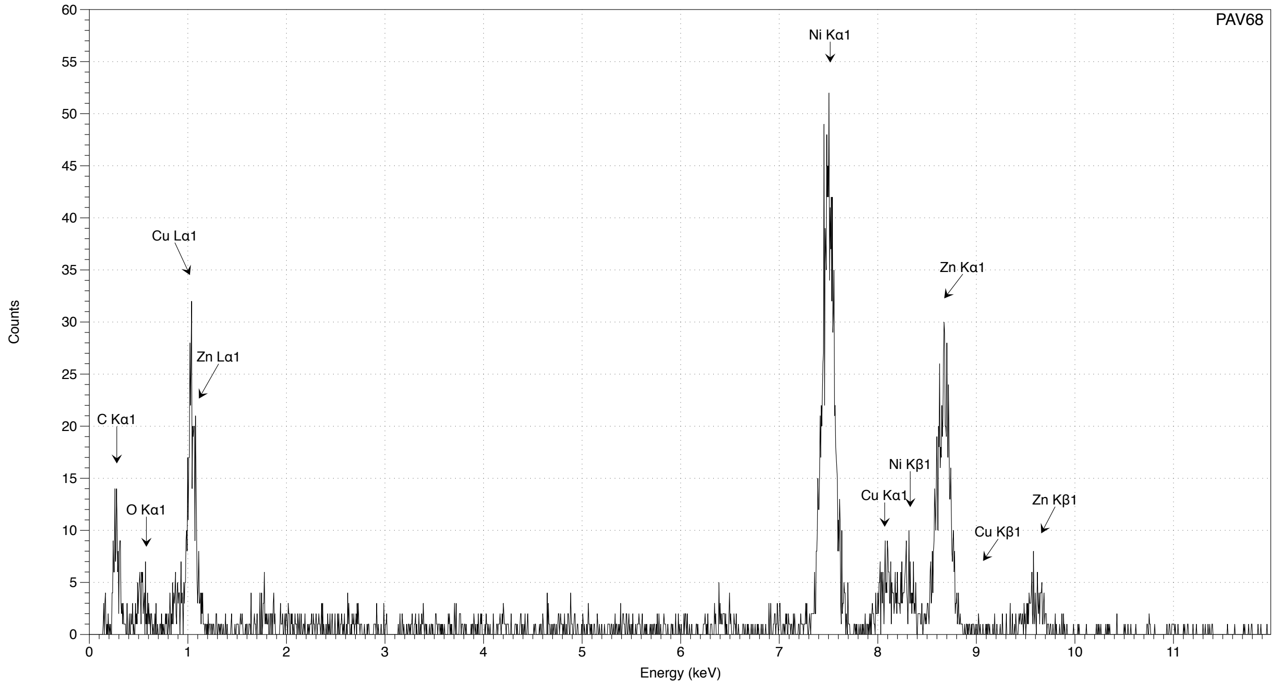

Figure S28d Representative narrow beam ED spectrum reveals weak emission lines for Cu and strong lines for Zn. Peak integration and background subtraction reveals the actual approximate Cu:Zn ratio for this region to be 0.08

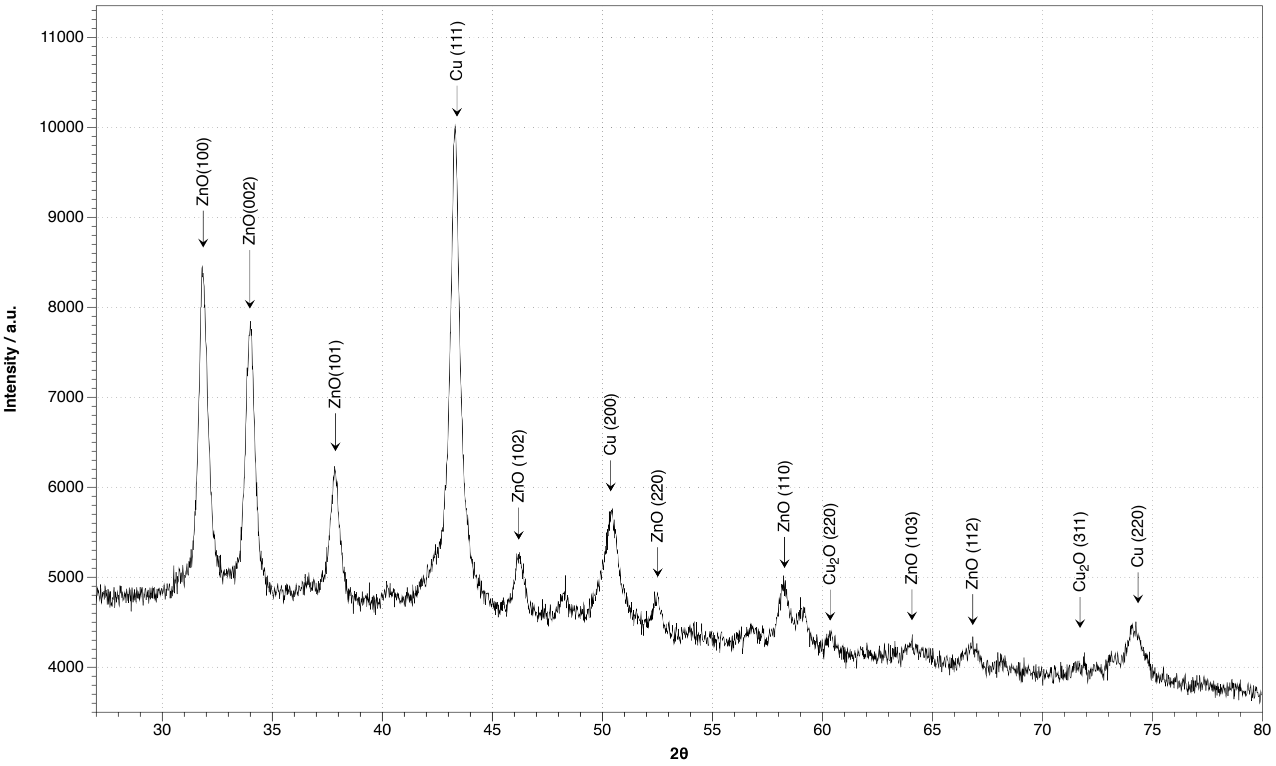

Figure S28e XRPD pattern demonstrates the presence of Cu, Cu_2O and ZnO

50:50 CuZn/PVPy60 29 (pav66)

$CuSO_4$ (79.81 mg, 0.50 mmol) and PVPy60 (1.05 g, 10.00 mmol) were dissolved in ethylene glycol (120 ml) under Ar and the mixture was stirred for 2 h at 80°C. This solution was cooled to 0°C and $ZnCl_2$ (68.15 mg, 0.5 mmol) in ethylene glycol (5 ml). The pH was adjusted to *ca*. 10 by adding NaOH (1M in ethylene glycol, 5ml). The mixture was stirred for 15 min after which NaH_2PO_2 (175.96 mg, 2.00 mmol) in ethylene glycol (5 ml) was added. The reaction was heated to 140°C for 90 min to give a crude NP dispersion, an aliquot of which was purified and redispersed as for catalyst 1.

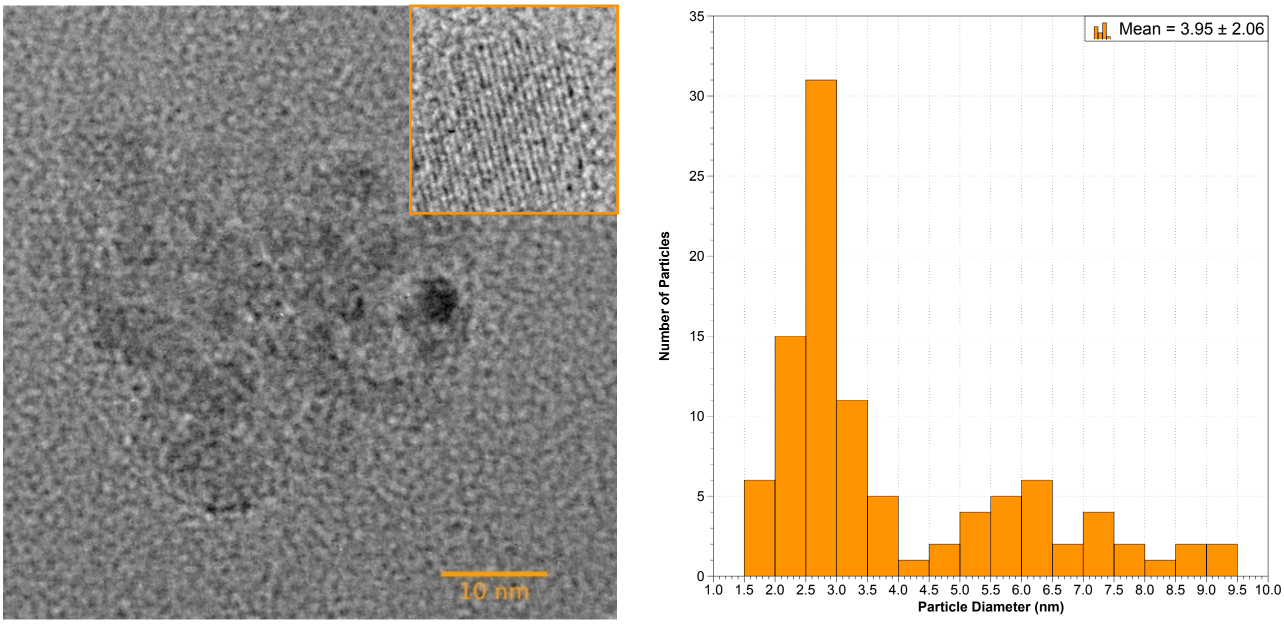

Figure S29a Representative TEM image of catalyst 29 at x300k with a magnified insert *(left)* and particle size distribution *(right)*

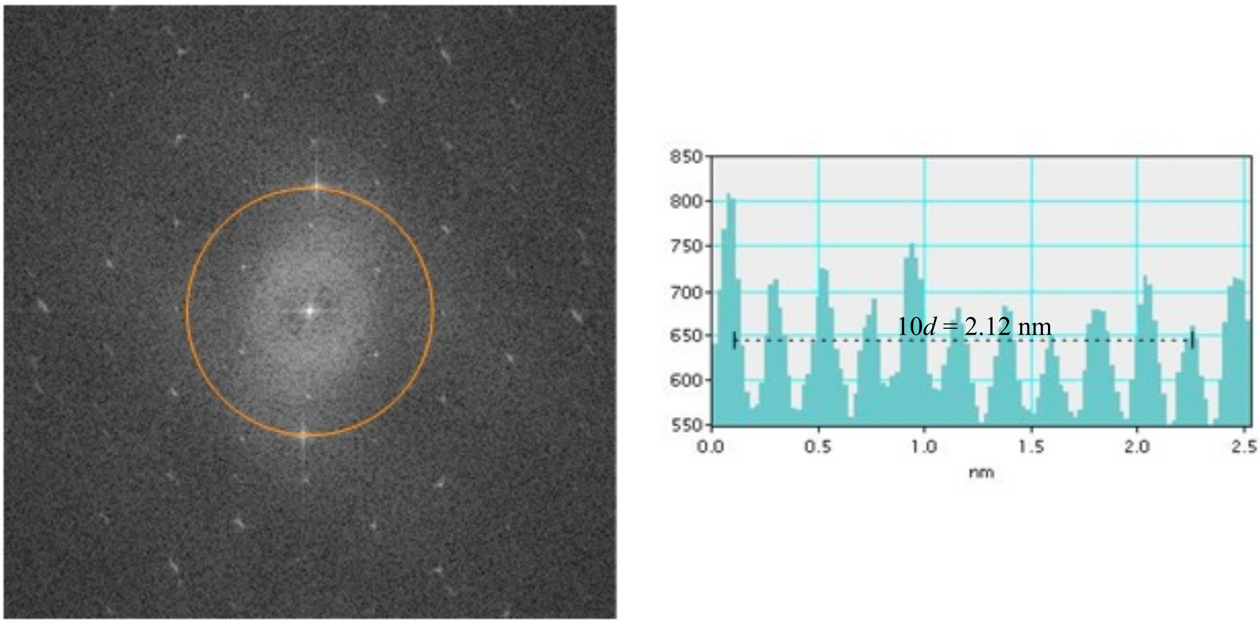

Figure 29b Fourier transform image and fringe space analysis for catalyst 29 demonstrate an average *d* spacing of 2.12 Å corresponding to Cu (111)

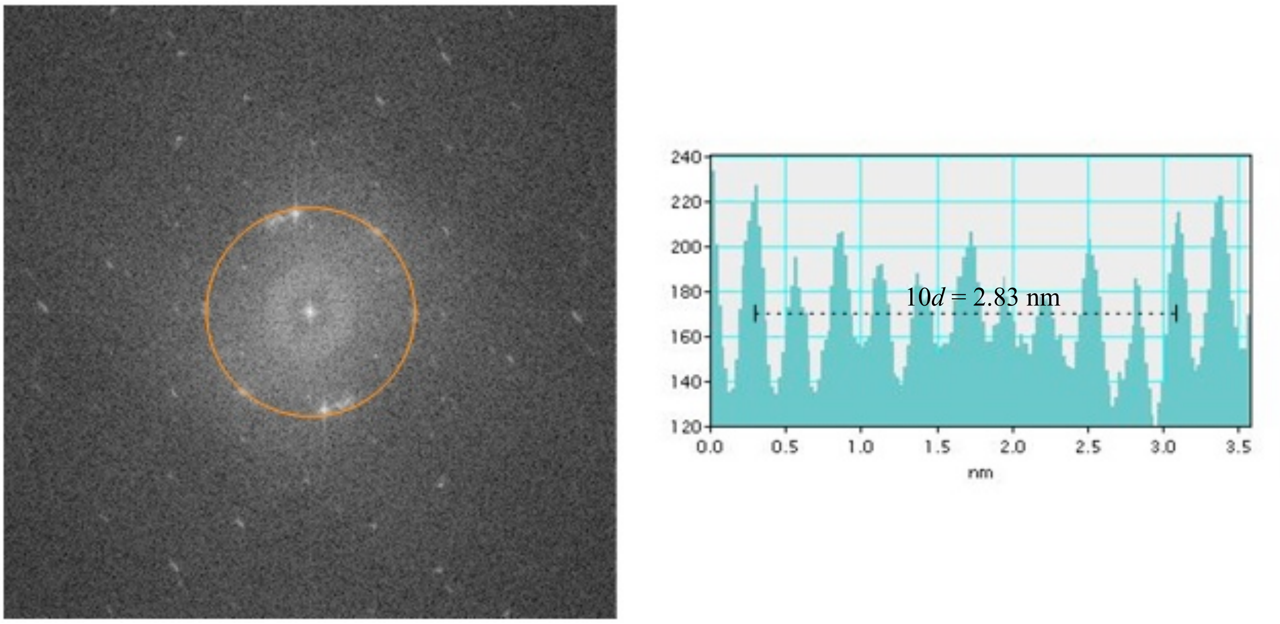

Figure 29c Fourier transform image and fringe space analysis for catalyst 29 demonstrate average d spacing of 2.83 Å corresponding to ZnO (100)

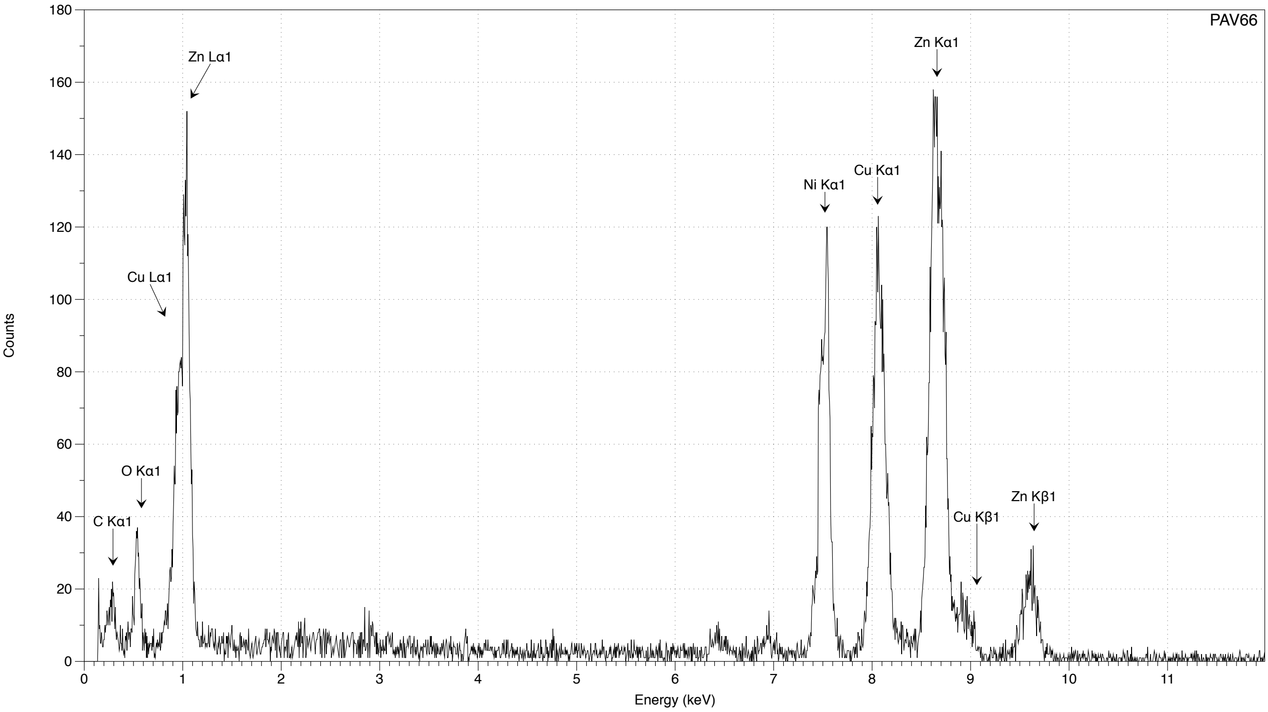

Figure S29d Representative narrow beam ED spectrum reveals emission lines for Cu and Zn. Peak integration and background subtraction reveals the actual approximate Cu:Zn ratio for this region to be 0.56

75:25 CuZn/PVPy60 30(reaction pav67)

$CuSO_4$ (119.71 mg, 0.75 mmol) and PVPy60 (1.05 g, 10.00 mmol) were dissolved in ethylene glycol (120 ml) under Ar and the mixture was stirred for 2 h at 80°C. This solution was cooled to 0°C and $ZnCl_2$ (34.07 mg, 0.25 mmol) in ethylene glycol (2 ml) was added. The pH was adjusted to *ca*. 10 by addingNaOH (in ethylene glycol) (1M, 5ml). The mixture was stirred for 15 min after which NaH_2PO_2 (175.96 mg, 2.00 mmol) in ethylene glycol (10 ml) was added. The reaction was heated to 140°C for 90 min to give a crude NP dispersion, an aliquot of which was purified and redispersed as for catalyst 1.

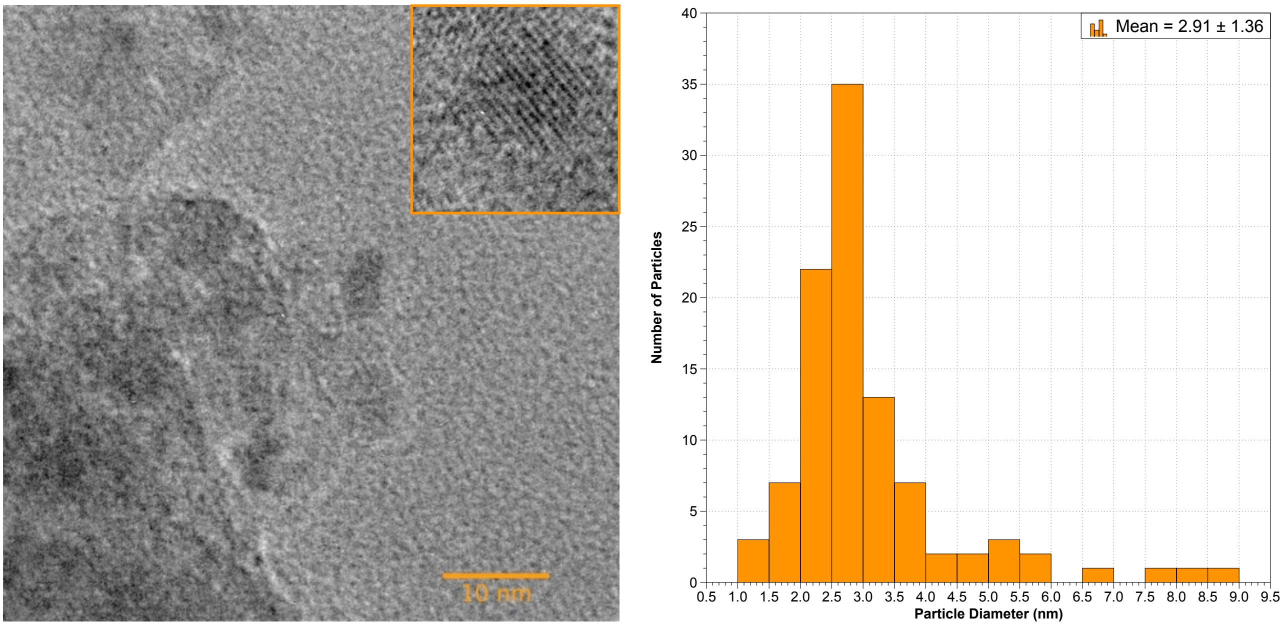

Figure S30a Representative TEM image of catalyst 30 at x300k with a magnified insert *(left)* and particle size distribution *(right)*

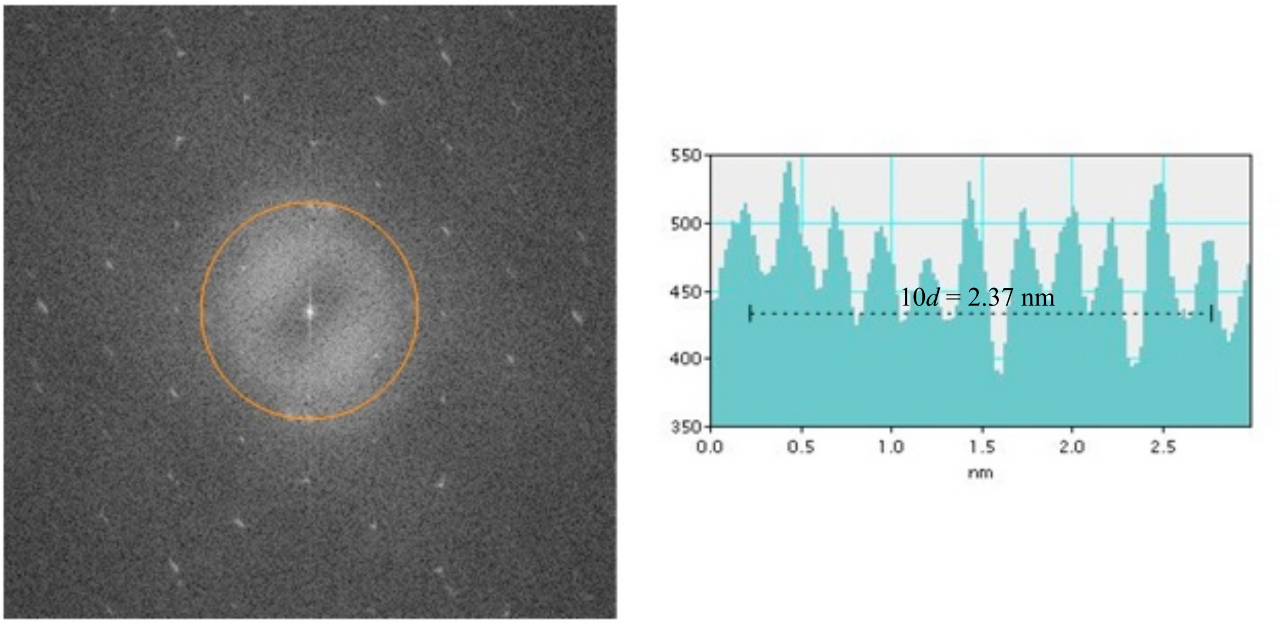

Figure 30b Fourier transform image and fringe space analysis for catalyst 30 demonstrate an average *d* spacing of 2.37 Å corresponding to Cu_2O (111)

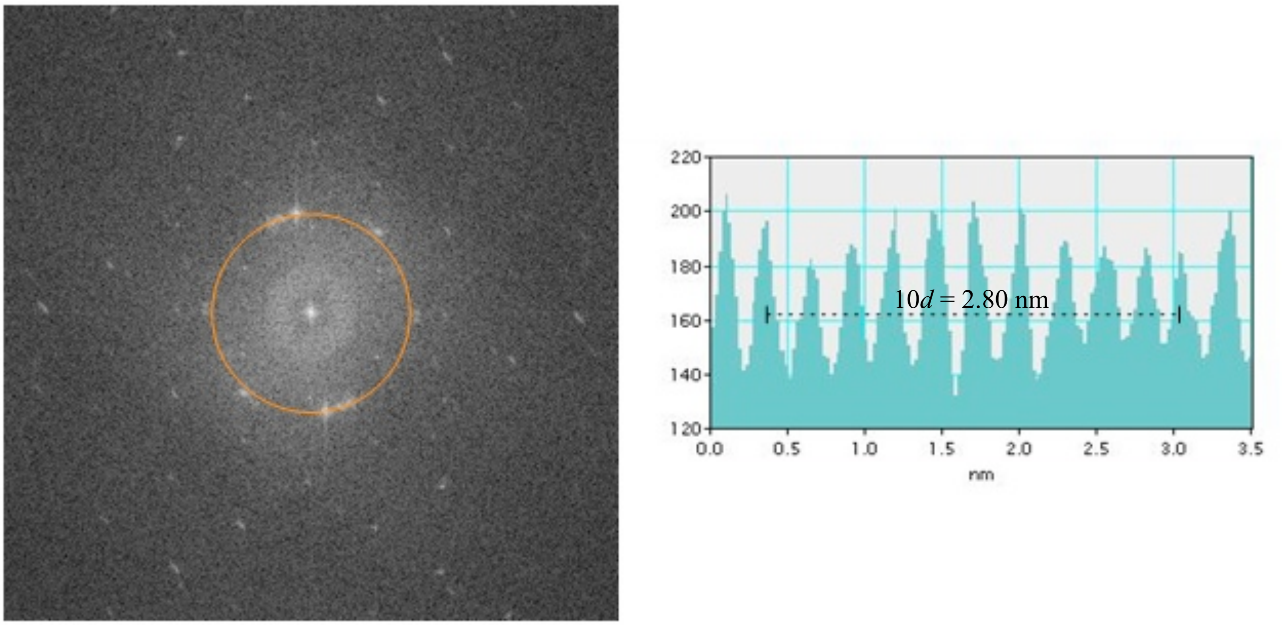

Figure 30c Fourier transform image and fringe space analysis for catalyst 30 demonstrate an average *d* spacing of 2.80 Å corresponding to ZnO (100).

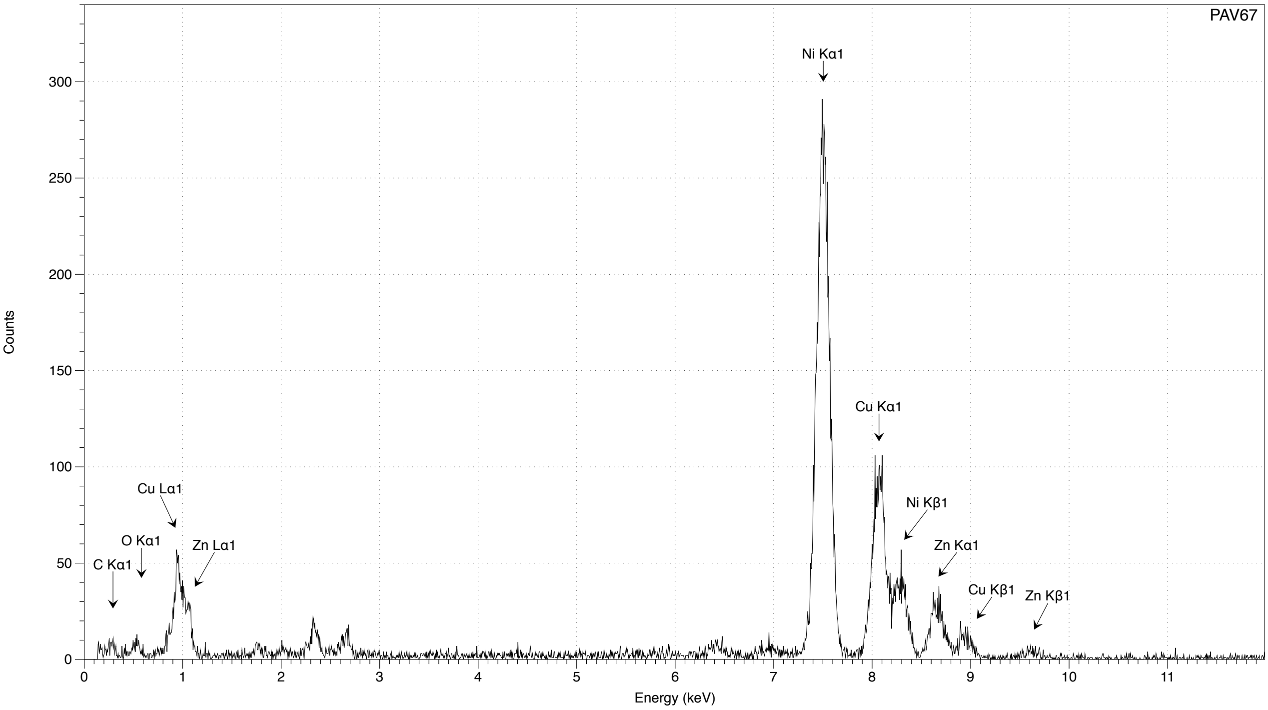

Figure S30d Representative narrow beam ED spectrum reveals strong emission lines for Cu and weak lines for Zn. Peak integration and background subtraction reveals the actual approximate Cu:Zn ratio for this region to be 3.31

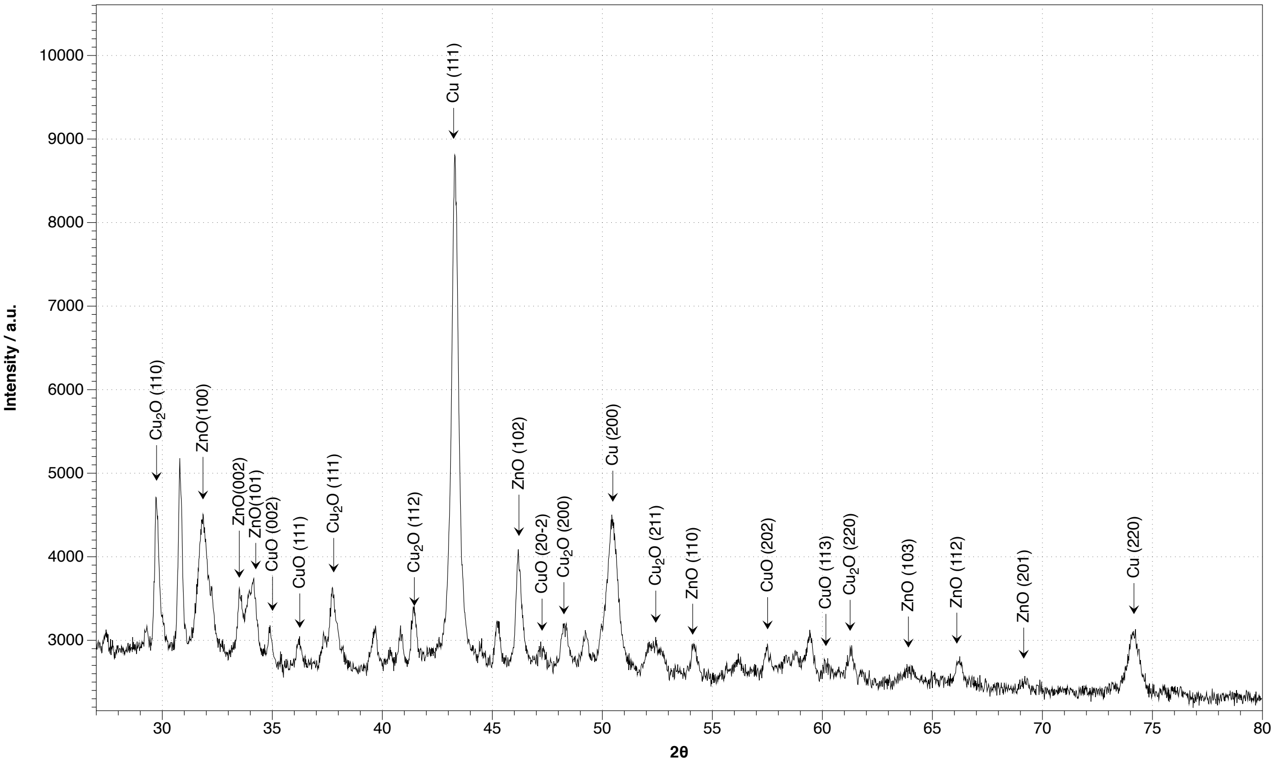

Figure S30e XRPD pattern demonstrates the presence of Cu, Cu_2O and ZnO

ICP-OES analysis of CuZn samples 22-30

Sample	Reaction stoichiometry (Cu:Zn)	Cu:Zn (ppm)	Cu:Zn (mol%)	Notes
22	25:75	184:1947	8.6:91.4	PVP29, hydrous preparation
23	50:50	77:132	36.9:63.1	
24	25:75	84:35	70.6:29.4	
25	25:75	266:7882	3.3:96.7	PVP29, anhydrous preparation
26	50:50	57:153	27.1:72.9	
27	25:75	156:44	77.8:22.2	
28	25:75	850:1350	38.6:61.4	PVPy60, anhydrous preparation
29	50:50	600:800	42.9:57.1	
30	25:75	1600:450	78.0:22.0	

Multicomponent synthesis of 1,2,3-triazoles

NaN_3 (72 mg, 1.1 mmol), organic halide [benzyl bromide (119 μl, 1 mmol) or 1-iodononane (197 μl, 1 mmol)], and phenylacetylene (110 μl, 1 mmol or 220 μl, 2 mmol) were added to a suspension of Cu NPs or CuZn NPs in MeOH (2 ml; the metal content of which had been determined by ICP-OES prior to dilution to a known concentration) under an atmosphere of air or argon. The reaction mixture was maintained at room temperature or at reflux for the specified time, with the progress being monitored by TLC. Water (30 ml) was added and the mixture extracted with EtOAc (3 × 10 ml). The organic phase was dried with anhydrous $MgSO_4$, and the solvent removed *in vacuo* to give crude material, which was analyzed by GLC and did not require any further purification when high conversions into the triazoles **3**, **5** and **6** were reached. Triazoles **3**,[1] **5**[2] and **6**[3] were characterized by comparison of their physical and spectroscopic data with those described in the literature.

Synthesis of 1-benzyl-4-phenyl-1,2,3-triazole 3 using Cu catalyst 1

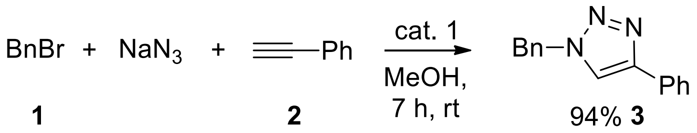

Synthesis of 1-benzyl-4-phenyl-1,2,3-triazole 3 using Cu catalyst 2

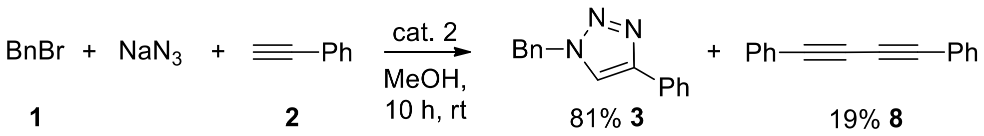

---

[1] F. Alonso, Y. Moglie, G. Radivoy and M. Yus, *Eur. J. Org. Chem.*, 2010, 1875.

[2] F. Alonso, Y. Moglie, G. Radivoy and M. Yus, *Org. Biomol. Chem.*, 2011, **9**, 6385.

[3] J. Deng, Y.-M. Wu and Q.-Y. Chen, *Synthesis*, 2005, 2730.

Synthesis of 1-benzyl-4-phenyl-1,2,3-triazole 3 using Cu catalyst 4

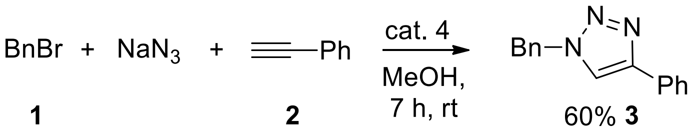

Synthesis of 1-benzyl-4-phenyl-1,2,3-triazole 3 using Cu catalyst 4

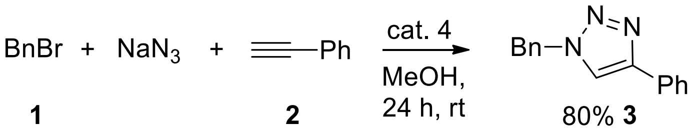

Synthesis of 1-benzyl-4-phenyl-1,2,3-triazole 3 using Cu catalyst 4

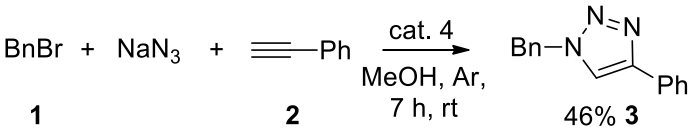

Synthesis of 1-benzyl-4-phenyl-1,2,3-triazole 3 using Cu catalyst 4

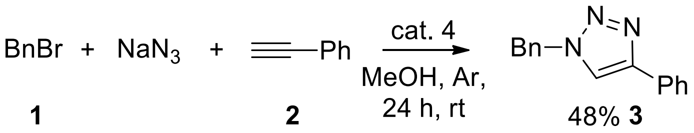

Synthesis of 1-benzyl-4-phenyl-1,2,3-triazole 3 using Cu catalyst 7

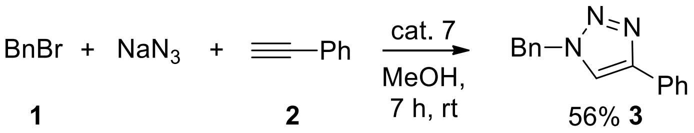

Synthesis of 1-benzyl-4-phenyl-1,2,3-triazole 3 using Cu catalyst 7

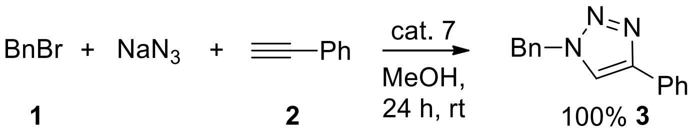

Synthesis of 1-benzyl-4-phenyl-1,2,3-triazole 3 using Cu catalyst 7

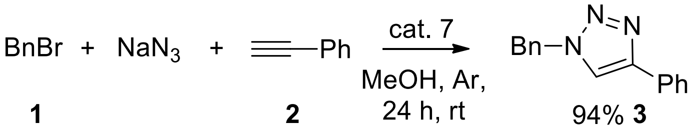

Synthesis of 1-benzyl-4-phenyl-1,2,3-triazole 3 using Cu catalyst 9

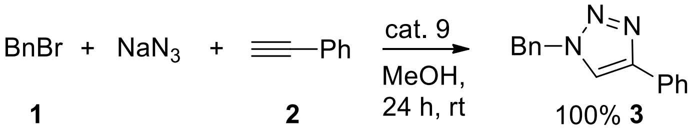

Synthesis of 1-benzyl-4-phenyl-1,2,3-triazole 3 using Cu catalyst 9

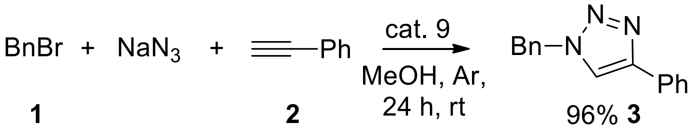

Attempted synthesis of 1-nonyl-4-phenyl-1,2,3-triazole 5 using Cu catalyst 9

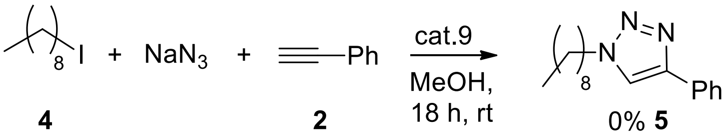

Synthesis of 1-nonyl-4-phenyl-1,2,3-triazole 5 using Cu catalyst 9

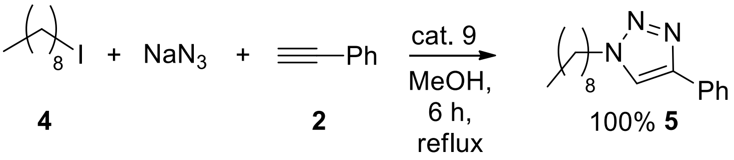

Synthesis of 1-benzyl-4-phenyl-1,2,3-triazole 3 using Cu catalyst 12

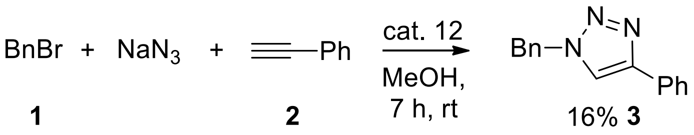

Synthesis of 1-benzyl-4-phenyl-1,2,3-triazole 3 using Cu catalyst 12

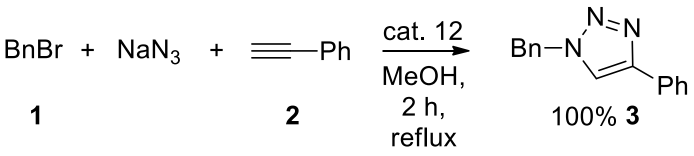

Attempted synthesis of 1-benzyl-4-phenyl-1,2,3-triazole 3 using Cu catalyst 15

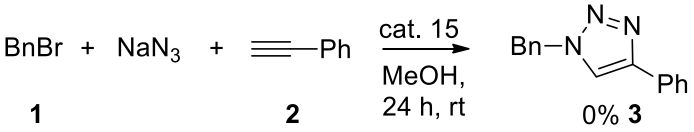

Synthesis of 1-benzyl-4-phenyl-1,2,3-triazole 3 using Cu catalyst 15

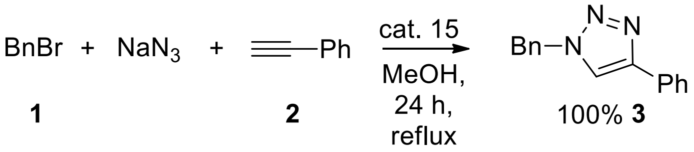

Attempted synthesis of 1-benzyl-4-phenyl-1,2,3-triazole 3 using Cu catalyst 15

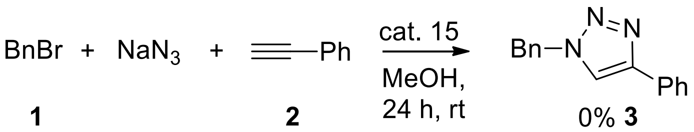

Attempted synthesis of 1-benzyl-4-phenyl-1,2,3-triazole 3 using Cu catalyst 17

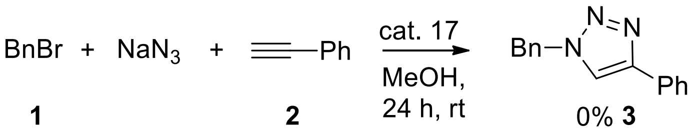

Synthesis of 1-benzyl-4-phenyl-1,2,3-triazole 3 using Cu catalyst 17

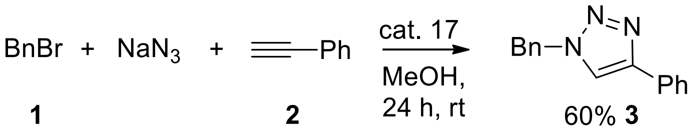

Attempted synthesis of 1-benzyl-4-phenyl-1,2,3-triazole 3 using Cu catalyst 17

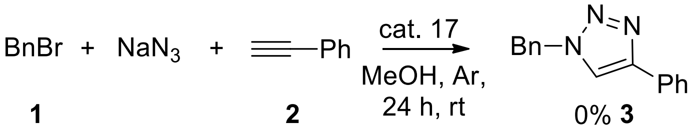

Synthesis of 1-benzyl-4-phenyl-1,2,3-triazole 3 using CuZn catalyst 23

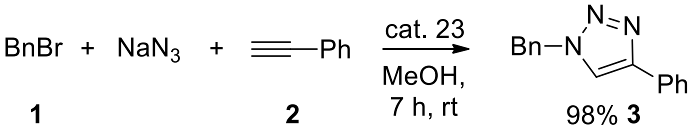

Synthesis of 1-benzyl-4-phenyl-1,2,3-triazole 3 using CuZn catalyst 24

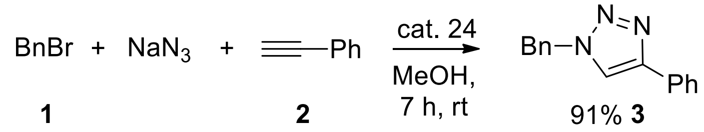

Synthesis of 1-benzyl-4-phenyl-1,2,3-triazole 3 using CuZn catalyst 25

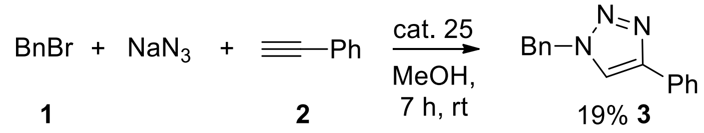

Synthesis of 1-benzyl-4-phenyl-1,2,3-triazole 3 using CuZn catalyst 26

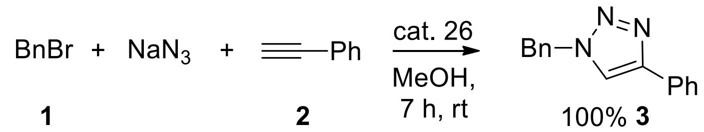

Synthesis of 1-nonyl-4-phenyl-1,2,3-triazole 5 using CuZn catalyst 26

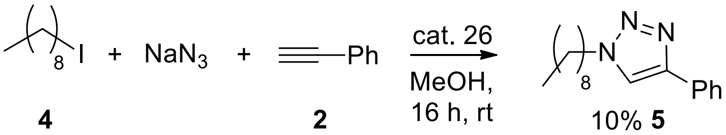

Synthesis of 1-nonyl-4-phenyl-1,2,3-triazole 5 using CuZn catalyst 26

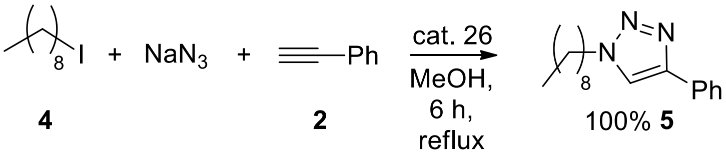

Synthesis of 1-benzyl-4-phenyl-1,2,3-triazole 3 using CuZn catalyst 28

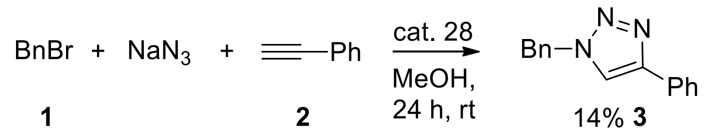

Synthesis of 1-benzyl-4-phenyl-1,2,3-triazole 3 using CuZn catalyst 28

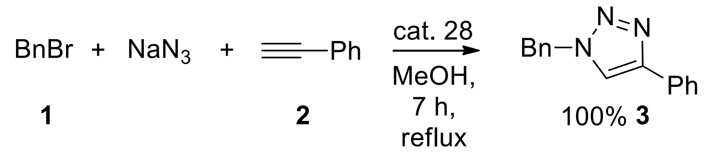

Synthesis of 1-benzyl-4-phenyl-1,2,3-triazole 3 using CuZn catalyst 29

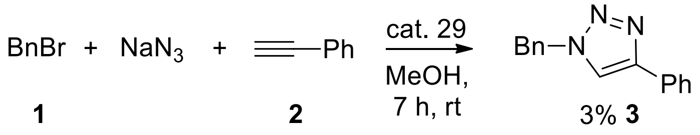

Synthesis of 1-benzyl-4-phenyl-1,2,3-triazole 3 using CuZn catalyst 29

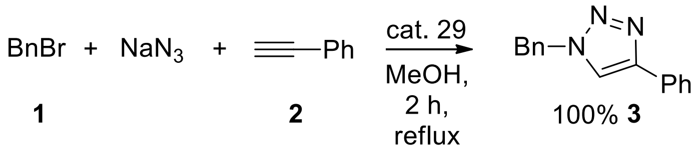

Synthesis of 1-benzyl-4-phenyl-1,2,3-triazole 3 using CuZn catalyst 30

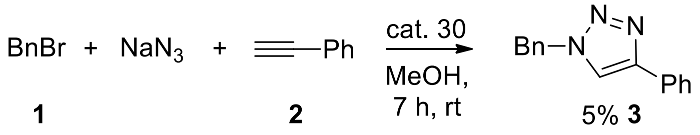

Synthesis of 1-benzyl-4-phenyl-1,2,3-triazole 3 using CuZn catalyst 30

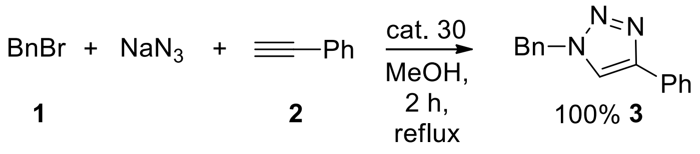

Synthesis of 1-benzyl-4-phenyl-5-phenylacetylido-1,2,3-triazole 6 using Cu catalyst 1

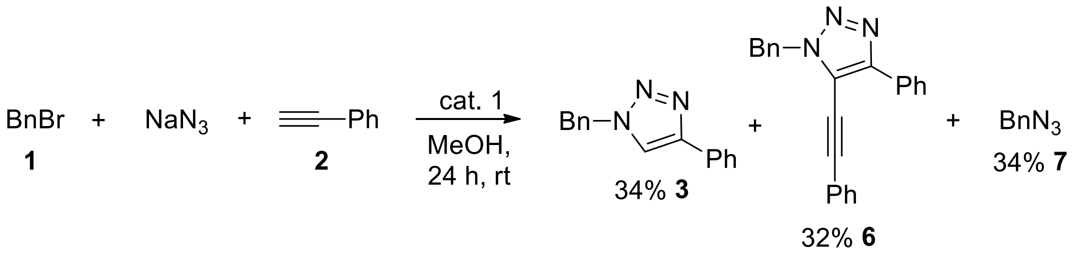

Synthesis of 1-benzyl-4-phenyl-5-phenylacetylido-1,2,3-triazole 6 using Cu catalyst 2

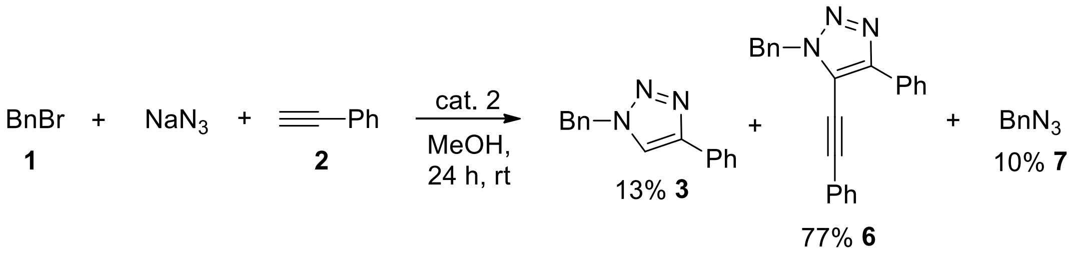

Synthesis of 1-benzyl-4-phenyl-5-phenylacetylido-1,2,3-triazole 6 using CuZn catalyst 23

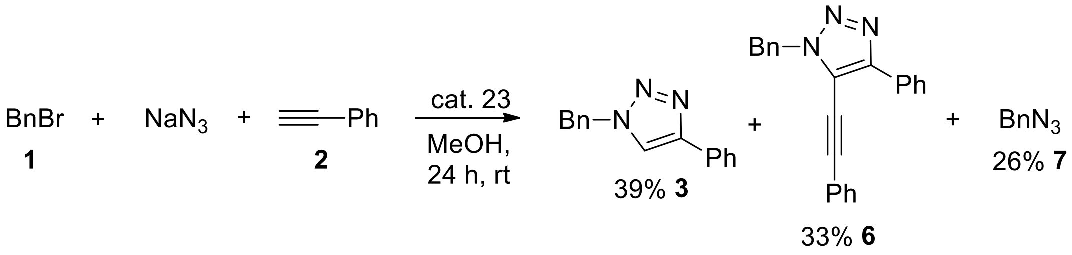

Synthesis of 1-benzyl-4-phenyl-5-phenylacetylido-1,2,3-triazole 6 using Cu catalyst 1

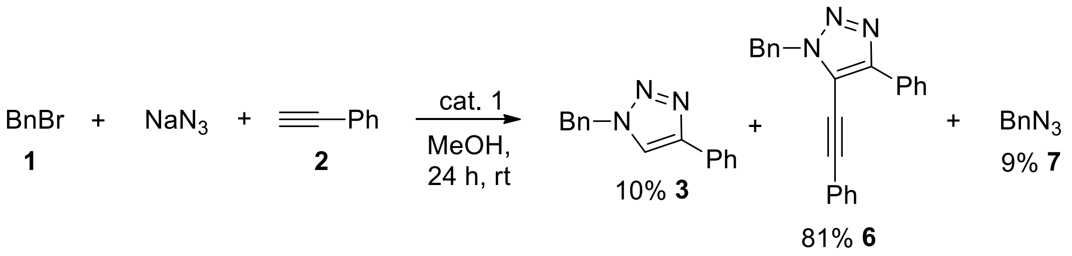

Attempted synthesis of 1-benzyl-4-phenyl-5-phenylacetylido-1,2,3-triazole 6 using CuZn catalyst 23

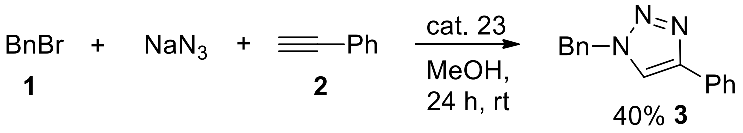

Synthesis of 1-benzyl-4-phenyl-5-phenylacetylido-1,2,3-triazole 6 using Cu catalyst 2

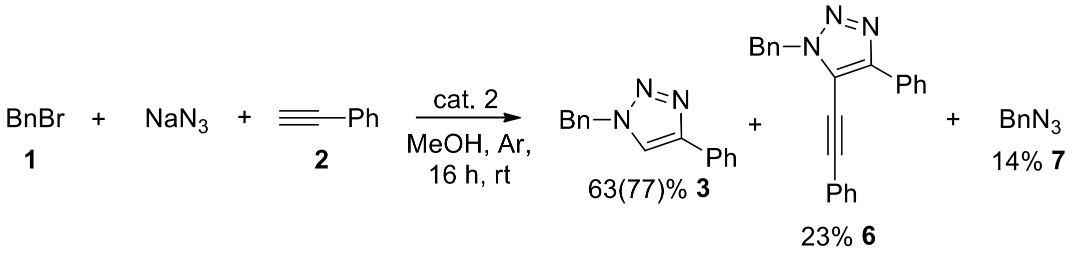

Attempted synthesis of 1-benzyl-4-phenyl-5-phenylacetylido-1,2,3-triazole 6 using Cu catalyst 2

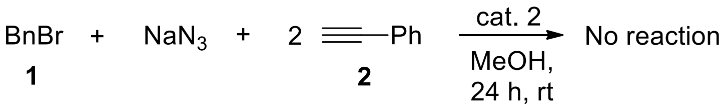

Synthesis of 1-benzyl-4-phenyl-5-phenylacetylido-1,2,3-triazole 6 using Cu catalyst 2

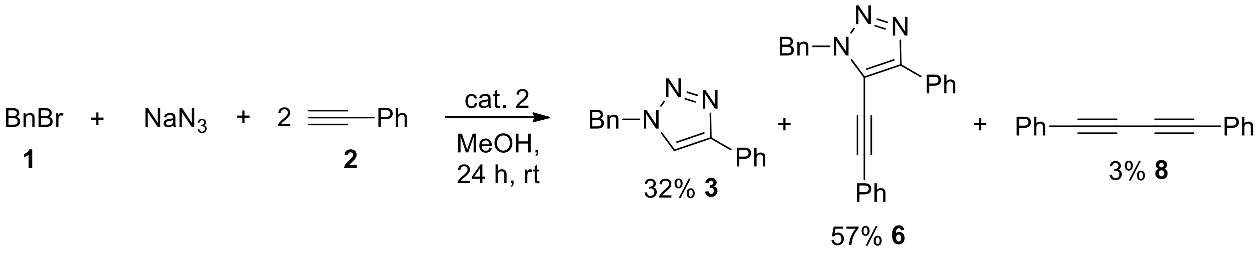

Synthesis of 1-benzyl-4-phenyl-5-phenylacetylido-1,2,3-triazole 6 using Cu catalyst 2

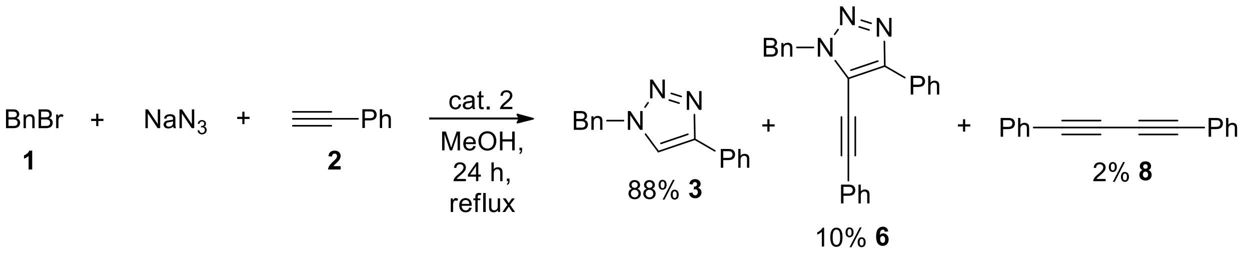

Synthesis of 1-benzyl-4-phenyl-5-phenylacetylido-1,2,3-triazole 6 using Cu catalyst 2

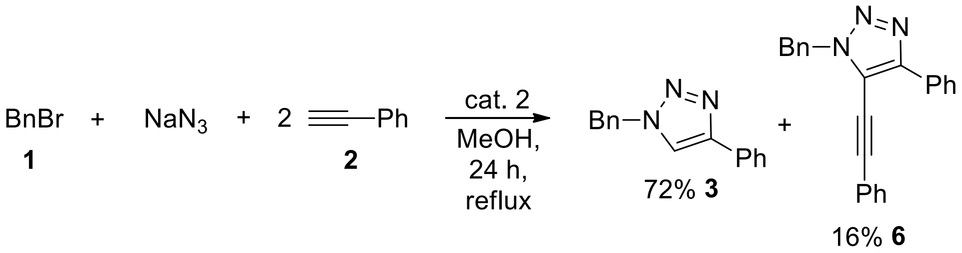

Synthesis of 1-benzyl-4-phenyl-5-phenylacetylido-1,2,3-triazole 6 using Cu catalyst 1

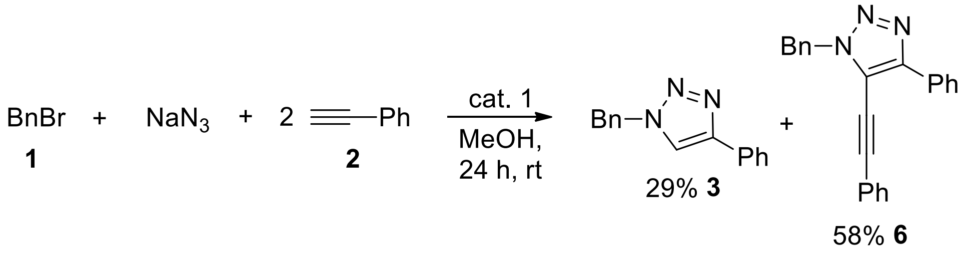

Synthesis of 1-benzyl-4-phenyl-5-phenylacetylido-1,2,3-triazole 6 using Cu catalyst 1

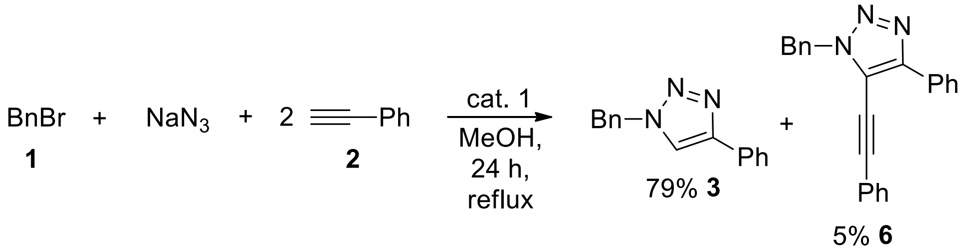

Attempted reaction of 1-benzyl-4-phenyl-1,2,3-triazole 3 with phenylacetylene using Cu catalyst 2

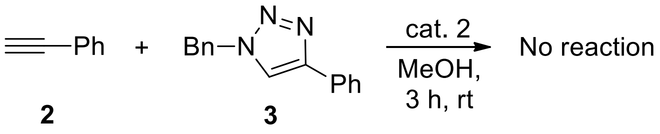

Attempted reaction of 1-benzyl-4-phenyl-1,2,3-triazole 3 with phenylacetylene using Cu catalyst 2

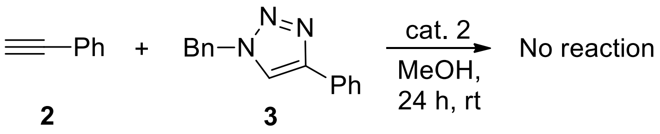

Attempted reaction of 1-benzyl-4-phenyl-1,2,3-triazole 3 with phenylacetylene using Cu catalyst 2

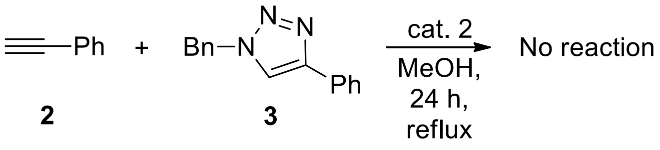

Attempted reaction of 1-benzyl-4-phenyl-1,2,3-triazole 3 with phenylacetylene using Cu catalyst 2

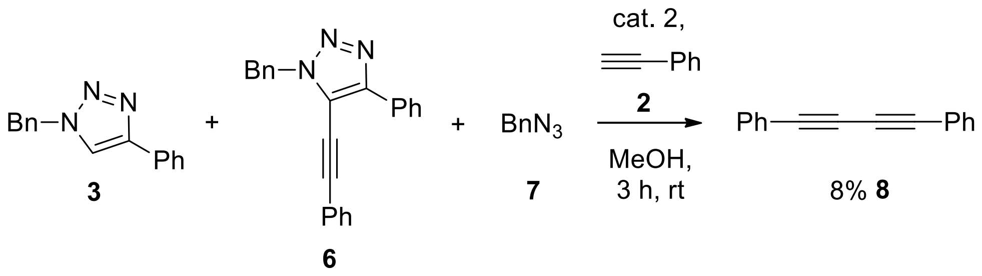

Attempted reaction of benzylbromide 1 with 1,4-diphenyl-1,3-diyne 8 using Cu catalyst 2